PONTIFICIA UNIVERSIDAD CATOLICA DE CHILE

ESCUELA DE INGENIERIA

FIBERS AND POROUS SCAFFOLDS FROM ALGINATE

TERESA R. CUADROS

Thesis submitted to the Office of Research and Graduate Studies in partial fulfillment of the requirements for the Degree of Doctor in Engineering Sciences

Advisor:

JOSÉ MIGUEL AGUILERA RADIC

Santiago de Chile, August, 2015

PONTIFICIA UNIVERSIDAD CATOLICA DE CHILE
ESCUELA DE INGENIERIA

FIBERS AND POROUS SCAFFOLDS FROM ALGINATE

TERESA R. CUADROS

Members of the Committee:

JOSÉ M. AGUILERA

JOSÉ M. DEL VALLE

CARMEN SAENZ

JORGE MORENO

MARÍA DEL PILAR BUERA

CRISTIAN VIAL

Thesis submitted to the Office of Research and Graduate Studies in partial fulfillment of the requirements for the Degree of Doctor in Engineering Sciences

Santiago de Chile, August, 2015

Dedicated to my parents and my family

ACKNOWLEDGEMENTS

In a special way, I wish to express my sincere gratitude to my advisor José Miguel Aguilera, for his constant teachings and his critical and constructive spirit. I have found in you a guide and model. Thank you!.

I would also like to thank the other members of the thesis commitee, Prof. María del Pilar Buera, Prof. Carmen Saenz, Prof. Jorge Moreno, Prof. José Manuel del Valle and Prof. Cristian Vial. Thanks for agreeing to join me in this mission and for the words and advice across this journey!.

I want to thank immensely every one of my lab-mates who contributed in some way to this work. I do not want to omit anyone. I thank all the people whom I went, consulted, talked, discussed, shared, helped and assisted me. Thank you very much to all!.

At this point of the road I must recognize the administrative guidance provided by Gloria Escobar, Debbie Meza and Fernanda Kattan of the Office of Research and Graduate Studies. Thank to them!.

Also, I was lucky to match and receive from Rosa and Jackelin, almost daily one word of encouragement especially in the most difficult moments. For them, my gratitude, thank for their joy!.

And as my source of encouragement and inspiration, I want to thank my family, Salvador and Orlando for their support, patience and wait. For me all this is priceless. Thank you from the bottom of my heart!

Ross

Financial support:

This thesis was supported by the National Commision for Scientific and Technological Research (CONICYT- Beca para estudios de Doctorado para extranjeros en Chile), as well as the School of Engineering and the Research Vice-rectory (VRI) of Pontificia Universidad Católica de Chile.

LIST OF CONTENTS

PONTIFICIA UNIVERSIDAD CATOLICA DE CHILE

ESCUELA DE INGENIERIA

FIBRES AND POROUS SCAFFOLDS FROM ALGINATE

Thesis submitted to the Office of Research and Graduate Studies in partial fulfillment of the requirements for the Degree of Doctor in Engineering Sciences by

TERESA R. CUADROS

ABSTRACT

Structures constructed from gels may find various applications. This thesis proposes that it is possible to manufacture fibers and porous matrices based on alginate gels with enhanced properties and different potential uses. By varying the composition and/or processing techniques the microstructure and physical and mechanical properties of these structures may be tailor-made. The overall objectives of this thesis were to prepare homogeneous structures (fibers and porous matrices) based on the gelation process of alginate, to determine their properties, and to suggest applications in the biomedical and/or food fields. Calcium alginate fibers of continuous and uniform diameter were successfully produced using a microfluidic device and their mechanical properties studied within a range of concentrations of calcium and alginate. The tensile stress of fibers increased with Ca^{2+} up to a certain concentration (maximum of 1.41%) and then the value decreased. This seems to indicate that a determined number and size of binding sites was attained along the polymeric chains of alginate. Their mechanical properties were directly related to the number of "egg-box" crosslinks formed. Furthermore, a biopolymeric porous matrix (BPM) of calcium alginate/gelatin was created by the porogen-leaching technique. The process involves incorporating the porogen (aerated gelatin solution), molding, gelling the alginate, re-molding, leaching the gelatin, and

lyophilizing. Cylinders of BPM showed a relative density of 0.027 ± 0.002, a porosity of 97.26 ± 0.18%, an average internal pore size of 204 ± 58 μm, and enhanced mechanical properties, this is, an apparent Young's modulus around 4.0 MPa. Following the steps for preparing porous matrices, two types of BPMs were produced (A and B, leached and non-leached, respectively). Each type of porous matrix was prepared using 1.5%, 2.25% and 3.0% alginate (called 1, 2, and 3 respectively). Their physical, mechanical, microstructural, and rehydration properties were evaluated. The average sizes of the internal pores decreased from 380 ± 88 to 204 ± 58 μm as the concentration of sodium alginate increased from 1.5% to 3.0%, respectively (samples A). Within each stage of preparation of BPMs (wet, lyophilized and rehydrated), the concentration of alginate showed no influence on the volume, but did show effect on the apparent Young's modulus. The rehydration kinetics of BPMs (A and B) showed a similar behavior. On rehydration at different temperatures (20 to 50 °C) the volume slightly decreased, while the water absorption and apparent Young's modulus remained stable. The highest water uptake was exhibited by the BPM with 1.5% alginate (A1) and at 25 °C, which exceeded 16 times its dry weight. Moreover, as one of the possible applications, the BPM with 3% alginate (A3) was tested as a scaffold for cell culture (tissue engineering). *In vitro* cell culture tests, using mesenchymal stem cells held within the BPM, showed an excellent response to MTT (3-(4,5-dimethylthiazol-2-yl)-2,5-diphenyltetrazolium bromide) assays and expression of alkaline phosphatase. The BPM provide a suitable microenvironment for the seeding, adhesion, proliferation, and osteogenic differentiation of cells. BPMs are structures with controllable properties that can be used in various applications in biomedicine, pharmacology, foods, environmental engineering, among others.

Members of the Doctoral Thesis Committee:

José M. Aguilera

José M. del Valle

Carmen Saenz

Jorge Moreno

María del Pilar Buera

Cristian Vial

Santiago, January 2015

PONTIFICIA UNIVERSIDAD CATOLICA DE CHILE
ESCUELA DE INGENIERIA

FIBRAS Y ANDAMIOS POROSOS DE ALGINATO

Tesis enviada a la Dirección de Investigación y Postgrado en cumplimiento parcial de los requisitos para el grado de Doctor en Ciencias de la Ingeniería

TERESA R. CUADROS

RESUMEN

Estructuras construidas a partir de geles pueden encontrar varias aplicaciones. Esta tesis propone que es posible fabricar fibras y matrices porosas basadas en geles de alginato con propiedades mejoradas y para diferentes potenciales usos. Variando la composición y las técnicas de procesamiento, tanto las propiedades físicas, mecánicas y micro-estructurales de estas estructuras pueden hacerse a la medida. Los objetivos generales de esta tesis fueron preparar estructuras homogéneas (fibras y matrices porosas) basadas en el proceso de gelación del alginato, determinar sus propiedades y sugerir aplicaciones en los campos de la biomedicina y/o los alimentos. Fibras de alginato de calcio de diámetro continuo y uniforme fueron producidas con éxito utilizando un dispositivo de microfluídos y sus propiedades mecánicas fueron estudiadas dentro de un rango de concentraciones de calcio y alginato. El esfuerzo tensil de las fibras aumentó con la concentración del catión Ca^{2+} hasta una determinada concentración (máximo de 1,41%), a concentraciones más altas de calcio, la fuerza tensil de las fibras disminuye. Este máximo, parece indicar que un determinado número y tamaño de sitios de unión se alcanza a lo largo de las cadenas poliméricas. Las propiedades mecánicas del gel están relacionadas directamente con el número de reticulaciones o "caja-huevos" formados. Además, una Matriz Porosa Biopolimérica (BPM) de alginato de calcio/gelatina fue creada mediante la técnica porógeno-lixiviación. El proceso implica la incorporación del

porógeno (solución de gelatina aireada), moldeo, gelificación del alginato, re-moldeo, lixiviación de la gelatina y liofilización. Cilindros de BPM mostraron una densidad relativa de 0.027 ± 0.002, porosidad de 97.26 ± 0.18%, un tamaño de poro interno promedio de 204 ± 58 µm y propiedades mecánicas mejoradas, esto es, un módulo de Young aparente alrededor de 4.0 MPa y un esfuerzo elástico máximo alrededor de 0.4 MPa. Siguiendo las etapas de preparación de las matrices porosas, dos tipos de BPMs fueron producidas (A y B, lixiviadas y no-lixiviadas, respectivamente). Cada tipo de matriz porosa fue preparada utilizando 1.5%, 2.25% y 3.0% de alginato (llamadas 1, 2, y 3, respectivamente). Sus propiedades físicas, mecánicas, microestructurales y de rehidratación fueron evaluadas. Los tamaños medios de los poros internos disminuyeron de 380 ± 88 a 204 ± 58 micras conforme la concentración de alginato de sodio aumenta de 1.5% a 3.0%, respectivamente (muestras A). Dentro de cada etapa de preparación de BPMs (húmeda, liofilizada y rehidratada), la concentración de alginato no mostró influencia sobre el volumen, pero sí tuvo efecto sobre el módulo de Young aparente. Las cinéticas de rehidratación de las BPMs mostraron un comportamiento similar. En cuanto a la rehidratación a diferentes temperaturas (20 a 50 °C) el volumen disminuyó ligeramente, mientras que la absorción de agua y módulo aparente de Young permanecieron estables. La mayor absorción de agua fue exhibida por las BPMs con 1,5% de alginato (A1) a 25 ° C, las cuales superaron 16 veces su peso en seco. Además, como una de las posibles aplicaciones, la BPM con 3% de alginato (A3) fue probada como andamio para el cultivo celular (ingeniería de tejidos). Pruebas de cultivo celular *in vitro* utilizando células madre mesenquimales mantenidas dentro de la BPM, mostraron una excelente respuesta a los ensayos MTT y a la expresión de la fosfatasa alcalina. La BPM proporcionó un microambiente adecuado para la siembra, adhesión, proliferación y diferenciación osteogénica de las células. Las BPMs son estructuras con propiedades controlables que se pueden utilizar en diversas áreas de las ciencias como la biomédica, farmacología, alimentos, ingeniería medioambiental, entre otras.

Miembros del Comité de Tesis Doctoral:

José M. Aguilera

José M. Del Valle

Carmen Saenz

Jorge Moreno

María del Pilar Buera

Cristian Vial

Santiago, Enero 2015.

LIST OF PAPERS

The present thesis is based on the following papers:

Chapter II: Gels as precursors of porous matrice for use in foods: a review. 2015. Cuadros, T.R. and Aguilera, J.M. Food Biophysics Journal, DOI 10.1007/s11483-015-9412-5, In press.

Chapter III: Mechanical properties of calcium alginate fibers produced with a microfluidic device. 2012. Cuadros T.R., Skurtys O. and Aguilera, J.M. Carbohydrate Polymers, 89(4), 1198-1206.

Chapter IV: Porous matrix of calcium alginate/gelatin with enhanced properties as scaffold for cell culture. 2015. Cuadros, T.R., Erices, A.A. and Aguilera, J.M. Journal of the Mechanical Behaviour of Biomedical Materials, 46, 331-342.

Chapter V: Porous matrices of calcium alginate/gelatin at different concentrations and temperatures. Cuadros, T.R. and Aguilera J.M. F. To be submitted.

Proceedings

Topics of this thesis and other made during the doctoral studies have also been presented at one national congress and two international events under the following references:

Cuadros, T.R., Skurtys, O. and Aguilera, J.M. Study of mechanical behaviour of calcium alginate fibers by a microfluidic device. In: Proceedings of the First Congress of Engineering Graduate Students, Mayo 28, Santiago, Chile (2010).

Cuadros, T.R., Skurtys, O., Aguilera, J.M. Mechanical behaviour of calcium alginate fibers by a microfluidic device. In: 11th International Symposium on the Properties of Water. (Isopow 11), September 5-9, Querétaro, México (2010).

Cuadros, T.R. and Aguilera, J.M. Porous matrices as supports for design of functional foods. In: Proceedings of the Course Advanced in Molecular Structuring of Food Materials. SPSAS ESPCA/Sao Paulo, School of Advanced Science. Selection for funding was performed by Scientific Committee of the Sao Paulo School on Advanced Science, April 6-7, Sao Paulo, Brasil (2013).

1. INTRODUCTION

1.1. Structuring by gelation

Gels are soft solids that hold abundant water (e.g., >90%) on an occluded aqueous solution within a three-dimensional polymeric network formed by proteins or polysaccharides. Gelation is a mechanism that can be used to generate structures that cover a wide range of length scales and properties. Several mechanisms take place during gelation, and their relative kinetic will determine the final structure and related properties.

Fibers and porous matrices can be obtained by different procedures that cause the re-organization of the biopolymer chains and the modification of the structure formed. More information regarding the relationship between the molecular properties and the junction zones is required to better understand the mechanisms involved in the formation of the gel network and subsequently in the gel properties (Hermansson, 2009). For example, properties related to the model of the eggs-box for alginate gelation with bivalent cations (Morris, 1986) or related to triple threads in the gelatin gels (Djabourov et al., 1988), among others. Although most polysaccharide gels networks have similar length scales, the kinetics of formation of gels may be different with respect to the molecular composition for gel formation.

1.2. Structures based on biopolymers

Biopolymers have been widely used for the fabrication of structures with biomedical and food applications. Advances in materials science are providing a good understanding of material-structure and structure-property relationships, keys to the design and control of their global properties. For example, the design of scaffolds for tissue engineering with desired properties (that is, with certain properties, such as geometrical, physical, chemical and mechanical) for cell implantation, proliferation, guide and tissue organization (Bhattarai et al., 2006; Leong et al., 2003; Shoichet, 2010). A scaffold is a

3D support structure which provides the chemical, physical, and mechanical properties required for cell survival and tissue formation. Similarly, polymeric networks composed from fibers (micro and nano) may have applications in tissue engineering. The basic manufacturing process may involve stacking fiber-reinforced sheets into true 3D fibrillar composites.

Apart from the medical field, the manufacture of 3D micro-porous structures is attractive for incorporating new components of interest in foods, pharmaceuticals, biotechnology products, etc. Microstructure is the spatial arrangement of different elements of less than 100 μm, such as pores and micropores, protein assemblies polymer networks, fibers and fibrils, granules, crystals, oil droplets, gas bubbles, colloidal particles, etc. (Aguilera, 2005).

If the porous matrix or designed structure is homogeneous, resistant, and has interconnected micropores, it could offer the following convenient attributes: easy incorporation of micronutrients (in solution) and their protection, and then, improvement of nutrients release and increased access to enzymatic activity during the digestion of food.

1.3. Alginates

1.3.1. Background

In 1881 the English chemist E.C.C. Stanford obtained a gelatinous mass from the digestion of brown algae (*Phaeophyceae*) with sodium carbonate, which he called "algin". Today the algins or alginates are extracted by means of an alkali and then subjected to bleaching, filtration, precipitation, coagulation, neutralization, drying and grinding. Commercial production began in 1929 by the Kelco Company in California, and following World War II the alginate industry started to grow in Europe (United Kingdom, Norway, France), Asia (China, Japan), USA (California), Australia and South Africa. In South America, Chile is the largest producer of alginate.

Alginate is a component of the cell walls of brown algae and its structural function is to give strength and flexibility. These algae are photosynthetic organisms and are not yet

classified as true plants. There is a huge variety of species that vary in size, shape, proportion and quality of alginates produced. The alginate content is about 2.5-3.0% of the total weight of alga (as alginic acid and salts of sodium, potassium and calcium). Currently over 200 different types of alginate and another equal number of alginate salts are available in the market.

Alginates are linear unbranched polymers based on two monomer units, β-(1→4)-linked D-mannuronic acid (M) and α-(1→4)-linked L-guluronic acid (G). The classical formulas of the monomeric molecules are shown in Figure 1.1; while Figure 1.2 shows the three-dimensional arrangement of them.

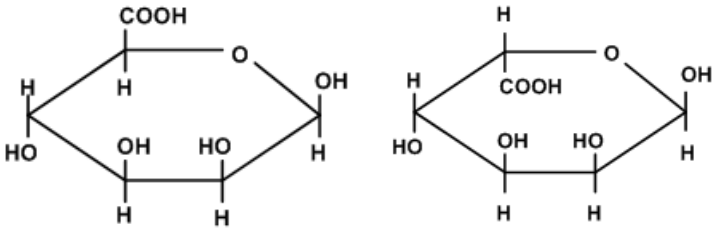

B-D-Mannuronic acid α-L-Guluronic acid

Figure 1.1. Classical formulas of the two monomeric units of the alginic acid.

The monomeric units are grouped into blocks of sequences MM, MG, linked by glycosidic bonds β-(1→4); and blocks GG, GM, joined by glycosidic bonds α-(1→4) (Figure 1.3). Each of these blocks has a different conformation and behavior. The alternate blocks occupy about 1/3 of chains, while polyguluronic blocks (GG) and polymannuronic (MM) change according to the species of algae. For example, an M/G ratio of around 1.5 has been found in *Macrocystis pyrifera* specie, while a ratio of 0.45 in the *Laminaria hyperborean* specie. Many domains of mannuronic acid (MMMMM) form elastic gels with low tendency to syneresis and ability to undergo deformation; whereas, many segments of guluronic acid (GGGGG), form stiff gels, with little binding of water and tendency to syneresis.

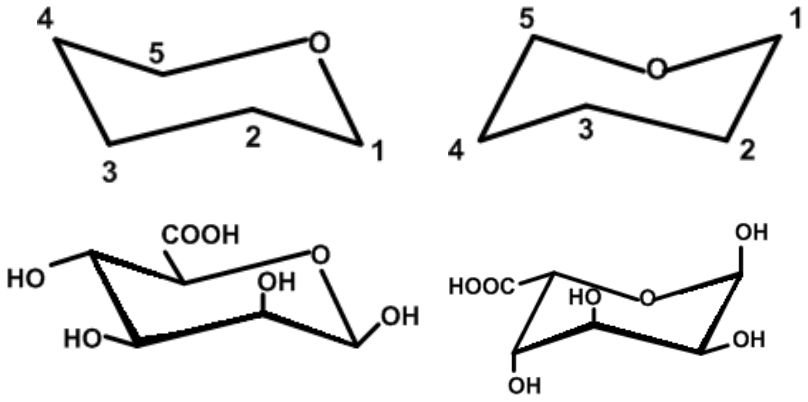

Figure 1.2. Chair conformations of the alginate monomers. Above: monomers are epimers and only differ at C_5. Down: D-mannuronic acid, M ($^4C_1$); and L-guluronic acid, G ($^1C_4$) of the tetrahydropyran ring.

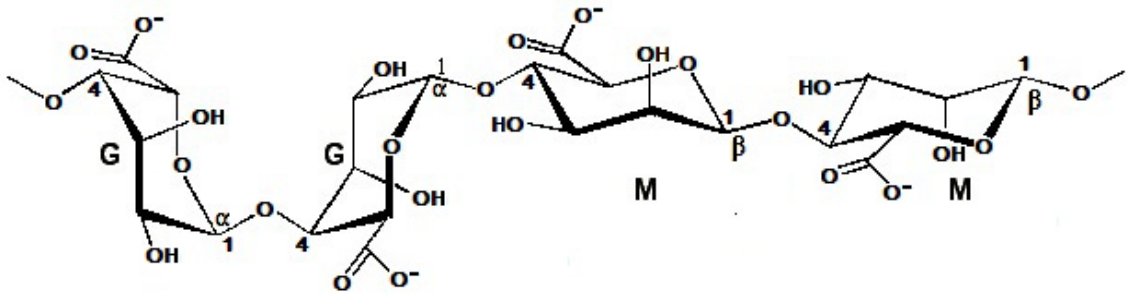

Figure 1.3. Linked monomers forming blocks G and M, poliguluronic and polimannuronic, respectively.

1.3.2. Physical and chemical properties

Sodium alginate as a dry powder stored in cool, dry place without sun exposure can have a shelf life of several months (i.e., temperature < 25 °C and moisture content between 10% and 13%). The Degree of Polymerization (DP) of the alginate gives the average molecular weight (MW) and corresponds to the number of uronic acid units in the polymer chain. Compounds with high DP are less stable than those with low DP. The

solubility of alginate powders in water depends on the particle size. Small particles will hydrate more quickly but with agglomeration (clumping), while large particles have a low rate of hydration but are usually more readily dispersed. Sodium alginate is one of the soluble forms most used in the food industry, whereas the calcium alginate is the form most used for gelation.

Solubilizing alginate is difficult if it occurs in presence of other compounds that compete for water molecules (e.g., proteins, starch, sugars, and salts of monovalent cations), so it is recommended to add the other components after alginate hydration. In presence of small amounts of polyvalent ions the hydration of alginates is inhibited and when present in large quantities lead to the precipitation of alginates. Sodium alginate is barely dissolved in hard water and milk due to the presence of ions which must be sequestered with sodium hexametaphosphate or ethylenediamine tetraacetic acid (EDTA) (Draget et al., 2006). Also, alginates are insoluble in aqueous solutions of alcohols and ketones. The glycosidic linkages are susceptible to both acid and alkaline degradation and oxidation by free radicals (Draget, 2000).

The viscosity of alginate solutions is important as it allows their use as thickeners, stabilizers, gelling agents, etc. The viscosity of sodium alginate solutions is almost independent of pH in the range between 5 and 10, showing higher stability while it is closer to neutrality (pH 6-8) because the molecule is extended by the repulsive effects of negatively charged carboxylic groups (COO^-). The viscosity of solutions decreases approximately 2.5% per degree of temperature increase. The process is reversible and the initial viscosity is recovered by cooling. If alginate solutions are kept at high temperature for extended periods, the viscosity decreases irreversibly due to depolymerization.

1.3.3. Alginate gel formation

The alginate gel is a network of stiff molecular chains (Draget et al., 2006). Polymannuronic segments do not have affinity for divalent cations; this is a property exclusive of the poliguluronic domains (Braccini and Pérez, 2001) (Figure 1.4). The

alginates (Alg) affinity for polyvalent cations, mainly calcium, occurs by an ion-exchange crosslinking reaction.

$$2\ AlgNa + Ca^{2+} \leftrightarrow Alg_2Ca + 2Na^{+}$$

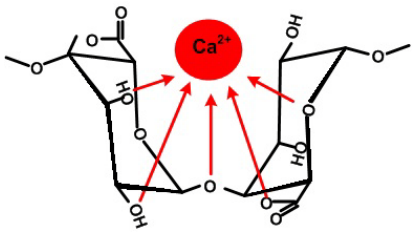

Figure 1.4. Probable chelation of ions by the -GG- blocks.

When calcium chloride is introduced into a solution of sodium alginate, a gel or precipitate is formed instantaneously. A rapid, strong and irreversible formation of junction zones in the gel occurs. This high rate of gelation makes it difficult to produce homogeneous gels free of lumps (known as fisheyes), even with high-speed stirring (Draget, 2000).

Alginates with a high content of guluronic acid are sensitive to changes in the strength of the alginate gel network, whereas alginates with a high content of mannuronic are not sensitive to such changes (Simpson et al., 2004). The strength of the alginate gel network is an important factor that influences, e.g., the protection of encapsulated components of interest or the growth of encapsulated cells. In general, the elastic modulus of an alginate gel depends on the number and strength of the cross-links and on the length and stiffness of the chains between cross-links. However, “it is still unclear whether the increase in elastic modulus is caused by a higher strength of the junction zones or if it is caused by a larger number of junction zones” (Draget et al., 2006).

1.3.4. Potential applications

Potential applications of alginate gels currently focus on the development of scaffolds for tissue engineering such as promotion of the culture, growth, and proliferation of, e.g.,

nerve (Pfister et al., 2008), bone (Eslaminejad et al., 2007), wound healing (Pereira et al., 2013) and the development of systems of controlled drug delivery and/or bioactive compounds because of its resistance (including heat resistance), non-toxicity, and biocompatibility.

1.4. Hypothesis and objectives

Hypothesis

It is possible to manufacture fibers and porous matrices based on alginate with tailor-made properties suitable for different applications. This can be accomplished by manipulating the composition of the gelling mixture, concentration of the gelling agent, the use of co-agents, and application of processing techniques.

Objectives

The overall objective of this thesis was to prepare homogeneous structures (fibers and porous matrices) based on alginate, to determine their properties, and to suggest applications in the food and biomedical fields.

1.5. Structure of the thesis

A general outline of this thesis is summarized in Figure 1.5, which considers Paper 1 to 4. Papers 1 to 3 are published while Paper 4 is written and prepared for publication (in Food Hydrocolloids).

Paper 1 reports an extended literature review on gelation of alginate and utilization of gels. The manufacture of calcium alginate fibers and their mechanical properties is detailed and discussed in Paper 2. The study of the effects of sodium alginate and calcium chloride concentrations were the basis to understand (a little more) the gelation

of alginate and it was the key in the preparation of the porous matrices with a maximum gel strength (Paper 3).

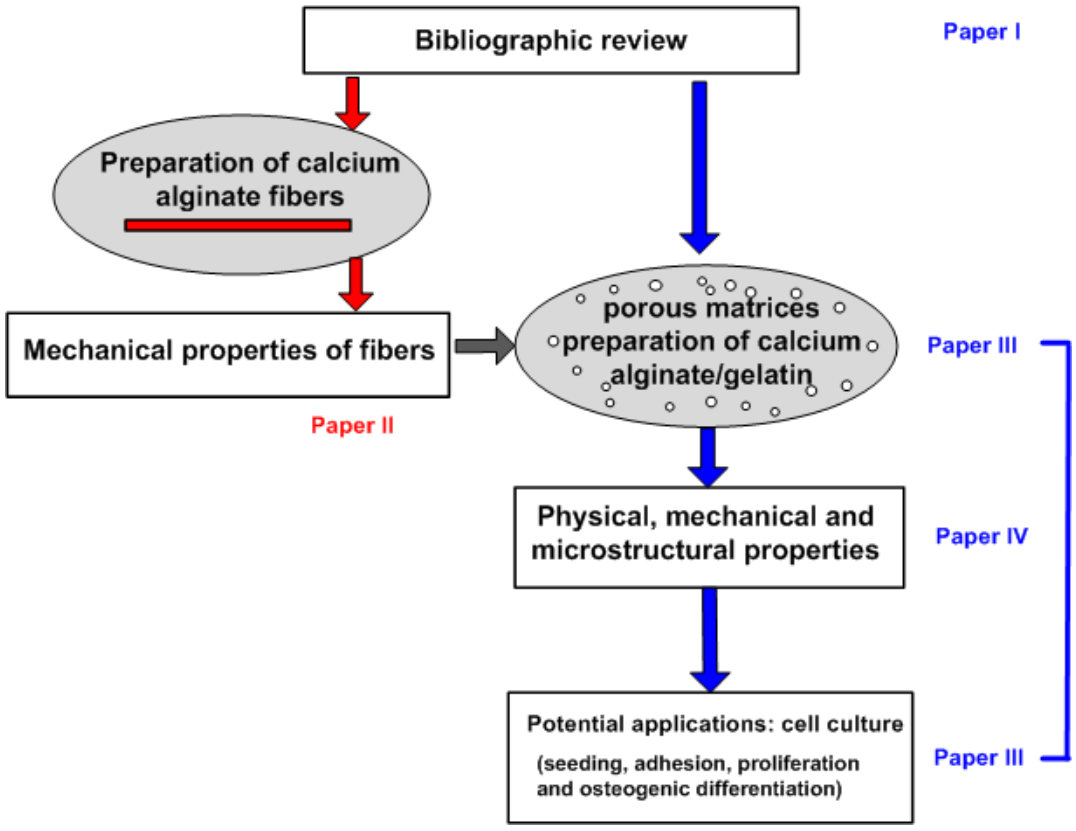

Figure 1.5. Overview of the procedure followed through this thesis and the relationship of the annexes or papers that form.

Paper 3 describes in detail the proposed method for preparing a biopolymeric porous matrix (BPM) of calcium alginate/gelatine with enhanced physical, mechanical, and microstructural properties, and their functionality as scaffolds for cell culture. Paper 4 describes the properties and behaviour of the porous matrix at different stages of preparation and under different formulations.

1.6. Conclusions and future work

1.6.1. General conclusions

- ✓ Non-porous (fibers) and porous (scaffolds) structures were fabricated using alginate as gelling material. Their physical, mechanical and microstructural properties were improved and could be tailored by varying the concentration of alginate, calcium chloride and modifying the preparation procedure.
- ✓ The tensile strength of calcium alginate fibers could be varied up to a maximum value when calcium chloride concentration was 1.41% (0.127 M). This value is several times the stoichiometric requirement to saturate the polymer's carboxyl groups.
- ✓ Biopolymeric porous matrix (BPM) were prepared by a unique top-down technique using aerated gelatin as porogen (scaffold). This is a relatively simple procedure to produce porous matrices with controlled pore size with enhanced physical, mechanical and microstructural properties. BPMs lyophilized samples prepared at different alginate concentrations 1.5%, 2.25% and 3.0% showed pore sizes in a range of 400 to 200 µm, high porosities between 98% to 96.5% and the water absorption was 8 to 16 times its dry weight. Also, there is a direct relationship between the alginate concentration and apparent Young's modulus.
- ✓ Finally, obtained matrices were tested as scaffolds in tissue engineering and provided an excellent environment for MSCs cell culture, adhesion, growth, proliferation and differentiation in osteogenesis.

1.6.2. Future studies

- ✓ In the case of fibers other food biopolymers may be used as raw materials.
- ✓ With respect to BPMs other types of cells may be analyzed for growth and stability. Also BPMs could be investigated as support and delivery systems for drugs and bioactive compounds.

References

Aguilera, J. M. (2005). Why food microstructure? *Journal of Food Engineering, 67*, 3-11.

Bhattarai, N., Li, Z., Edmondson, D. and Zhang, M. (2006). Alginate-based nanofibrous scaffolds: structural, mechanical and biological properties. *Advanced Materials, 18*, 1463-1467.

Braccini, I. and Pérez, S. (2001). Molecular basis of Ca^{2+}-induced gelation in alginates and pectins: the egg-box model revisited. *Biomacromolecules, 2*(4), 1089-1096.

Djabourov, M., Leblond, J. and Papon, P. (1988). Gelation of aqueous gelatin solutions. I. Structural investigation. *Journal Physics (Paris), 49*, 319-332.

Draget, K. (2000). Alginates. In G. O. Phillips and P. A. Williams (Eds.). *Handbook of Hydrocolloids* (Cap. 22). Cambridge, Woodhead Publishing Limited.

Draget, K., Moe, S., Skjak-Braek, G. and Smidrod, O. (2006). Alginates. In A. M. Stephen, G. O. Phillips and P. A. Williams (Eds.). *Food Polysaccharides and Their Applications* (pp. 289-334). Boca Raton, FL, CRC Press.

Eslaminejad, M., Mirzadeh, H., Mahamadi, Y. and Nickmahzar, A. (2007). Bone differentiation of marrow-derived mesenchymal stem cells using *B*-tricalcium phosphate-alginate-gelatin hybrid scaffolds. *Journal of Tissue Engineering Regenerative Medicine, 1*, 417-424.

Hermansson, A.-M. (2009). Structuring water by gelation. In J. M. Aguilera and P. J. Lillford (Eds.). *Food Materials Science: Principles and practice* (pp. 255-280), Springer.

Leong, K. F., Cheah, C. M. and Chua, C. K. (2003). Solid freeform fabrication of three-dimensional scaffolds for engineering replacement tissues and organs. *Biomaterials, 24*, 2363-2378.

Morris, E. R. (1986). Molecular interactions in polysaccharide gelation. *British Polymer Journal, 18*, 14-21.

Pereira, R., Carvalho, A., Vaz, D. C., Gil, M. H., Mendes, A. and Bártolo, P. (2013). Development of novel alginate based hydrogel films for wound healing applications. *International Journal of Biological Macromolecules, 52*, 221-230.

Pfister, L. A., Alther, E., Papaloïzos, M., Merkle, H. P. and Gander, B. (2008). Controlled nerve growth factor release from multi-ply alginate/chitosan-based nerve conduits. *European Journal of Pharmaceutics and Biopharmaceutics, 69,* 563-572.

Shoichet, M. S. (2010). Polymer scaffolds for biomaterials applications. *Macromolecules, 43,* 581-591.

Simpson, N. E., Stabler, C. L., Simpson, C. P., Sambanis, A. and Constantinidis, I. (2004). The role of the $CaCl_2$-guluronic acid interaction on alginate encapsulated BTC3 cells. *Biomaterials, 25,* 2603-2610.

Paper 1

Gels as Precursors of Porous Matrices for Use in Foods: A Review

Data on manufacture of porous matrices.

Food Biophysics
DOI 10.1007/s11483-015-9412-5

REVIEW ARTICLE

Gels as Precursors of Porous Matrices for Use in Foods: a Review

Teresa R. Cuadros[1] · **José M. Aguilera**[1]

Received: 25 January 2015 / Accepted: 4 August 2015

Abstract Gelation is a structuring mechanism commonly used in foods to produce soft and homogeneous structures. Techniques applied in other areas of science (e.g., bioengineering, biotechnology and electronics) aims at producing wet and dried porous gel matrices and they may find applications in foods. This review describes several processes to manufacture porous structures such as scaffolding, ice templating, use of porogens, oleogelation, incorporation and entrapment of bubbles, enzymatic modifications, microfluidics and microfabrication techniques, among others. Several examples are also presented. Beyond textural properties, porous gels and sponges may be tailored in their mass transfer characteristics to achieve specific rates of release of bioactive molecules, nutrients and flavors.

Keywords Food gels · Porous solids · Cellular solids · Hydrocolloids · Microstructure

Introduction

Food microstructure may be defined as the spatial arrangement of identifiable elements in a food unseen by the naked eye and the interactions among them that relate to some of its properties [1]. Similarly, the concept of "food matrix" points to the fact that food components are usually arranged as microstructures that may be of natural origin (e.g., tissue or cellular matrices) or created by processing (e.g., gels, emulsions, foams, etc.).

A gel is a colloidal system in which the continuous phase is a network swollen by a liquid. Gels are ubiquitous structures in high-moisture foods, having densities and transport properties similar to liquids and mechanical responses that resemble those of soft solids. Many food biopolymers form gels through two main mechanisms. Some gels are formed from disordered biopolymer molecules (e.g., carrageenan, alginate, pectin, gelatin, etc.) cross-linked or entangled at a few points to avoid slipping of the chains. Other gel networks involve specific local interactions between long chains of aggregates (e.g., those of thermally denatured globular proteins and casein) leading to a permanent 3D structure [2, 3]. The food industry has used proteins and polysaccharides for many years as structuring agents to immobilize large quantities of water at room temperature in the form of gels [1, 3, 4]. This ample availability of edible gelling materials offers opportunities for the design of high-moisture structures with tailored properties, both in industry and in gastronomy [5].

Highly porous sponges of biodegradable polymers are frequently utilized in areas such as tissue engineering or medical technology to replace damaged organs or tissues, in the transplant of cells or as a template for tissue regeneration [6–9]. Several techniques described in the literature refer to porous or "cellular solids" from hydrocolloids [10, 11]. Some of the architectures that can be achieved in porous gels representing different designs and key structural elements are shown in Fig. 1: (a) channels [12]; (b) pores [8]; (c) scaffolds [13]; (d) micro-honeycombs [12]; (e) irregular pores [14]; (f) interconnected pores [15]; (g) microporous spheres [16]; and (h) microbubbles [17].

This paper reviews the formation of porous gel matrices and sponges based on biopolymers that are employed mostly in fields of science other than foods and describes some

✉ Teresa R. Cuadros
tcuadroc@uc.cl

[1] School of Engineering, Department of Chemical and Bioprocess Engineering, Pontificia Universidad Católica de Chile, P.O. Box 306, Santiago 22, Chile

Published online: 13 August 2015

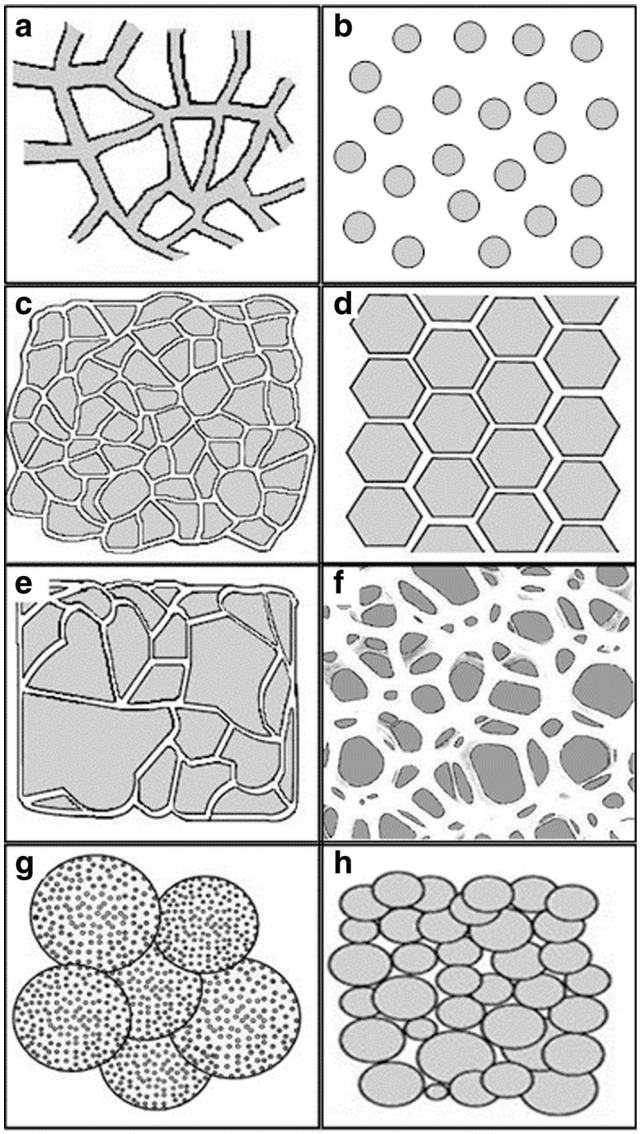

Fig. 1 Diagrams of some architectures of porous gels representing different designs and structural elements (*shaded areas* represent voids): **a** channels, **b** closed air cells, **c** scaffolds, **d** micro-honeycomb, **e** irregular pores, **f** interconnected pores, **g** micro-porous spheres, **h** micro-bubbles

relevant structural features. Some of the techniques are presented and potential applications of modified gel structures in food are discussed.

Description and Classification of Manufacturing Techniques of Porous Matrices

Three criteria were used to classify the manufacturing techniques leading to porous gel matrices, namely, the type of process (top-down or bottom-up), the number of chemical components (excluding water) intervening in structure formation, and whether pores were formed before or after gelation (Fig. 2). Top-down techniques are conventional methods where the porous gel structure is formed in bulk and in a single step. However, they may involve some post-production procedures such as washing and freeze-drying. As a result, pore size and interconnectivity are neither well controlled nor designed. On the contrary, the bottom-up approach tries to control structure formation starting at the nano- or micro-scales, through sequential stages of fabrication until a final structure is achieved. For example, bottom-up techniques to obtain highly organized 3D scaffolds [18] may include the use of 3D printing [19], laser micro-stereolithography (SL), photolithography patterning and multilayering. The physical characteristics of these scaffolds, such as porosity and interconnectivity, can be tailored by precise control of the architecture, distribution and geometry of the pores, and will influence the mechanical and transport properties. Microfabrication technologies have emerged from the automotive, microelectronics and aerospace industries and are being transferred to the biological sciences and bioengineering. Despite these significant advantages over conventional top-down methods, the bottom-up techniques may involve expensive robotic control and often time-consuming pixel-by-pixel programming [18].

A second way of classification refers to the number of compounds (excluding water) used in the process. Some techniques describe the use of up to three compounds (e.g., biopolymer, cross-linking agent and a gas) while most of them use more than three compounds.

A third mode of classification looks at whether the pores are promoted before or during gelation or after formation of the gel matrix. The most common pre-gelation pore-forming techniques include all methods of air (or gas) incorporation to the parent solution or suspension. Examples of techniques applied after gel formation are washing of porogens, all forms of drying or removal of separated phases and breakdown of the structure through the action of enzymes. A simple schematic of this third category is shown in Fig. 3 which illustrates some techniques used before and after gelation, for example: (a) setting the pores by lyophilization [15], (b) increasing the size of existing pores through enzymatic action [10] and, (c) the incorporation of sugar crystals as porogens followed by leaching [20].

Techniques most commonly reported in the scientific literature and patents are top-down and those that use multiple compounds. A large number of procedures have found applications in tissue engineering, with a smaller number developed for pharmacology, foods and biotechnology, probably because they involve the use of potentially toxic chemical compounds (e.g., solvents). The use of these compounds requires excessive washing of scaffolds, usually first with ethanol-water and then with copious amounts of water [19, 21, 22]. Washing is also done to adjust the pH of the porous matrix. After these long washing processes, additional tests are required in order to ensure complete removal of any toxic organic solvent or reagent [23–25]. For example, some techniques that utilize

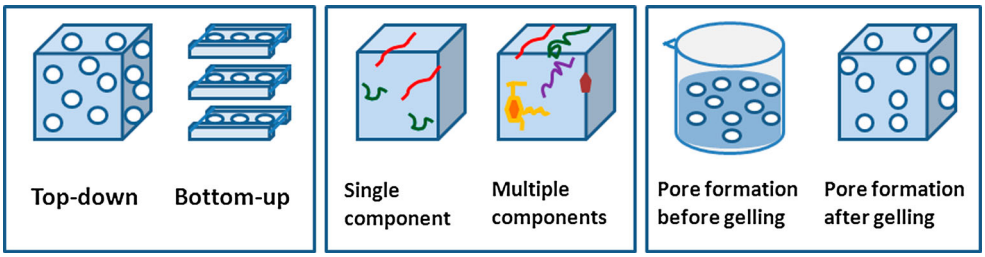

Fig. 2 Classification criteria for techniques used in manufacturing porous gel matrices reported in the literature

gelatin for scaffold manufacturing involve chemical cross-linking to stabilize the lateral functional groups between the protein chains ("hardened gelatin"). Among cross-linking agents reported in the literature are glutaraldehyde (GTA) [22, 26], *N*-(3-dimethylaminopropyl)-*N*'-ethylcarbodiimide hydrochloride (EDC) [22], tripolyphosphate (TPP) [22], *N*-hydroxysuccinimide (NHS) [27], diisocyanates, polyepoxy compounds, acyl azides and molecules with methacrylamide side groups [19, 28]. GTA is the most widely used compound due to its high levels of efficiency, though it does show local toxicity and subsequent calcification in long-term implants for tissue engineering [22, 28, 29].

Compounds that are added to create pores in the gel structure are called porogens and include sucrose crystals [20], sodium chloride [30] and other salt crystals, starch [31], lipids [10] and wax particles [24]. For example, crystals of calcium salts have two functions in alginate gels: as a porogen and as reacting internal gelation agent (e.g., $CaCO_3$ in D-glucono-δ-lactone induced gels). Sedimentation problems of the porogen leading to uneven distribution of pores [32] have been solved by preparing thin sheets (1–2 mm thick) to facilitate the uniform dispersion and removal of the porogen or residual salt crystals while forming the pores [20] followed by stacking of the sheets into 3D structures. Something similar happens when starch is added as a porogen and later subjected to the action of the enzyme α-amylase. Initially the enzyme breaks down starch located on the surface of the gel and a longer the exposure to the enzyme increases the size of surface pores [10]. There may also be a physical interaction between particles of the porogen left in a gel and the biopolymer network. The presence of residual particles or their debris may affect the rheological properties of the gel matrix depending on their nature, concentration and degree of interaction with the matrix [33, 34].

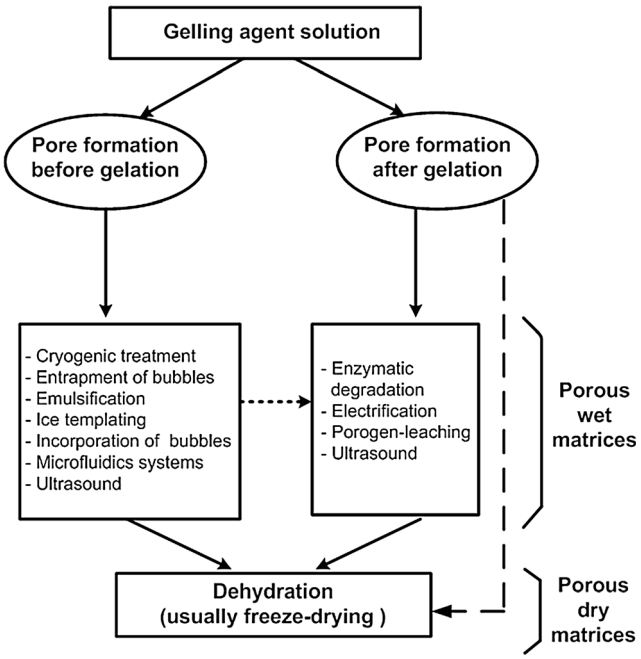

Fig. 3 Manufacturing techniques of porous matrices based on whether pore formation occurs either before or after gelation

Manufacture of Porous Matrices

Table 1 shows in alphabetical order a list of the techniques commonly used in the preparation of porous gel matrices. Some of these techniques are described below.

Ice Templating

Recently, great attention has been paid to ordered porous materials with micro-/mesopores that can be used as absorbents, separation materials, or catalyst supports in applications ranging from water treatment to microdevices for analytical techniques [49]. The performance of these materials is strongly influenced by porosity and the morphology of the porous structure. The majority of materials with ordered macropores are synthesized using a 'sacrificial' template (e.g., from phase-separated polymer solutions [13, 22], colloidal crystals [66], and microemulsions [67]) around which the skeletal material is formed. A template is a temporary medium responsible for formation pores or interstices in the resulting matrix. It is then removed using a physical and/or chemical treatment and the voids become the macropores. Some templates may take the form of polymer lines (nylon) to create microvasculature in vitro [75]. Unique materials with ordered macropores may be obtained through such templating methods, although they present several drawbacks. First, the templates used are in most cases expensive and second, the removal process generally requires extreme conditions such as high or low pH and/or high temperatures.

Table 1 Techniques used in the manufacture of porous matrices from gels (alphabetical order)

Description of the techniques	See also section
Centrifugal force. Gelation under the action of a centrifugal force. The gel morphology can be manipulated by controlling the rotational speed and formulation. Gels formed are multilayered and stable [14, 35].	Centrifugal force
Cryogenic treatment or freezing regime. Gels are formed after phase separation between the non-frozen liquid phase and the growing ice crystals [13, 22, 25, 36, 37]. The biopolymer concentration, cooling rate and the applied temperature gradient have large effects on the pore size and geometry.	Scaffold techniques
CTD (computational topology) or **CAD** (computer-aided) **design**. Structures are built layer-by-layer and the 3D scaffolds are constructed by stacking these monolayer structures [26, 38]. These systems may include a bioplotter, which is a commercial machine developed to "print" a range of biomaterials.	Scaffold techniques
Electrification. Consists of subjecting dried gels to direct current (DC). The porous structures exhibit a slight increase in internal surface and surface porosity, but are basically similar to the non-treated material [39].	Electrification
Electrospinning. Various macromolecules are electrospun into ultrafine fibers as thin as several nanometers and later formed into a mat or fibrous matrix. Polymer properties such as molecular weight, viscosity, conductivity and surface tension are important parameters as well as electrospining conditions such as applied electric voltage, tip-to-collector distance, etc. [40–42].	
Entrapment of gases. Involve the dispersion of gas usually generated by chemical reactions. This causes the formation of bubbles and the expansion of the volume of the product [43].	Incorporation and entrapment of bubbles
Enzymatic action. The enzyme decomposes starch (used as porogen) on the gel surface causing the enlargement of pores. Longer exposure to the enzyme action leads to larger surface pores, contributing to a change in the mechanical properties of the sponges [10, 44].	Enzymatic action
Freeze-drying. A simple technique used to fabricate porous scaffolds from almost any gelled material. Water is sublimated from the frozen gelled system, maintaining good retention of structure. 3D sponges may be prepared by a three-step procedure: i.e., gelation (crosslinking), freezing, and removal of the ice crystals by sublimation [13, 15, 36, 45].	Scaffold techniques
Freeze-fixation and freeze-gelation. A porous structure is generated during freezing of a polymer solution, followed by solvent extraction or the polymer is gelled under freezing conditions [22, 46].	Scaffold techniques
FDM (fused deposition modeling)**.** Employs melt extrusion to form successive parallel layers of material. It is possible to change the direction of material deposition and generate controllable pore morphologies and complete pore interconnectivity [47].	
Gluten Structures. Heated viscoelastic doughs and their mixtures can result in a variety of bi- and tri-dimensional sponges with different physico-chemical, rheological, and mechanical properties [48].	Gluten structures
Ice templating. Ice crystals are easy to form and can be removed by simply thawing and drying the material. They provide unique porous materials with ordered morphology. Cryogels structures varied depending on freezing conditions and gave well-defined microhoneycomb structures [12, 49].	Ice templating
Incorporation of bubbles. Bubbles can be dispersed in the bulk of liquid solutions or a viscous dispersion by several mechanisms [50]. For example, the incorporation of a high pressure gas to produce porous hydrogels [8, 17, 51–54].	Incorporation and entrapment of bubbles
Microfluidic systems. Highly monodisperse drops or bubbles are generated in fine capillaries and may be deformed by forcing them through a narrow channels of different geometries [55, 56]. The application of microfluidic devices and porous membranes to incorporate microbubbles (i.e., diameters$<$100 μm) is a subject of intensive research [5, 57, 58].	Microfluidic systems
Oleogels. An oleogel is obtained when a liquid oil phase is entrapped within a structure such as a biopolymer network [59]. For example, edible oleogels were prepared using a combination of water-soluble food polymer (e.g., methylcellulose and xanthan gum mixture) [60]. The result is a structured matrix with a high liquid oil content (>97 wt%) solid [61].	Oleogels
Polymerization. Hydrogel formation is performed by polymerization of modified polymers in aqueous solution by thermal or photochemical methods. For example, a series of methacrylate derivatives of dextran, functionalized dextrans and hyaluronan were synthesized by reaction with glycidyl methacrylate. Then, porous hydrogels were fabricated by adding a porogen to the curing mixture and leaching after polimerization [62].	
Porogen-leaching. Uses a particulate porogen, such as crystals of sucrose [20, 62], sodium chloride [30, 63] or calcium carbonate added to the polymer solution, which are leached or dissolved after hydrogel formation.	Scaffold techniques
SFF (Solid freeform fabrication)**.** Structures are built layer-by-layer and the 3D scaffold is then constructed by stacking these monolayer structures [26]. SFF is also known as rapid prototyping. Three SFF techniques have been extensively researched: three-dimensional printing (3DP), fused deposition modeling (FDM), selective laser sintering (SLS).	Scaffold techniques
SL (Stereolithography) or **PSL** (projection stereolithography)**.** Microfabrication technique based on computer aided design (CAD) [26] and used to design intricate [19, 64] that can mimic the microarchitecture of tissues.	Scaffold techniques
SLS (selective laser sintering)**.** Employs a laser beam to selectively sinter polymers or composite powders to form layers of materials. The laser beam is directed by a high precision laser scanning system [47].	
Sacrificial template. Materials with ordered macropores are synthesized using a "sacrificial≅template (e.g., from phase-separated polymer solutions [65], colloidal crystals [66] or microemulsions [67]). The template is removed by physical and/or chemical treatment and the voids formed become the macropores.	Scaffold techniques

Table 1 (continued)

Description of the techniques	See also section
TIPS (thermally induced phase separation) [36, 68, 69]. In this technique the solution temperature is lowered to induce phase separation of the homogeneous polymer solution into a continuous phase and a solvent-rich phase which is usually removed by freeze-drying.	Scaffold techniques
Three-D printing [47, 70, 71]. Freeform fabrication method that uses an ink-jet type of printing head to dispense powders or melts according to a CAD program. 3DP has been used to directly print porous scaffolds with designed characteristics (shape, interconnected porosity and controlled chemistry) [72] with predefined multilevel internal architectures via stacking monolayer structures.	Scaffold techniques
Ultrasound [73]. Is a commonly used method for the generation of microbubbles. The interaction of ultrasound with solid–fluid interface can produce a micro-stirring in the fluid [74].	Ultrasound

Toxicity problems may be overcome by using ice crystals as the template. Freezing leading to ice crystal formation is a relatively low-cost process and ice can be removed by simply thawing or freeze-drying the frozen material. An ice template may be produced in two ways: freeze-gelation and unidirectional freezing. It has been found that the morphology can change from microhoneycombs to polygonal fibers, passing through intermediate morphologies (lamella sheets, flat fibers), as is commonly found in silica and resorcinol-formaldehyde sol–gel systems [12, 49, 76]. At the start the hydrogels presented a micro-honeycomb structure and when hydrogels were frozen unidirectionally microfibers with polygonal cross sections were obtained [76] (Fig. 1-d). The cell size (micro/meso/macroporosity) of micro-honeycombs can be controlled by changing the freezing conditions (e.g., immersion rate and temperature) [12]. Micro-honeycombs and polygonal fibers morphologies may be simple to achieve in some small foods since freezing is a widely used preservation process.

Scaffold Techniques

In tissue engineering, scaffolds act as an analogue of the extracellular matrix, providing physical support for cell growth by means of a suitable porous structure that is biocompatible and biodegradable [51]. The scaffolds should have high porosity, large surface area, suitable pore size, and a highly interconnected pore structure.

Freeze-drying is the simplest technique to produce porous scaffolds (Table 1). Three-D sponges may be prepared using a three-step procedure consisting of gelation (cross-linking) of a solution to form a hydrogel, followed by freezing and finally removal of the ice crystals by sublimation [13, 15, 36, 45]. Other methods reported for the production of porous scaffolds include porogen leaching [22, 38, 62, 63, 77–79], saturation and release of CO_2 [6, 80], 3D printing [38, 70, 71, 81], formation of microemulsions and phase separation techniques [68, 82].

Porous hydrogels are produced using porogen-leaching (Table 1) by adding a particulate porogen (e.g., sucrose crystals) to the mixture and leaching out the porogen after the hydrogel is formed [20, 62]. Paraffin spheres were used as porogens to fabricate biodegradable poly(D-L-lactic-co-glycolic acid) porous scaffolds with potential use in tissue engineering or in situ tissue induction [63]. The pore structure, pore size, and density were easily changed by controlling the properties and content of the porogen. 3D hydrophilic gels based on poly[2-hydroxyethyl methacrylate] were designed as scaffolds for the regeneration of soft tissues, e.g., nerve tissue [79] with anisotropic macropores of sizes ranging from 10 to 50 μm using fibers of organic poly(*L*-lactide) as porogen.

In tissue regeneration the scaffold design must meet complex 3D anatomical shapes. Advances in both computational topology design (CTD) and solid free-form manufacturing (SFF) or structures built layer-by-layer, have made it possible to create scaffolds with controlled architectures [38]. Biodegradable polymers are preferred over synthetic polymers matrices because they disintegrate or bioresorb once they have served their purpose while contributing to in situ formation of the natural tissue structure. Another method used to produce scaffolds is thermally-induced phase separation (TIPS) [36, 68, 69]. In this technique the temperature is lowered to induce phase separation of the polymer solution. Phase separation may occur by liquid-liquid demixing or solid–liquid demixing. In the first case a polymer-poor phase becomes dispersed in a polymer-rich liquid phase and is later removed to originate the pores. If the temperature is low enough to allow freezing of the solution, the phase separation mechanism would be solid–liquid demixing, consisting in a frozen solvent phase and a concentrated polymer solution. Solvent removal is critical to retain the porous structure, therefore, sublimation is usually used for solvent removal, otherwise, a rise in temperature during the sublimation stage could result in remixing of the phase- separated solution or melting of the frozen solution. Depending on the polymer concentration, type of solvent, or cooling rate, phase separation takes place via different mechanisms resulting in scaffolds with various morphologies [9, 83].

Freeze-fixation and freeze-gelation can be used to prepare highly porous scaffolds ("Ice templating" section). The porous structure is generated during freezing of a polymer

solution, after which the solvent is extracted by a non-solvent or the polymer is gelled under freezing conditions. This requires that the porous structure is not destroyed during any subsequent drying stage. These methods are time- and energy-saving compared to freeze drying, leave less residual solvent, and are easier to scale up [9]. In a freeze-gelation method for fabricating porous chitosan scaffolds for tissue engineering applications the scaffolds were cross-linked using glutaraldehyde (GTA), N-(3-dimethyl-aminoprophil)-N'-ethylcarbodiimide hydrochloride (EDC), or tripolyphosphate (TPP) [22]. Mechanical properties significantly increased with the addition of the cross-linking agent GTA but not as much by the addition of EDC and TPP. The fabrication of a novel 3D chitosan/gelatin scaffold with predefined multilevel internal architectures combined SFF, microreplication and lyophilization techniques [26, 38]. A computer model of the scaffold was designed incorporating biological data such as branching angle of the liver vascular system [26]. Stereolithography, a type of SFF technique was utilized to build a resin mould based on poly-dimethylsilicone (PDMS) and produced by microreplication. A chitosan/gelatin mixture solution was then cast onto the PDMS mould prior to freezing and the monolayer porous structures with organized internal morphology were obtained upon lyophilization. Then, 3D structures are assembled by staking monolayers of 2D structures [26].

Some of the components used in the construction of biological scaffolds are not permitted in food manufacturing but it is up to the food technologist to investigate which food-grade materials could be used as appropriate substitutes.

Gluten Structures

Wheat gluten proteins in the absence of plasticizers are fragile and become difficult material to process and handle [84]. They can be thermally processed using plasticizers, commonly water, and bubbles are formed during heating by steam generation and air expansion. The addition of polysaccharides usually enhances the functional properties of gluten protein matrices acting as fillers or interacting with protein molecules in different ways depending on the load and degree of aggregation of the protein. This results in a variety of bi- and tri-dimensional structures with different physico-chemical, rheological and mechanical properties [48]. For example, the mechanical properties (e.g., tensile strength, elastic modulus) were enhanced with the addition of methylcellulose to wheat protein and the glass transition temperature of the wheat gluten matrix was increased [85]. In wheat gluten-chitosan mixtures the extensibility, toughness and water solubility improved with increasing chitosan content [86]. The addition of tannins promoted the polymerization of gluten proteins, modified the secondary structures of the gluten network, and improved the dough mixing time and strength [87]. Gels of protein-polysaccharide complexes are more effective than single protein or polysaccharides gels because covalent bonds may be formed between branching monosaccharides and amino acid residues [88]. NaCl increased the non-covalent interactions and β-sheet structure formation in gluten proteins [89] and it was observed by microscopy (SEM and CLSM) that it induced a more marked cross-linking and orientation of the gluten network while the addition of hydrocolloids led to more open matrices [90].

Incorporation and Entrapment of Bubbles

Semi-solid foams have important applications as food products and in gastronomy (e.g., cakes, marshmallows, soft meringues, mousses, etc.). Introducing a dispersed gas phase into a food matrix affects its texture and firmness, making the product softer and lighter, changing its appearance, color, and mouth-feel [91]. Bubbles in semi-solid foods are initially dispersed in the bulk of a liquid solution or a viscous dispersion through a variety of mechanisms, and the final structure is achieved by gelation [52]. Entrapment of gas bubbles can either be induced mechanically, chemically or by heating [52]. Although gas hold-up is a common measure of the level of gas incorporated into a matrix, the relevant properties are usually determined by the average bubble size, bubble size distribution and the architecture of the foam (e.g., Fig. 1-h) [51, 52]. It is known that size uniformity of air cells in liquid foams is an important factor increasing their longevity. Thus, a foam with a monodisperse array of bubbles has structural and stability advantages [57, 92, 93].

Recently, membranes have been used to incorporate gas bubbles into solutions of food biopolymers, yielding a highly monodisperse bubble size distribution [94]. Membrane processes use an applied pressure to disperse a gaseous phase through the membrane into the continuous liquid phase [95]. In membrane processing, bubble diameter increases with gas flow rate and membrane pore size, and it is usually larger than the nominal pore dimension [94]. The main limitation of the membrane process is a low flow of the dispersed phase through the membrane. Once the foamed solutions are formed, gelation of the biopolymer matrix can be induced.

Microfluidic Systems

Microfluidic systems offer convenient methods for controlling the formation of bubbles (and droplets) of sizes below the 100 micron [17]. Microfluidic devices used are varied. For example, highly monodisperse drops were generated in a concentric capillary geometry and their shape was changed by passing them through a narrow rectangular channel [55, 56]. Other geometries include the T-junction [53, 96], the cross-junction of four crossed channels [57, 96] and the adapted hyperbolic flow generated in a four-roll mill (4RM) [97, 98]. Different flow regimes and wetting properties of the channels give rise to varied foam structures. The diameter of the formed bubble generally scales with the diameter of the capillary

orifice and there is an interplay between geometrical parameters and the gas and liquid flow rates. A foam architecture of monodisperse bubbles has structural and stability advantages [57]. Highly monodisperse bubble sizes can be generated in liquids using an axi-symmetric flow-focusing system with bubble sizes ranging between 5 and 120 μm and a polydispersity index within a variation of 2 % [99]. Another reason for using a microfluidic device to produce a foamed gel is that gravitational effects are small compared to surface tension effects, yielding small Bond numbers (Bo), typically around 0.01 [96], thus, minimizing liquid drainage and increasing foam stability resulting in a better control over the final pore size in the gel [53, 96].

Microfluidic systems can be used to reduce the volume/energy ratio, improve the homogeneity of products, form double emulsions (W/O/W or O/W/O), foam mixtures and dispersions under continuous flow, thus, allowing the formation of multicomponent gels with controlled architectures [97].

Oleogels

Oleogels are colloidal systems in the form of lipids trapped within gel network [100, 101]. Alternatively, they may be viewed as potential porous structures of hydrophobic polymers that exhibit viscoelastic properties while having an organic liquid (oil) entrapped [59, 101]. Oil gels in food are called "oleogels" unlike "organogels" which use organic solvents and are widely applied in the chemical industry [102]. Since most food biopolymers are hydrophilic there are few oleogel systems that can be formed directly for use in foods [103]. Ethylcellulose (EC) is a food-grade biopolymer capable of solubilizing in oil when heated above a transition temperature of approximately 140 ° C and forming a gel network upon subsequent cooling. The 3D network of EC oleogels has been found to have voids (3–4.5 μm) filled with oil [104]. Oil in EC oleogels may be solvent-extracted leaving an aerogel with micropores whose biopolymeric walls entrap some residual oil. Alternatively, hydroxyl propyl methyl cellulose (HPMC) foams can be freeze-dried and the resulting porous template impregnated with oil and subjected to shear to form sheets of dispersed polymer that effectively encapsulate the oil [100]. Oleogels are of increasing interest due to the ease of preparation and good chemical and mechanical stability, finding applications in pharmaceuticals and foods for drug delivery and texture enhancement, respectively [101, 102]. Oleogelation may represent an interesting alternative to structure lipids reducing the use of saturated fats and eliminating trans fats from food products [60] and culinary dishes [103].

Enzymatic Action

The use of enzymes in food processing presents a number of advantages due to their high specificity and action under mild conditions, especially temperature, so applications in tailoring porous matrices abound. A cellular structure was obtained by α-amylase action on starch-agar gels prior to freeze-dehydration [44]. Starch content (0.5–1.5 %), enzyme concentration (1000–1500 ppm) and exposure times changed the structure (e.g., large pores in the outer region) and mechanical properties of the gels. Initially, the enzyme decomposed starch on the gel surface, while longer exposure to the enzyme action led to larger surface pores, thus a change in the mechanical properties of the sponge [10]. Indirect action of enzymes is another technique to produce bubbles, whereby the action of yeast enzymes converts sugar into alcohol and CO_2. Agar sponges have been made by immobilizing yeast in agar gels and then immersing in a 5 % sucrose solution for 3 to 7 days, followed by drying. Long fermentation times lowered the pH of the gel and reduced the strength and stiffness of porous gels [105]. A matrix of starch and polyacrylic acid formed a compact structure by intermolecular H-bonds in an acid environment, with a minimum release of an encapsulated drug. In contrast, there was a maximum release of the drug in a slightly alkaline pH (i.e., at colonic pH of 7.4) due to the degradation of the starch by the α-amylase present in the solution. The enzymatic degradation of starch (pH 7.4 and 37 °C) produces sugar that diffuses out of the matrix, thus forming macro pores that facilitate the release of the encapsulated drug [106]. Porous cross-linked enzyme aggregates (p-CLEAs) of papain were formed after the precipitation of the dissolved enzyme and subsequent covalent cross-linking [31]. The p-CLEAs were prepared by adding starch (as a pore-forming agent) to the enzyme solution in order to form an enzyme-starch precipitate before removing starch using α-amylase and washing away the sugars after enzyme hydrolysis. Another study includes the effect of trypsin on the enzymatic degradation of non-porous and porous samples of poly(lactide-co-glycolide) copolymers (PLGA) [107]. Trypsin had a greater effect on the degradation of porous PLGA than on non-porous PLGA, because of the larger surface area of the porous samples. Porous PLGA matrices are more desirable for tissue engineering applications as their properties can be tailored and controlled.

Centrifugal Force

The procedure of gelation under dynamic conditions was initially assayed by applying a centrifugal force to a mixture of two polysaccharides, chitosan and *k*-carrageenan [14]. The appearance of the gel depends on the prevalent conditions during the gelation step. An opaque gel was formed when gelation took place after conventional magnetic stirring while a transparent gel was created under centrifugal force [14]. Gelation under dynamic conditions (450 rpm) was useful to induce order in a fibrin network, giving rise to transparent and stable gels with fibrils arranged in parallel fashion (as

observed by AFM and LTSEM), similar to *k*-carrageenan-chitosan gel [14].

A patent presents a method for producing porous structures using a rotational spinning technique. Phase separation occurred due to an increase in density of one phase resulting in its sedimentation at the periphery. After gelation the excess solvent at the center was removed allowing for multilayering and the formation of hollow structures while maintaining good mechanical properties [35].

Ultrasound

Ultrasound is an effective form of localizing high pressure and temperature in a medium. In the laboratory ultrasound is usually applied to a given volume of sample using an ultrasonic bath or a probe at frequencies >20 kHz [3]. Ultrasonic waves produce a series of rapid compressions and expansions of the medium similar to a sponge being squeezed and released repeatedly [108]. Under this "sponge effect" liquid exits/enter the sample producing micro-channels or micro-tunnels (Fig. 4) which are suitable for fluid movement [110]. High-intensity ultrasound (generally between 20 and 100 kHz) was applied to study the effect of the degree of denaturation on aggregation and surface properties of β-lactoglobulin used as surfactant to incorporate bubbles to gelatin gels [3]. The resulting gels were weaker and less ductile than non-aerated gels.

Electrification

An electric field (direct current, DC) of a relatively low strength can be used to increase the surface porosity and surface area of a gel. Freeze-dried gels of different origin (collagen, agarose, alginate, agar, and gellan [39, 111–113]) were immersed in distilled water, placed between a pair of platinum electrodes and subjected to a low electrical field (up to 40 V/cm) [39]. Major changes (e.g., increased porosity, increased surface area) occurred in the interior of gels (e.g., cut alginate gel beads) but not on the outer surface possibly due to ionic migration and development of pH gradients [114].

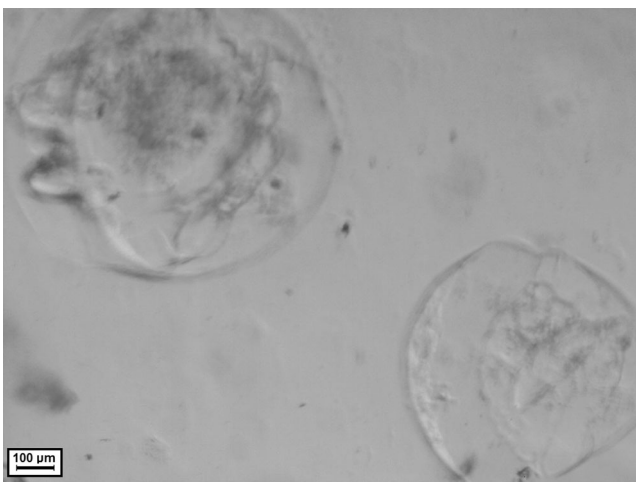

Fig. 4 Image of a 2 % alginate gel after treatment by ultrasound. Pores with almost circular cross section are about 700 µm on average and similar to those in acrylamide gels [109]

Mass Transfer Process – Incorporation of Micronutrients

Much of the theoretical and practical attention given to gels is due to their mass transport properties in a wide context of applications: fluid biological systems, separation technologies, and matrix formation, among others. Gels are a unique form of "semi-solid water" at room temperature having the consistency of biological tissue. However, the diffusivities of small solutes (ions, sugars) and uncharged macromolecules in gels are typically lower than in an aqueous solution due to a combination of hydrodynamic and steric interactions (derived from the gel matrix). Nevertheless, porous gels filled with fluid (liquid or gas) may provide the necessary mass transfer rates by combining free and hindered diffusion within a tailor-made matrix, extending their versatility and possible uses (e.g., controlled release, encapsulation) [115].

Transport of solutes in non-porous gels is generally considered to occur by molecular diffusion while mass transport in porous gels it is a more complex phenomena involving also capillarity and microconvection [116].

Mass transport resistance inside non-porous gel matrices is high and depends mainly on the structural characteristics of the matrix (Table 2), and to a minor extent on temperature [115, 132]. Porous materials are sometimes defined as those having pore diameter greater than or equal to 10^{-7} m and capillary-porous as those having pore diameter of less than 10^{-7} m [116]. Pores may be interconnected so that mass transport through the pores is faster than through the gel matrix. If pores are closed, solutes will still have to diffuse through the walls surrounding the pores. Data to calculate diffusion coefficients (D) of solutes in gels are determined using various experimental techniques and D values estimated using Fick's second law which masks all structural and interaction effects in an "effective diffusion coefficient" [117, 129]. Mass transport in porous gels has been described as highly anomalous and not susceptible to be described by Fick's law alone [133]. The values of the effective diffusion coefficients in hydrogels are lower than those found in water because the path length for the diffusing solute is increased due to obstructions caused by the gel network, possible interactions between the gel matrix and the diffusing substances, and a reduced volume available for diffusion [119]. Data on the influence of the concentration of small molecules (glucose, sucrose, lactose and others) and the degree of cross-linking on diffusivity vary greatly. Table 2 shows some selected values of D for different gel systems and specific solutes. As polymer concentration increases and

Table 2 Some examples of diffusion coefficients (D) of solutes in non-porous and porous gels

Gel system	Component	D value, m^2s^{-1}	Comments	Reference
Non-porous gels				
Polymer/silicate gel (polyacrylamide, silicate, $AlK(SO_4)_2$, $CaCl_2$)			25 °C	[117]
	H_2O	6.4×10^{-9}	C_{SiO2}=50 g/L + C_P=2 g/L + C_{HCl}=0.155 mol/L	
	D_2O	2.6×10^{-9}		
Poly(acrylamide-co-methyl methacrylate)			25 °C	[118]
	KCl	4.57×10^{-10}		
	LiCl	3.14×10^{-10}		
PAAG (polyacrylamide gel)			20 °C	[119]
	glucose	4.63×10^{-10}		
	maltose	3.23×10^{-10}		
Hydroetilcelluloses cationic (1 %):	ibuprofen 6 %		25 °C	[120]
PQ-4(poliquaternium-4)		5.68×10^{-9}		
PQ-10(poliquaternium-10)		1.98×10^{-9}		
Guar gums cationic (1 %):	ibuprofen 6 %			
E-14(ecopol 14S)		0.983×10^{-9}		
E-261(ecopol 261S)		0.883×10^{-9}		
Agarose 4 %			25 °C	
Different methods with high salt concentration to shield electrostatic interactions				
a) Diffusion cell	Lysozyme	10.7×10^{-11}		[121]
	BSA (Bovine serum albumin)	2.8×10^{-11}		
b) HLI (holographic laser interferometry)	Lysozyme	6.8×10^{-11}		[122, 123]
	BSA	3.0×10^{-11}		
c) ESPI (electronic speckle pattern interferometry)	Lysozyme	7.3×10^{-11}		[124]
	BSA	2.1×10^{-11}		
Agarose	nisin		10 °C	[125]
3.2 %		4.2×10^{-11}		
3.9 %		3.4×10^{-11}		
6.7 %		2.5×10^{-11}		
Agarose	nisin			[126]
3.0 %		1.92×10^{-11}	5.4 °C	
3.0 %		8.14×10^{-11}	22.3 °C	
Collagen 5 %			4 °C	[127]
	glucose	6.65×10^{-11}		
	ovalbumin	0.598×10^{-11}		
	^3H_2O	33×10^{-11}		
Kappa-carrageenan 0.45 %			37 °C	[128]
	sucrose (10 %)	5.9×10^{-10}		
	sucrose (15 %)	7.3×10^{-10}		
	aspartame (0.08 %)	6.1×10^{-10}		
	aspartame(0.12 %)	7.7×10^{-10}		
Kappa-carrageenan 0.9 %			37 °C	[128]
	sucrose (10 %)	3.8×10^{-10}		
	sucrose (15 %)	4.3×10^{-10}		
	aspartame (0.08 %)	5.9×10^{-10}		
	aspartame (0.12 %)	4.8×10^{-10}		
Protanal LF20/60, 2 %	glucose	6.07×10^{-10}	40 °C	[129]
	lactic acid	10.3×10^{-10}	40 °C	
Alginate calcium	glucose		30 °C	[129]
3 %		6.23×10^{-10}		
4 %		3.20×10^{-10}		

Table 2 (continued)

Gel system	Component	D value, m^2s^{-1}	Comments	Reference
Porous gels				
Chitosan	paracetamol		37 °C	[130]
1 %		4.45×10^{-8}	pore size 240 μm	
2 %		1.87×10^{-8}	pore size 98 μm	
3 %		0.30×10^{-8}	pore size 65 μm	
5 %		0.08×10^{-8}	pore size 25 μm	
PNIPA, poly(N-isopropylacrylamide) gel	rhodamine B	5.0×10^{-11}	33 °C; pore size 33 Å	[131]
		15×10^{-11}	25 °C; pore size 59.7 Å	

matrix pore size decreases, the diffusion coefficient also decreases. However, if the polymer concentration remains constant and the concentration of solute increases (see sucrose in k-carrageenan, Table 2), the diffusion coefficient increases. Different procedures have been applied to increase the kinetics of mass transfer in gelled biomaterials, including the use of a vacuum [134], centrifugal forces, electric pulses [135], and pressure waves such as sonic or high intensity ultrasound [108]. External factors and the characteristics of polymer chains (such as hydrophobicity, hydrophilicity, charge on a chain, the geometry or shape of the chains, etc.) influence the diffusivity values in a gel system (Table 2, d). Pore size has a strong influence on D values of porous matrices (see cases in which the gel system is PNIPA and chitosan, Table 2). An increased diffusivity coefficient was observed in gel systems with larger pore sizes. For example, a chitosan gel showed an increase from 0.1×10^{-8} to 5×10^{-8} m [2] s^{-1} (50 times) in D values when the pore size increased from 25 to 240 μm. Thus, porous gels matrices may be tailored as unique structures for the release of active biomolecules, nutrients, and flavors incorporated into their pores.

Potential Applications in Foods

Gels are ubiquitous food structures in dairy, meat and processed fruit products and in gastronomy. Many of the techniques for manufacturing porous gels and porous matrices revised in this paper may be adapted to obtain edible sponges of interest to the food industry after circumventing the fact that possible toxic components or nonfood-grade ingredients are used. Physical properties such as porosity, pore size, density as well as mechanical (e.g., texture, lightness) and transport properties (e.g., flavor release) that are of major importance in food products may be expanded and controlled by addition of a dispersed phase to food gels. Edible porous matrices may find many applications in "healthy products" as carriers of vitamins and minerals or other functional components of interest, as well as in the control of satiety [136]. Cellular hydrocolloid gels have already found numerous applications in foods and gastronomy ranging from analogs of fresh fruits and caviar [137–142] to carriers of vitamins and other essential micronutrients [10, 23, 141, 143, 144]. Other applications include artificial 'cherries' in pie fillings and low-calorie jams

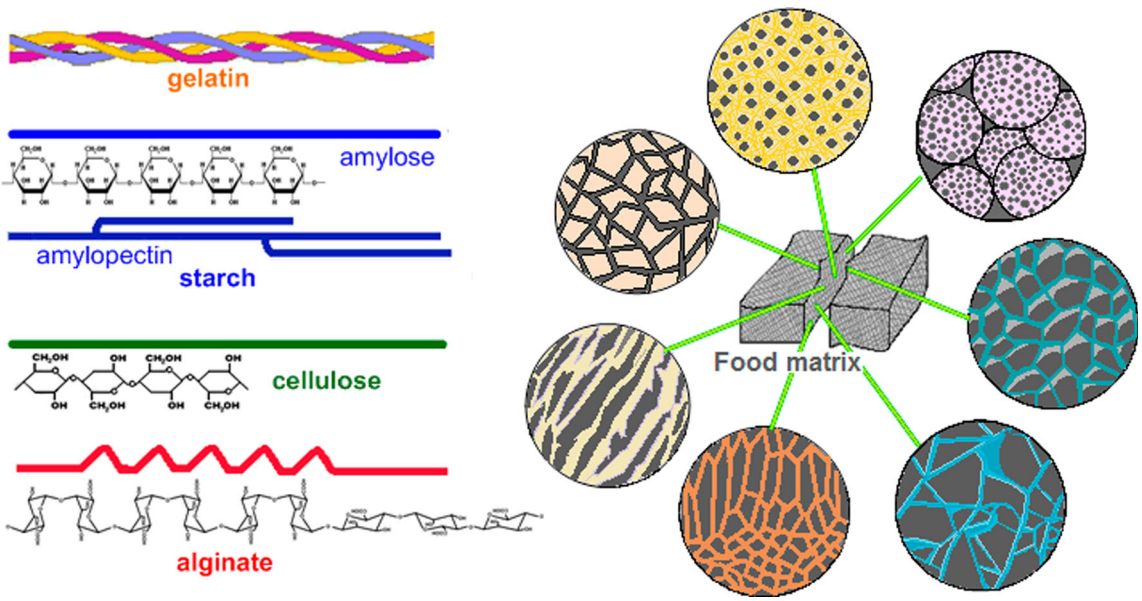

Fig. 5 Examples of food biopolymers and possible porous architectures of gelled systems for use in foods

and jellies that take advantage of the excellent flavor release offered by gels [142]. Gels can be used to create odd shapes (Fig. 5), encapsulate flavors and aromas improve satiety control and create novel structures in gastronomy [5, 145]. An attractive area in food development is the design of soft structures for the elderly. Porous microspheres from gels with a variety of micro-nutrients encapsulated and with different mechanical properties could be used in the case of dysphagia (difficulty in swallowing the food bolus) [146].

Conclusions

The food industry has often adapted and applied knowledge and technologies developed in other fields. The various techniques for manufacturing porous matrices described in this paper and already being implemented in the fields of tissue and biomedical engineering and pharmaceuticals offer a plethora of opportunities for food product design and innovation. In general, the properties of porous structures depend their composition and on the manufacturing technique as the former influences the rate of degradation, texture and mass transport properties and the latter affect the pore size, porosity and matrix architecture (Fig. 5). Much work has been advanced in top-down approaches and is now the time to explore into bottom-up techniques that require computational topological designs and manipulation at the microlevel. Further work should be based on how properties of porous wet and dry matrices fit the demands from consumers in health, wellbeing, weight control, convenience and pleasure. Food technologists ought to select the appropriate biopolymers and fabrication procedures to meet these targets while food engineers should be responsible for scaling-up processes into cost-efficient manufacturing technologies.

Acknowledgments We are grateful to CONICYT (Comisión Nacional de Investigación Científica y Tecnológica de Chile) for the financial support to T. R. Cuadros and FONDECYT project 1150395 (Prof. Aguilera).

Conflict of Interest The authors declare that they have no conflict of interest.

References

1. J.M. Aguilera, in *Physical Chemistry of Foods*, ed. by H. Schwartzberg, R. Hartel (Marcel Dekker Inc, New York, 1992), pp. 387–421
2. G. Tabilo-Munizaga, G.V. Barbosa-Cánovas, J. Food Eng. **67**, 147–156 (2005)
3. R.N. Zúñiga, U. Kulozik, J.M. Aguilera, Food Hydrocoll. **25**, 958–967 (2011)
4. P. Harris (ed.), *Food Gels* (Elsevier Science Publisher Ltd., London, 1990)
5. R. Zuñiga, J.M. Aguilera, Trends Food Sci. Technol. **19**, 176–187 (2008)
6. D. Mooney, D. Baldwin, N. Suh, J. Vacanti, R. Lange, Biomaterials **17**, 1417–1422 (1996)
7. L. Shapiro, S. Cohen, Biomaterials **18**, 583–590 (1997)
8. P. Eiselt, J. Yeh, R.K. Latvala, L.D. Shea, D.J. Mooney, Biomaterials **21**, 1921–1927 (2000)
9. H. Ming-Hua, K. Pei-Yun, H. Hsyue-Jen, H. Tzu-Yang, H. Lein-Tuan, L. Juin-Yih, W. D-Ming, Biomaterials **25**, 125–138 (2004)
10. A. Nussinovitch, Mol. Nutr. Food Res. **49**, 195–213 (2005)
11. L. Gibson, M. Ashby, *Cellular Solids: Structure and Properties* (Cambridge University Press, Cambridge, 1997)
12. S.R. Mukai, H. Nishihara, T. Yoshida, K.-I. Taniguchi, H. Tamon, Carbon **43**, 1563–1565 (2005)
13. S. Zmora, R. Glicklis, S. Cohen, Biomaterials **23**, 4087–4094 (2002)
14. E.M.D. Doncel-Pérez, E. Martín-López, L. Vásquez, M. Nieto-Sampedro, E. Ruiz-Hitzky, J. Mater. Sci. Mater. Med. **17**, 795–802 (2006)
15. D.J. Griffon, M.R. Sedighi, D.V. Schaeffer, J.A. Eurell, A.L. Johnson, Acta Biomater. **2**, 313–320 (2006)
16. T. Sobisch, D. Lerche, S. Fischer, C. Fanter, Progr. Colloids Polym. Sci. **133**, 169–172 (2006)
17. O. Skurtys, P. Bouchon, J.M. Aguilera, Food Hydrocoll. **22**, 706–714 (2008)
18. C.-C. Wang, K.-C. Yang, K.-H. Lin, H.-C. Liu, F.-H. Lin, Biomaterials **32**, 7118–7126 (2011)
19. R. Gauvin, Y.-C. Chen, J.W. Lee, P. Soman, P. Zorlutuna, J.W. Nichol, H. Bae, S. Chen, A. Khademhosseini, Biomaterials **33**, 3824–3834 (2012)
20. J. Weng, M. Wang, J. Mater. Sci. Lett. **20**, 1401–1403 (2001)
21. Y.A. Petrenko, R.V. Ivanov, A.Y. Petrenko, V.I. Lozinsky, J. Mater. Sci. : Mater. Med. **22**, 1529–1540 (2011)
22. H. Cheng-Hsuan, T. Sung-Pei, H. Ming-Hwa, W. Da-Ming, L. Chung-En, H. Cheng-Hsuan, T. Hsien-Chung, H. Hsyue-Jen, Carbohydr. Polym. **67**, 124–132 (2007)
23. R. Barbucci, G. Leone, A. Vecchiullo, J. Biomater. Sci. Polym. Ed. **15**, 607–619 (2004)
24. X. Liu, P.X. Ma, Biomaterials **30**, 4094–4103 (2009)
25. F.M. Plieva, B. Mattiasson, Ind. Eng. Chem. Res. **47**, 4131–4141 (2008)
26. H. Jiankang, L. Dichen, L. Yaxiong, Y. Bo, L. Bingheng, L. Quin, Polymer **48**, 4578–4588 (2007)
27. J.S. Pieper, P.M. van der Kraan, T. Hafmans, J. Kamp, P. Buma, J.L.C. van Susante, W.B. van den Berg, J.H. Veerkamp, T.H. van Kuppevelt, Biomaterials **23**, 3183–3192 (2002)
28. A.I. Van Den Bulcke, B. Bogdanov, N. De Rooze, E.H. Schacht, M. Cornelissen, H. Berghmans, Biomacromolecules **1**, 31–38 (2000)
29. K.Y. Lee, D.J. Mooney, Prog. Polym. Sci. **37**, 106–126 (2012)
30. M.S. Sader, M. Ferreira, M.L. Dias, Polím. Cienc. Tecnol. **16**, 12–18 (2006)
31. M. Wang, C. Jia, W. Qi, Q. Yu, X. Peng, R. Su, Z. He, Bioresour. Technol. **102**, 3541–3545 (2011)
32. K. Draget, in *Handbook of Hydrocolloids*, ed. by G.O. Phillips, P.A. Williams (Woodhead Publishing Limited, Crambridge, 2000). **Cap. 22**
33. T. van Vliet, Colloid Polym. Sci. **266**, 518–524 (1988)
34. J.M. Aguilera, H.-G. Kessler, J. Food Sci. **54**, 1213–1217 (1989)
35. P.D. Dalton, M.S. Schoichet. In *WO/2001/085417*, ed. by S.B. Sciences (Regen Corp. Toronto, 2001), p 8
36. S. van Vlierberghe, V. Cnudde, P. Dubruel, B. Masschele, A. Cosijns, I. De Paepe, P.J. Jacobs, L. Van Hoorebeke, J.P. Remon, E. Schacht, Biomacromolecules **8**, 331–337 (2007)
37. V. Lozinsky, Russian Chemical Bulletin, International Edition 57, 1015–1032 (2008)

38. S.J. Hollister, Nat. Mater. **4**, 518–524 (2005)
39. A. Nussinovitch, R. Zvitov-Marabi, Food Hydrocoll. **22**, 364–372 (2008)
40. X. Geng, O.-H. Kwon, J. Jang, Biomaterials **26**, 5427–5432 (2005)
41. J.M. Holzwarth, P.X. Ma, Biomaterials **32**, 9622–9629 (2011)
42. H.-J. Jin, J. Chen, V. Karageorgiou, G.H. Altman, D.L. Kaplan, Biomaterials **25**, 1039–1047 (2004)
43. A.B. Bennion, B.S.T. Bamford, C. a. Hall (ed.) (London, 1997)
44. Z. Gershon, A. Nussinovitch, Food Hydrocoll. **12**, 105–110 (1998)
45. E. Öztürk, C. Agalar, K. Kececi, E.B. Denkbas, J. Appl. Polym. Sci. **101**, 1602–1609 (2006)
46. H. Ming-Hua, K. Pei-Yun, H. Hsyue, H. Tzu-Yang, H. Lein-Tuan, L. Juin-Yih, W. Da-Ming, Biomaterials **25**, 129–138 (2004)
47. K.F. Leong, C.M. Cheah, C.K. Chua, Biomaterials **24**, 2363–2378 (2003)
48. L.S. Zárate-Ramírez, A. Romero, C. Bengoechea, P. Partal, A. Guerrero, Carbohydr. Polym. **112**, 24–31 (2014)
49. H. Nishihara, S.R. Mukai, D. Yamashita, H. Tamon, Chem. Mater. **17**, 683–689 (2005)
50. R.N. Zúñiga, J.M. Aguilera, Food Hydrocoll. **23**, 1351–1357 (2009)
51. N. Annabi, S.M. Mithieux, E.A. Boughton, A.J. Ruys, A.S. Weiss, F. Dehghani, Biomaterials **30**, 4550–4557 (2009)
52. K. Niranjan, S. Silva, in *Food Materials Science - Principles and Practice*, ed. by J.M. Aguilera, P. J. Lillford (Food Engineering Springer, 2008)
53. S. Martynov, X. Wang, E.P. Stride, M.J. Edirisinghe, Int. J. Food Eng. **6**(3), 1–12 (2010)
54. A. Nussinovitch, R. Velez-Silvestre, M. Peleg, Biotechnol. Prog. **8**, 424–428 (1992)
55. B. Walther, L. Hamberg, P. Walkenström, A.-M. Hermansson, J. Colloid Interface Sci. **270**, 195–204 (2004)
56. B. Walther, C. Cramer, A. Tiemeyer, L. Hamberg, P. Fischer, E.J. Windhab, A.-M. Hermansson, J. Colloid Interface Sci. **286**, 378–386 (2005)
57. O. Skurtys, J.M. Aguilera, J. Colloid Interface Sci. **318**, 380–388 (2008)
58. J. Raven, P. Marmottant, F. Graner, Eur. Phys. J. B **51**, 137–143 (2006)
59. A. Marangoni, J. Am. Oil Chem. Soc. **89**, 749–780 (2012)
60. A.R. Patel, N. Cludts, M.D.B. Sintang, A. Lesaffer, K. Dewettinck, Food Funct. **5**, 2833–2841 (2014)
61. A.R. Patel, P.S. Rajarethinem, N. Cludts, B. Lewille, W.H. De Vos, A. Lesaffer, K. Dewettinck, Langmuir **31**, 2065–2073 (2015)
62. S. Möller, J. Weisser, S. Bischoff, M. Schnabelrauch, Biomol. Eng. **24**, 496–504 (2007)
63. J. Zhang, H. Zhang, L. Wu, J. Ding, J. Mater. Sci. **41**, 1725–1731 (2006)
64. F.P.W. Melchels, J. Feijen, D.W. Grijpma, Biomaterials **30**, 3801–3809 (2009)
65. N. Nakamura, R. Takahashi, S. Satoshi, T. Sodesawa, Y. Satoshi, Phys. Chem. Chem. Phys. **2**, 4983–4990 (2000)
66. K. Kulinowski, P. Jiang, H. Vaswani, V. Colvin, Adv. Mater. **12**, 833–838 (2000)
67. V. Manoharan, A. Imhof, J. Thorne, D. Pine, Adv. Mater. **13**, 447–450 (2001)
68. Y. Nam, T. Park, J. Biomed. Mater. Res. **47**, 8–17 (1999)
69. K. Whang, C. Thomas, K. Healy, Polymer **36**, 837–842 (1995)
70. C.X.F. Lam, X.M. Mo, S.H. Teoh, D.W. Hutmacher, Mater. Sci. Eng. C **20**, 49–56 (2002)
71. S. Bose, S. Vahabzadeh, A. Bandyopadhyay, Mater. Today **16**, 496–504 (2013)
72. A. Park, B. Wu, L. Griffith, J. Biomat. Sci. Polym. Ed **9**, 89–110 (1998)
73. F. Chemat, E.H. Zill, M.K. Khan, Ultrason. Sonochem. **18**, 813–835 (2011)
74. B. Pugin, A. Turner (eds.), *Influence of Ultrasound on Reaction with Metals* (JAI Press, London, 1990)
75. T. Neumann, B.S. Nicholson, J.E. Sanders, Microvasc. Res. **66**, 59–67 (2003)
76. S. Mukai, H. Nishihara, H. Tamon, Catal. Surv. Jpn. **10**, 161–171 (2006)
77. G. Chen, T. Ushida, T. Tateishi, J. Biomed. Mater. Res. **51**, 273–279 (2000)
78. G. Chen, T. Ushida, T. Tateishi, Biomaterials **22**, 2563–2567 (2001)
79. H. Studenovská, M. Slouf, F. Rypácek, J. Mater. Sci. Mater. Med. **19**, 615–621 (2008)
80. L. Harris, D. Baldwin, D. Mooney, J. Biomed. Mater. Res. **42**, 396–402 (1998)
81. Y. Park, K. Nam, S. Ha, J. Control Release **43**, 151–160 (1997)
82. C. Schugens, V. Maquet, C. Grandfils, R. Jerome, P. Teyssie, J. Biomed. Mater. Res. **30**, 449–461 (1996)
83. N. Lorén, A.-M. Hermansson, M. Williams, L. Lundin, T. Foster, C. Hubbard, A. Clark, I. Norton, E. Bergström, D. Goodall, Macromolecules **34**, 289–297 (2001)
84. C. Bengoechea, A. Arrachid, A. Guerrero, S.E. Hill, J.R. Mitchell, J. Cereal Sci. **45**, 275–284 (2007)
85. Y. Song, Q. Zheng, Ind. Crop. Prod. **29**, 446–454 (2009)
86. F. Chen, X. Monnier, M. Gällstedt, U.W. Gedde, M.S. Hedenqvist, Eur. Polym. J. **60**, 186–197 (2014)
87. Q. Wang, Y. Li, F. Sun, X. Li, P. Wang, J. Sun, J. Zeng, C. Wang, W. Hu, J. Chang, M. Chen, Y. Wang, K. Li, G. Yang, G. He, Food Res. Int. **69**, 64–71 (2015)
88. C. Schmitt, L. Aberkane, C. Sanchez, in *Handbook of hydrocolloids*, ed. by G.O. Phillips, P.A. Williams (Woodhead Publishing Limited, Cambridge, 2009)
89. M. Wang, T.V. Vliet, R.J. Hamer, J. Cereal Sci. **39**, 341–349 (2004)
90. M.J. Correa, E. Ferrer, M.C. Añón, C. Ferrero, Food Hydrocoll. **35**, 91–99 (2014)
91. G.M. Campbell, E. Mougeot, Trends Food Sci. Technol. **10**, 283–296 (1999)
92. H. Oguz, A. Prosperetti, J. Fluid Mech. **257**, 111–145 (1993)
93. R.A.M. Al-Hayes, R.H.S. Winterton, Int. J. Heat Mass Transf. **24**, 223–230 (1981)
94. A. Bals, U. Kulozik, J. Membr. Sci. **220**, 5–11 (2003)
95. G.T. Vladisavljevic, R.A. Williams, Adv. Colloid Interf. Sci. **113**, 1–20 (2005)
96. O. Skurtys, J.M. Aguilera, Food Biophys **3**, 1–15 (2008)
97. B. Walther, P. Walkenström, A.-M. Hermansson, P. Fischer, E.J. Windhab, Food Hydrocoll. **16**, 633–643 (2002)
98. L. Hamberg, M. Wohlwend, P. Walkenström, A.-M. Hermansson, Food Hydrocoll. **17**, 641–652 (2003)
99. A.M. Gañán-Calvo, J.M. Gordillo, Phys. Rev. Lett. **87**, 274501 (2001)
100. A.R. Patel, *Alternative routes to oil structuring,* (Springer International Publishing, 2015)
101. T.A. Stortz, A.K. Zetzl, S. Barbut, A. Cattaruzza, A.G. Marangoni, Lipid Technol. **24**, 151–154 (2012)
102. L.S.K. Dassanayake, D.R. Kodali, S. Ueno, Curr. Opin. Colloid Interface Sci. **16**, 432–439 (2011)
103. M.A. Rogers, T. Strober, A. Bot, J.F. Toro-Vazquez, T. Stortz, A.G. Marangoni, Int. J. Gastronomy Food Sci. **2**, 22–31 (2014)
104. A.K. Zetzl, A.J. Gravelle, M. Kurylowicz, J. Dutcher, S. Barbut, A.G. Marangoni, Food Struct. **2**, 27–40 (2014)
105. A. Nussinovitch, Z. Gershon, Food Hydrocoll. **11**, 231–237 (1997)
106. S.K. Bajpai, S. Saxena, React. Funct. Polym. **61**, 115–129 (2004)
107. Q. Cai, G. Shi, J. Bei, S. Wang, Biomaterials **24**, 629–638 (2003)

108. J. Floros, H. Liang, Food Technol. **48**, 79–84 (1994)
109. H. Tamagawa, S. Popovic, M. Taya, Polymer **41**, 7201–7207 (2000)
110. H. Muralidhara, D. Ensminger, A. Putnam, Dry. Technol. **3**, 529–566 (1985)
111. R. Zvitov, A. Nussinovitch, Food Hydrocoll. **15**, 33–42 (2001)
112. R. Zvitov, A. Schwartz, E. Zamski, A. Nussinovitch, Biotechnol. Prog. **19**, 965–971 (2003)
113. R. Zvitov, A. Nussinovitch, Food Hydrocoll. **19**, 997–1004 (2005)
114. Y. Hirose, G. Giannetti, J. Marquardt, T. Tanaka, J. Phys. Soc. Jpn **61**, 4085–4097 (1992)
115. E.L. Cussler (ed.), *Diffusion : Mass Transfer in Fluid Systems* (Cambridge University Press, 2009)
116. A.K. Datta, J. Food Eng. **80**, 80–95 (2007)
117. I. Lakatos, J. Lakatos-Szabó, Colloids Surf. A Physicochem. Eng. Asp. **246**, 9–19 (2004)
118. A.J.M. Valente, A.Y. Polishchuk, V.M.M. Lobo, G. Geuskens, Eur. Polym. J. **38**, 13–18 (2002)
119. D. Yankov, Enzym. Microb. Technol. **34**, 603–610 (2004)
120. R. Rodriguez, C. Alvarez-Lorenzo, A. Concheiro, *VI Congreso SEFIG y 3as Jornadas TF* (Granada-España, 2002)
121. J. Gutenwik, B. Nilsson, A. Axelsson, Biochem. Eng. J. **19**, 1–7 (2004)
122. C. Mattisson, P. Roger, B. Jönsson, A. Axelsson, G. Zacchi, J. Chromatogr. B Biomed. Sci. Appl. **743**, 151–167 (2000)
123. P. Roger, C. Mattisson, A. Axelsson, G. Zacchi, Biotechnol. Bioeng. **69**, 654–663 (2000)
124. D. Karlsson, G. Zacchi, A. Axelsson, Biotechnol. Prog. **18**, 1423–1430 (2002)
125. A. Carnet Ripoche, E. Chollet, E. Peyrol, I. Sebti, Innovative Food Sci. Emerg. Technol. **7**, 107–111 (2006)
126. I. Sebti, D. Blanc, A. Carnet-Ripoche, R. Saurel, V. Coma, J. Food Eng. **63**, 185–190 (2004)
127. M. Shaw, A. Schy, Biophys. J. **34**, 375–381 (1981)
128. S. Bayarri, I. Rivas, E. Costell, L. Durán, Food Hydrocoll. **15**, 67–73 (2001)
129. W. Zhang, S. Furusaki, Biochem. Eng. J. **9**, 73–82 (2001)
130. B. Falk, S. Garramone, S. Shivkumar, Mater. Lett. **58**, 3261–3265 (2004)
131. F. Tsunomori, H. Ushiki, Phys. Lett. A **258**, 171–176 (1999)
132. S. Simal, J. Benedito, E. Sánchez, C. Roselló, J. Food Eng. **36**, 323–336 (1998)
133. N. Fatin-Rouge, K. Starchev, J. Buffle, Biophys. J. **86**, 2710–2719 (2004)
134. P. Fito, J. Food Eng. **22**, 313–328 (1994)
135. N. Rastogi, M. Eshtiaghi, D. Knorr, J. Food Sci. **64**, 1020–1023 (1999)
136. I.T. Norton, W.J. Frith, S. Ablett, Food Hydrocoll. **20**, 229–239 (2006)
137. C. Pelaez, M. Karel, J. Food Process. Preserv. **5**, 63–81 (1981)
138. C. Gehin-Delval, R. Redgwell, D. Curti, B. Former, E. Labat, A. Raemy. In *Nestec, 1800 Vevey, Switzerland*, ed. by N. SA (Switzerland, 2008)
139. N. Luh, M. Karel, J.M. Flink, J. Food Sci. **41**, 89–93 (1976)
140. H.P. Fogel. In *Richland, MI*, ed. by G. F. Corporation (General Foods Corporation, White Plains, 1985)
141. A. Nussinovitch, N. Jaffe, M. Gillilov, Food Hydrocoll. **18**, 825–835 (2004)
142. O. Ben-Zion, A. Nussinovitch, Lebensm. Wiss. Technol. **29**, 129–134 (1996)
143. S. Jaya, T. Durance, J. Texture Stud. **39**, 183–197 (2008)
144. D. Rassis, I. Saguy, A. Nussinovitch, J. Agric. Food Chem. **46**, 2981–2987 (1998)
145. H. This (ed.), *Molecular Gatronomy* (Columbia University Press, New York, 2006)
146. A. Zargaraan, R. Rastmanesh, G. Fadavi, F. Zayeri, M.A. Mohammadifar, Food Sci Human Wellness **2**, 173–178 (2013)

Paper 2

Mechanical Properties of Calcium Alginate Fibers Produced with a Microfluidic Device

Manufacture alginate fibers and their properties.

Carbohydrate Polymers 89 (2012) 1198–1206

Contents lists available at SciVerse ScienceDirect

Carbohydrate Polymers

journal homepage: www.elsevier.com/locate/carbpol

Mechanical properties of calcium alginate fibers produced with a microfluidic device

Teresa R. Cuadros [a,*], Olivier Skurtys [b], José M. Aguilera [a]

[a] Pontificia Universidad Católica de Chile, School of Engineering, Department of Chemical and Bioprocess Engineering, P.O. Box 306, Santiago 22, Chile
[b] Universidad Técnica Federico Santa María, Department of Mechanical Engineering, Av. Vicuña Mackenna 3939, Santiago, Chile

ARTICLE INFO

Article history:
Received 28 September 2011
Received in revised form 12 January 2012
Accepted 29 March 2012
Available online 5 April 2012

Keywords:
Alginate gel
Diffusion
Mechanical properties
Microfluidic
Fibers
Eggs-box model

ABSTRACT

Fibers are important microstructural elements in many foods. The main objective of this research was to produce calcium alginate fibers with uniform diameters (about 300 and 550 μm) using a microfluidic device (MFD) and to study the effect of concentration of sodium alginate [Alg] and calcium chloride [$CaCl_2$] on their mechanical properties (MP). Moisture content (MO) and MP as maximum tensile stress (σ_{max}), tensile strain at break ($\Delta L/L_0$) and apparent Young's modulus (E) of fibers were determined and a statistical model and surface responses were developed as a function of [Alg] and [$CaCl_2$]. As [$CaCl_2$] increased first a strengthening and then a weakening of fibers were observed. Furthermore, σ_{max} increased with the addition of Ca^{2+} and a maximum of σ_{max} was obtained for a [$CaCl_2$] around 1.4% (exceeding several times the stoichiometric requirements of the carboxylate groups of the polymer). Such behavior prompted a molecular explanation of what happens during gelation based on the "egg-box model" and this model is tried to complete. Moreover, fibers with [Alg] ≥1.8% showed high extensibility ($\Delta L/L_0$ around 100%) and low values of MO. High values of E (~0.5 MPa) were obtained for [$CaCl_2$] close to 1.4%. A greater understanding is needed of the interaction between cation-polysaccharide-water, taking into account [Alg] and [$CaCl_2$] to predict the mechanical behavior of fibers. Calcium alginate fibers are important in food engineering as texture and microencapsulation agents.

1. Introduction

Structure formation in food materials is influenced by ingredient properties and processing conditions, including shearing forces. The use of well-defined flows, such as simple shear, turned out to be essential to study and control the structure formation process in fibrous foods (van der Goot, Peifhambardoust, Akkermans, & van Oosten-Manski, 2008). Recently, several microfluidic applications for producing various microstructural elements, such as bubbles, particles, fibers, strips, microcapsules have been reported (Bhattarai, Li, Edmondson, & Zhang, 2006; Fan, Du, Huan, Wang, Wang, & Zhang, 2005; Mikolajczyk & Wolowska-Czapnik, 2005; Shin et al., 2007; Skurtys & Aguilera, 2008a,b; Skurtys, Bouchon, & Aguilera, 2008; Vreeker, Li, Fang, Appelqvist, & Mendes, 2008).

Alginate is a powerful thickening, stabilizing and gel-forming agent used in foods to produce a variety of gel products (cold instant puddings, fruit gels, dessert gels, onion rings, imitation caviar) (Belitz, Grosch, & Schieberle, 2004). In particular, calcium alginate fibers may find applications in the structuring of various food analogs since alginate is an inexpensive and easily available natural biomaterial. Alginate fibers are also currently used to encapsulate flavor, enzymes, proteins, drugs and active components (Bhattarai et al., 2006; Mikolajczyk & Wolowska-Czapnik, 2005; Tonnesen & Karlsen, 2002; Wang, Liu, Gao, Liu, & Tong, 2008). Several methods have been utilized to fabricate alginate fibers with diameters smaller than 100 μm: extruding-spinning achieving fiber diameters of 40–50 μm (Fan et al., 2005); electrospinning of nanofibers such as alginate-PEO(poly-ethylene oxide) fibers with diameters between 20 and 100 nm (Bhattarai et al., 2006), and 40–200 nm (Moon, Ryu, Choi, Jo, & Farris, 2009); spinning machine yielding fiber diameters <80 μm (Mikolajczyk & Wolowska-Czapnik, 2005); and, a microfluidic device (similar to the one in this study) whose fibers have diameters ~20 μm (Shin et al., 2007). However, all these studies lack of a detailed study of the mechanical properties of the resulting fibers.

Alginate belongs to a family of linear copolymers of (1 → 4)-linked β-D-mannuronic acid (M) and α-L guluronic acid (G) residues, with M and G residues present in varying proportions and sequences depending on the alginic acid source. Alginate gelation occurs when divalent cations (usually Ca^{2+}) interact with blocks of G residues. In the dialysis method, calcium ions diffuse into the alginate solution with a rapid, strong and irreversible formation of gel (Draget, Moe, Skjak-Braek, & Smidsrod, 2006). These gels have

* Corresponding author. Tel.: +56 2 3544237; fax: +56 2 3545803.
E-mail addresses: tcuadroc@uc.cl, trcuadro@ing.puc.cl, trcuadros@gmail.com (T.R. Cuadros).

0144-8617/$ – see front matter © 2012 Elsevier Ltd. All rights reserved.
http://dx.doi.org/10.1016/j.carbpol.2012.03.094

the particular feature of being cold setting and heat stable. When forming alginate gels, two contiguous, diaxially linked guloronic residues form a cavity that acts as a binding site for calcium ions "cooperative binding". This behavior, usually described as the "egg-box model", results in the formation of a 3D gel network (Grant, Morris, Rees, & Smith, 1973; Sime, 1990). Although the egg-box model has been amply used it has been questioned several times and is still subject to controversy. Numerous studies have been performed to characterize the mechanisms and structural features involved in the gelation of alginate. These have shown a two-stage process in the mechanism of calcium alginate gelation: first, the formation of strongly linked dimer associations with important contributions from van der Waals and hydrogen bonding interactions, followed by the formation of weaker inter-dimer associations that display no particular specificity, and being mainly governed by electrostatic interactions (Braccini & Pérez, 2001; Morris, Rees, Thom, & Boyd, 1978; Sikorski, Mo, Skjak-Braek, & Stokke, 2007).

Rheological or mechanical properties (MP) of alginate fibers may have a major influence on the acceptance of a product because texture properties of foods are linked to deformation, disintegration and flow under strain. Due to the very rapid and irreversible binding reaction between multivalent cations and alginates, a direct mixing of these two components rarely produces homogeneous gel networks (Draget, 2000, Chap. 22). When the ion (that is, Ca^{2+}) diffuses into a stream of alginate solution, a gel is immediately formed at the interface and MP of alginate fibers are directly related to their chemical structure (Fabra, Talens, & Chiralt, 2010). Values of tensile strength in calcium alginate fibers may depend on intra- or intermolecular associations (Espino-Díaz et al., 2010), indeed, the physical properties of biopolymers depend on whether the molecules are in the disordered or ordered state. In the disordered state, interactions depend mainly on space-occupancy considerations, whereas in the ordered state, molecular interactions create structures capable of stable association into compact networks (Lazaridou, Biliaderis, & Kontogiorgios, 2003). The importance of the G units in the gelation of alginate is highlighted by the fact that the gel strength is a function of the total content and length of contiguous G-blocks as well as the concentration of the cation (Sikorski et al., 2007; Simpson, Stabler, Simpson, Sambanis, & Constantinidis, 2004), whereas changes in frecuency and length of contiguous G units alter the overall strength of the gel (Simpson et al., 2004).

The fracture stress is a measure of the "strength" of a material (Walstra, 2003). This suggests that material fracture takes place when the stress overcomes the cohesive/adhesive forces within the material. For that reason, the fracture stress of alginate gels is proportional to the network crosslink density (Zhang, Daubert, & Foegeding, 2005). The change in density of the gel matrix depends on the concentration either of sodium alginate or calcium salt (Stokke, Draget, Smidsrod, Yuguchi, Urakawa, & Kajiwara, 2000). Contrary to engineering polymers, the mechanical properties (like fracture mechanisms) for many food biopolymer gels are still poorly understood. Despite the wide use of alginate fibers, studies on their MP are limited in the scientific literature.

Hence, the main objective of this research was to produce uniform calcium alginate fibers using a microfluidic device (MFD) and study the effect of concentration of alginate [Alg] and calcium chloride [$CaCl_2$] on their mechanical properties.

2. Materials and methods

2.1. Preparation of sodium alginate and calcium chloride solutions

Solutions of sodium alginate powder Gelymar (Natural Extracts S.A., Chile) used was from *Macrocystis pyrifera* with the following average composition: 16% G [α-L guluronic acid], 38% M [β-D-mannuronic acid] and 46% of MG alternating units (low viscosity, 50–200 cP for a 1% aqueous solution at 20 °C). Sodium alginate at concentrations between 1.25% and 2.5% (until complete dissolution) were prepared. A small amount of red dye (red Laca FC-2030), 0.5% (w/w) was emulsified (by an Ultra Turrax, basic mixer during a two-step, 5 min at 25,000 rpm) into each alginate solution in order to distinguish the fiber at the outlet of the MFD. Finally, solutions were allowed to stand for 24 hours at 4 °C before use. $CaCl_2$ solutions ($CaCl_2{\cdot}2H_2O$ p.a., CA-0520, Heyn, Santiago, Chile) were prepared at different concentrations, % (w/v) based on weight of the anhydrous salt.

2.2. Production of calcium alginate fibers

In Fig. 1, a sketch of the microfluidic device (MFD) used to produce calcium alginate fibers is presented. It was fabricated by combining transparent polycarbonate plates using microfabrication technique and a metal needle. A detailed view of the MFD, to create the coaxial flow, is presented inside the dotted circle in Fig. 1. The metal needle (inner diameter D_{needle} = 0.51 mm) and the polycarbonate capillary tube ($D_{capillary}$ = 3 mm) were co-axially assembled. The $CaCl_2$ solution was injected through the outer capillary whereas the alginate solution was introduced in the inner capillary. Two digital syringe pumps (Model 1000, New Era Pump System Inc., Farmingdale, NY, USA) were employed to produce a controlled flow rate. A fixed alginate flow rate were used, for Q_{Alg} = 1 mL min^{-1} and calcium chloride Q_{CaCl_2} = 5 mL min^{-1}. The calcium alginate fibers moved downward in the vertical laminar flow (this position is important to avoid clogging), while at the interface of both fluids, the Alg solutions met with the polycation (Ca^{2+}) from the $CaCl_2$ solution. A long outlet capillary tube was employed to form the calcium alginate gel on the fiber surface. The polymerized calcium alginate fibers were immediately collected in a beaker that contained 1000 cm^3 of $CaCl_2$ solution to the same concentration that was entered to the MFD.

2.3. Alginate calcium fiber diameter measurements

Measurements of the diameter of single alginate calcium fibers (D_{fiber}) were obtained using a stereo microscope (Olympus SZX7, Optical Co. Ltd., Tokyo, Japan), at magnifications up to 85.5×. Images were recorded with a digital CCD camera Cool Snap Pro Color (Photometrics Roper, Division Inc, Tucson, AZ, USA), processed and analyzed using Image-Pro Plus software (Media Cybernetics, Inc., Silver Spring, MD, USA). Ten samples were measured for each experimental run.

2.4. Moisture content

Moisture content of calcium alginate fibers (about 2–3 g from the container A, Fig. 2) were determined by drying the samples in a convective hot air oven at 105 °C until constant weight and expressed in percentage. Measurement were run in triplicates.

2.5. Mechanical properties measurements

Mechanical properties of calcium alginate fibers [tensile stress at fracture (σ_{max}), tensile strain at fracture or break ($\Delta L/L_0$) and apparent Young's modulus (E)] were measured at room temperature (25 °C) using a Universal Texture Analyser TA.XT2i (Stable Micro Systems, Godalming, Surrey, GU7 1YL, UK) in the tension mode. The calibration was carried out using a 5 kg load cell and initial grip separation was set at 50 mm. The specimen consist of a bundle of parallel, untangled, calcium alginate fibers, that is, a set of 20 fibers (Fig. 2). A constant deformation speed of 0.1 mm/s was

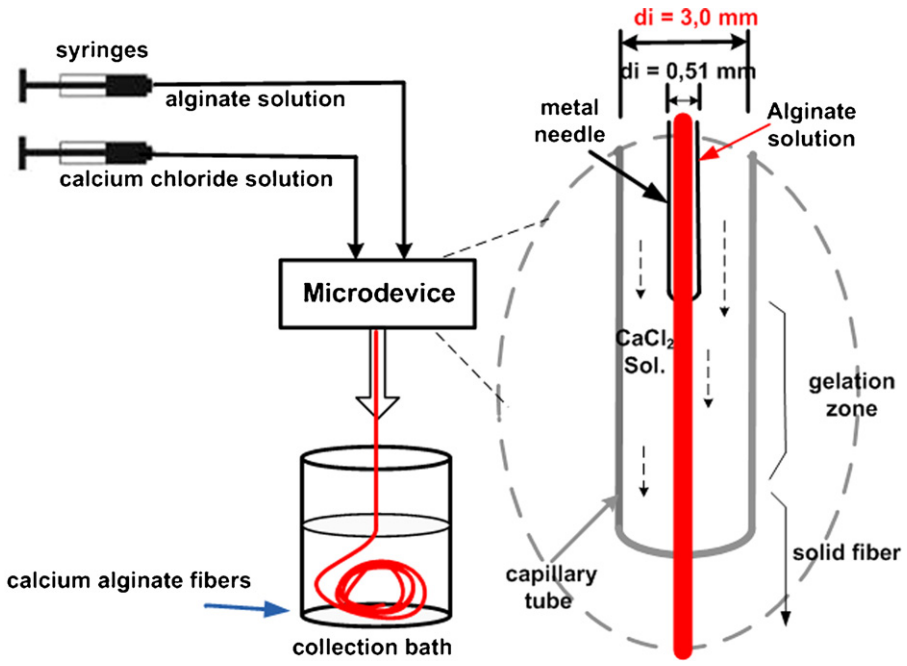

Fig. 1. Sketch of the experimental setup for generating calcium alginate fibers.

applied up to a tension strain beyond the break point. The force versus distance data was recorded for six replicates.

2.6. Experimental design and data analysis

The effect of the independent variables [Alg] and [$CaCl_2$] (in coded or real levels) on dependent variables MO (y_1) and MP [tensile stress at break (y_2), tensile strain at break (y_3) and apparent Young's modulus (y_4)] was studied using response surface (RS) methodology. The selected range of [Alg], between 1.25% and 2.5%, was chosen after performing preliminary experiments so that it was possible to continuously produce calcium alginate fibers with an almost constant diameter. Below the lower limit of [Alg] (<1.25%), we obtained very weak fibers, which did not record data of texture, and above the upper limit (>2.5%) we could not obtain continuous fibers, probably due to the high viscosity of the solutions of sodium alginate, making it difficult to have a continuous flow through the MFD. The coded levels (x) of independent variables were −1, 0 and +1 while the real levels (X_1 for [Alg]) were 1.25%, 1.875% and 2.5% and (X_2 for [$CaCl_2$]), 0.5%, 1.5% and 2.5%.

The experimental values of concentration (%) of sodium alginate solutions used in the experimental design correspond to 11.42, 17.13 and 22.84 mM; and the values that correspond to the calcium chloride solutions (%) are: 45.05, 135.16 and 225.27 mM. The amount of divalent cation, Ca^{2+}, required to react stoichiometrically with G-blocks can be calculated by considering that two guluronic acid units plus one divalent cation are required to create one ionic crosslink (Morris, Rees, Thom, & Boyd, 1978). The stoichiometric amount of Ca^{2+} required to saturate the carboxylates groups of alginate solutions are: 5.71, 8.57 and 11.42 mM. The values of the ratio ($Ca^{2+}{}_{experimental}/Ca^{2+}{}_{stoichiometric}$) vary from 3.9 (for [Alg] = 2.5% or 22.84 mM and [$CaCl_2$] = 0.5% or 45.05 mM) to 39.5 (for [Alg] = 1.25% or 11.42 mM and [$CaCl_2$] = 2.5% or 225.27 mM), and a value of 15.8 for the center point, where [Alg] = 1.875% or 17.13 mM and [$CaCl_2$] = 1.5% or 135.16 mM.

A 3-levels factorial design in 3 blocks which studied the effects of 2 factors ([Alg] and [$CaCl_2$]), was executed twice including an extra centerpoint per block, resulting in 24 runs (Table 1). All experiments were performed randomly and experimental data were analyzed to fit polynomial models as RS using an analysis of variance (ANOVA). Statistical significance was determined using the Statgraphics Plus software (Statistical Graphics Corporation, version 5.1, Rockville, USA), at a probability level of 0.05 ($p < 0.05$). A stepwise procedure was employed to simplify the models and three-dimensional surface plots were generated. The dependent variables were expressed individually as a function (Y) of the aforementioned independent variables (coded or real level of variables) using the following model polynomial Eq. (1):

$$Y = \beta_0 + \beta_1 x_1 + \beta_2 x_2 + \beta_{11} x_1^2 + \beta_{22} x_2^2 + \beta_{12} x_1 x_2 \quad (1)$$

3. Results and discussion

3.1. Effect of residence time on mechanical properties

Residence time was defined as the time during which the alginate fibers bundle remained exposed to the same [$CaCl_2$]. After producing a continuous fiber calcium alginate for about 5 min into the calcium chloride bath, the fiber was cut (Fig. 2), and measuring of residence time began. The residence time in Fig. 2 was the amount of time the fibers remained in the container A and B but the time in the first container was much higher than in the second ($t_A \gg t_B$). The container B was used solely to facilitate handling and formation of the fibers bundle of calcium alginate. Fig. 3 shows that the signatures derived from the mechanical testing of the bundle of fibers with [Alg] = 2% formed in [$CaCl_2$] = 0.5% were similar after a residence time exceeding 30 min. For other combinations of concentrations of the experimental design, the behavior was similar, not observed changes in mechanical properties of fibers after this time, so the tensile stress measurements were conducted at residence times greater than 30 min ($t > 30$ min). During exposure to the $CaCl_2$ bath the gelation interface moves from the surface to the centre of the fiber. As a first approach, the minimum gelation time can be obtained from Fick's second law $\partial C/\partial t = D(\partial^2 C/\partial x^2)$ expression which is possible to approximate as $C/t_{gel} \approx D(C/L^2)$ where L is a characteristic length given by radius of a cylindrical fiber (~200 μm), and D the diffusion coefficient of the calcium chloride in water: 10^{-9} m^2/s (Ribeiro et al., 2008). Thus the minimun gelation

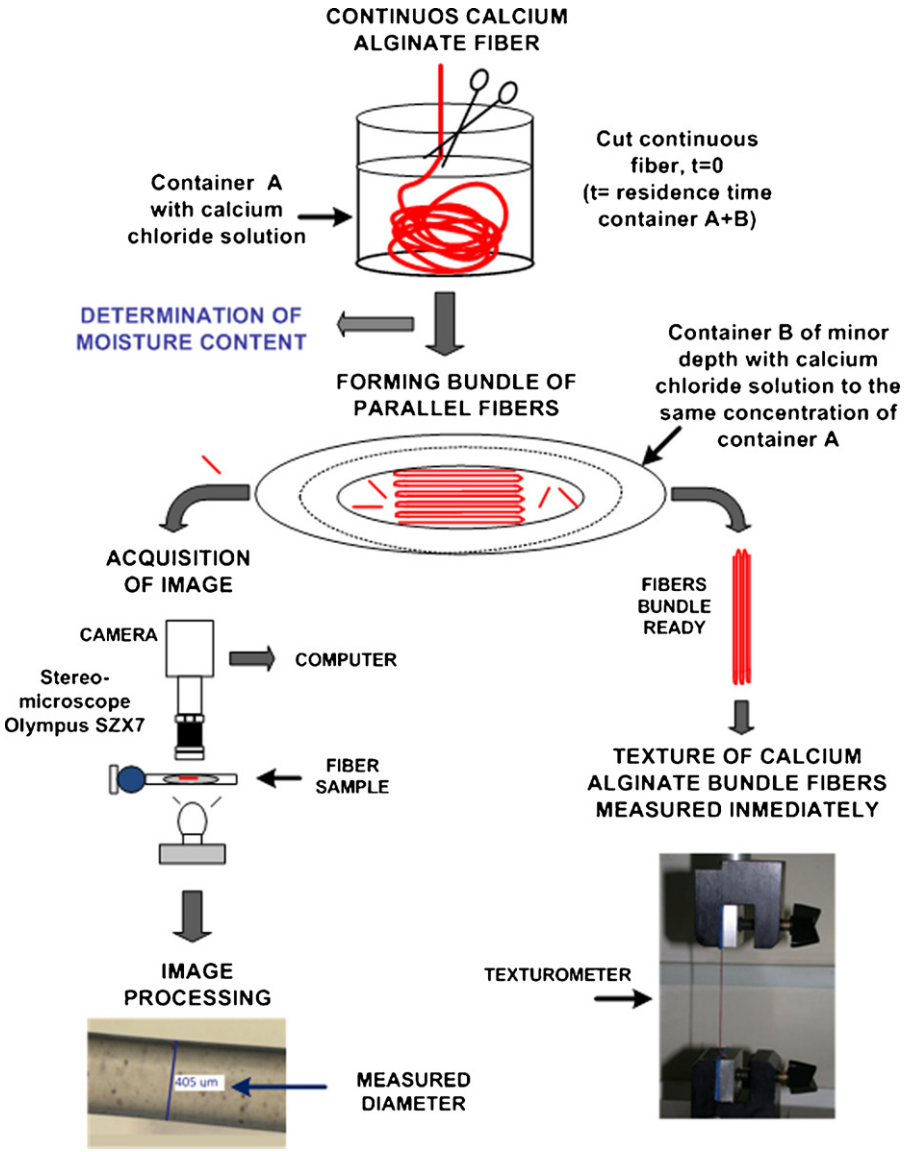

Fig. 2. Procedures showing moisture content, diameter of individual fibers and texture determinations of fiber bundles (total residence time t_{total}, is the sum of the times that the bundle of fibers is in containers A and B, $t_{total} = t_A + t_B$; $t_A \gg t_B$).

time, $t_{gel} \approx L^2/D$ is estimated be close to 40 s. This estimated time to gel was the minimum time that a fiber needs to gel completely assuming that D is constant. However, when the fiber begins to gel, D decreases and t_{gel} increases. The present experimental result was consistent with other reported studies where gelation depends on diffusion of calcium ions through interface or gel membrane that requires times from seconds (Shin et al., 2007) to several hours, e.g., up to 24 h for pieces of 3.2 cm diameter in the case restructured scallops (Roopa & Bhattacharya, 2008; Suklim, Flick, Marcy, Eigel, Haugh, & Granata, 2004).

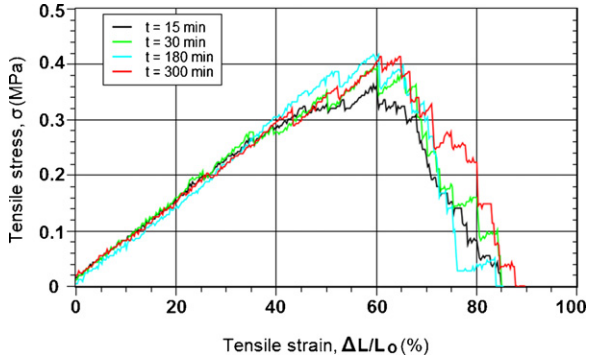

Fig. 3. Signatures of the mechanical test as a function of residence time in the $CaCl_2$ solution. Tensile stress (MPa) vs strain (%) for [Alg] = 2% and [$CaCl_2$] = 0.5%.

3.2. Diameter of fibers

The MFD used to produce alginate fibers was a slightly modified model of that developed by Skurtys and Aguilera (2009) and similar to the one reported by Shin et al. (2007) (Fig. 1). The fibers produced with the MFD had a uniform diameter (10% variation around mean diameter) and showed the advantage of being easily manipulated allowing the formation of fibers bundle (Fig. 2). The procedure for measuring the diameter of individual fibers is as shown in Fig. 2, the mean diameter was used to calculate the cross sectional area of the fibers bundle (Eq. (3)) and this value was used subsequently to calculate the tensile stress. The mean diameter of calcium alginate fibers ranged between 300-550 μm, Table 1.

Table 1
Experimental design in coded and real independent variables (x or X) and observed responses of the dependent variables (y).

Test N°	Sodium Alginate (%)		Calcium Chloride (%)		Diameter[a]	Moisture[a]	Mechanical properties		
	Coded level x_1	Real coded X_1	Coded level x_2	Real coded X_2	D_{fiber}, (μm)	MO (%) y_1	σ_{max} (MPa) Y_2	$\Delta L/L_0$ Y_3	E (MPa) y_4
1	−1.0	1.25	−1.0	0.5	365(26)	96.3(0.3)	0.260	0.372	0.459
2	0.0	1.875	0.0	1.5	461(34)	94.9(0.4)	0.465	0.733	0.540
3	1.0	2.5	1.0	2.5	548(16)	91.1(0.4)	0.354	0.686	0.324
4	0.0	1.875	0.0	1.5	451(41)	94.2(0.5)	0.437	1.052	0.540
5	0.0	1.875	−1.0	0.5	473(21)	94.7(0.2)	0.383	0.811	0.446
6	1.0	2.5	0.0	1.5	539(18)	93.6(0.4)	0.699	0.999	0.408
7	−1.0	1.25	1.0	2.5	301(34)	94.5(0.4)	0.230	0.930	0.171
8	0.0	1.875	0.0	1.5	456(37)	94.0(0.2)	0.424	0.773	0.563
9	1.0	2.5	−1.0	0.5	451(42)	95.4(0.2)	0.510	1.118	0.243
10	−1.0	1.25	0.0	1.5	408(37)	94.6(0.2)	0.330	0.525	0.533
11	0.0	1.875	1.0	2.5	439(32)	92.8(0.3)	0.424	1.143	0.217
12	0.0	1.875	0.0	1.5	461(46)	93.9(0.4)	0.432	1.110	0.485
13	−1.0	1.25	−1.0	0.5	374(27)	96.3(0.3)	0.263	0.370	0.378
14	0.0	1.875	0.0	1.5	455(34)	94.6(0.3)	0.454	0.842	0.498
15	1.0	2.5	1.0	2.5	530(27)	91.9(0.3)	0.362	0.683	0.322
16	0.0	1.875	0.0	1.5	461(39)	94.9(0.4)	0.442	0.843	0.523
17	0.0	1.875	−1.0	0.5	475(23)	95.1(0.3)	0.374	0.859	0.435
18	1.0	2.5	0.0	1.5	545(21)	93.2(0.4)	0.711	1.166	0.390
19	−1.0	1.25	1.0	2.5	292(32)	94.5(0.4)	0.216	0.841	0.186
20	0.0	1.875	0.0	1.5	471(27)	94.6(0.5)	0.444	0.732	0.499
21	1.0	2.5	−1.0	0.5	461(45)	95.3(0.2)	0.509	1.153	0.340
22	−1.0	1.25	0.0	1.5	399(25)	94.7(0.3)	0.339	0.490	0.568
23	0.0	1.875	1.0	2.5	446(34)	92.6(0.3)	0.427	1.148	0.217
24	0.0	1.875	0.0	1.5	436(19)	93.9(0.1)	0.475	0.804	0.508

[a] Average and standard deviation in parentheses for diameter and moisture content.

3.3. Effect of the factors on response surface (RS)

The RS graphs were obtained from the regression equations, keeping the response function on the Z-axis with X- and Y- axes representing the two independent variables related to concentration. The response functions were approximated by a second degree polynomial (Eq. (1)) with linear, quadratic and interaction effects (Table 2).

3.3.1. Moisture content

Fig. 4 shows contour plots of RS for moisture content (MO). The model estimates was statistically significantly ($p < 0.05$; $R^2 = 0.92$) and using the notation of Eq. (1), the best fit of the coded model is:

$$Y_1 = 94.2129 - 0.8408 \cdot x_1 - 1.2908 \cdot x_2 + 0.0938 \cdot x_1^2 - 0.1263 \cdot x_2^2 - 0.6755 \cdot x_1 x_2 \quad (2)$$

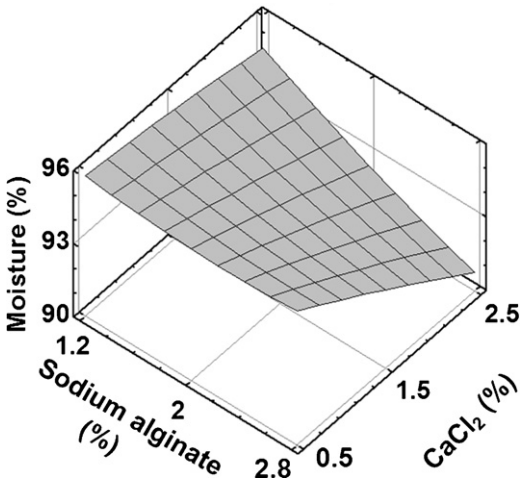

Fig. 4. Response surface for moisture content (MO) as a function of the concentration of sodium alginate and calcium chloride.

Regression coefficients and analysis of variance for MO are shown in Table 2 and maximum and minimum values of model are shown in Table 3. Fig. 4, indicate that MO decreased slightly with an increase in the [Alg] and decreases drastically with increasing the [$CaCl_2$]. Higher values of tensile strain ($\Delta L/L_0 \sim 100\%$ for [Alg] $\geq 1.8\%$) showed values of MO below 95%. An important variable in MP is the moisture content of calcium alginate fibers, so the presence of a high [$CaCl_2$] could affect the hydration of the alginate fibers showing a drastic decrease in MO. In alginate gels, the swelling rate constant decreases with an increase in the calcium concentration, indicating that the diffusion rate decreases at higher calcium concentrations (Davidovich-Pinhas & Bianco-Peled, 2010). High values in the tensile strain and low values in the tensile stress, could be related to the fact that water acts as plasticizer in fibers and reduces interactions between the adjacent chains in the biopolymers, making them more elastic thereby increasing mobility and flexibility of the fibers. This behavior was also observed in pigskin gelatin films (Bergo & Sobral, 2007).

3.3.2. Maximum tensile stress (σ_{max})

Maximum tensile stress (σ_{max}) was calculated by dividing the maximum force applied (at break) by the original cross-sectional area through which the force is applied (A_{bundle}). The cross-sectional area of the bundle of calcium alginate fiber was estimated from radius of a single fiber, R_{fiber}, multiplied by the number of fibers in the bundle (Eq. 3):

$$A_{bundle} = 20 \cdot \pi \cdot R_{fiber}^2 = \pi \cdot R_{bundle}^2 \quad (3)$$

Contour plots of RS for maximum tensile stress (σ_{max}) are depicted in Fig. 5. Strengthening and weakening of fibers were observed. The tensile stress increases with increasing [$CaCl_2$] up to a maximum around [$CaCl_2$] $\approx 1.41\%$ (Table 3), then values of tensile stress decreased (weakening) as [$CaCl_2$] increased. A similar pattern was observed by Mao, Tang, and Swanson (2000) for 1.5% mixed gellan gels (high acyl to low acyl ratio, 50/50) where a maximum tensile stress of 0.108 MPa was reported. In another study by Zhang et al. (2005) the authors concluded, on the contrary, that the tensile

Table 2
Coefficients of the regression equations for response functions (Y) in coded and real levels of independent variables.

Coefficients polynomial[a]	Coded level of variables				Real level of variables			
	Moisture	Mechanical Properties			Moisture	Mechanical Properties		
	MO (%) Y_1	σ_{max} (MPa) Y_2	$\Delta L/L_0$ Y_3	E (MPa) Y_4	MO (%) Y_1	σ_{max} (MPa) Y_2	$\Delta L/L_0$ Y_3	E (MPa) Y_4
β_0	92.2146	0.4693	0.8870	0.5164	96.5074	−0.0670	2.0956	0.2748
β_1	−0.8667*	0.1257*	0.1896*	−0.0223	−0.9187*	0.1472*	2.2924*	0.1377
β_2	−1.3083*	−0.0237	0.0622	−0.0720*	1.1329*	0.3036	0.6699	0.2666*
β_{11}	0.1313	0.0046	−0.1436*	−0.0352	0.336	0.0119	−0.3677*	−0.0901
β_{22}	−0.0938	−0.1130*	0.0517	−0.1814*	−0.0938	−0.1129*	0.0517	−0.1814*
β_{12}	−0.72*	0.0039	−0.2543*	0.0686*	−1.152*	0.0062	−0.4068*	0.1098*
mae	0.2789	0.0369	0.0935	0.0343	0.2789	0.0369	0.0935	0.0343
R^2	0.92	0.86	0.78	0.89	0.92	0.86	0.78	0.89

mae: the mean absolute error or the average value of the residuals. R^2: the R-squared statistic indicates that the model as fitted explains the % of the variability in the dependent variables.

[a] Polynomial model (coded variables): $Y = \beta_0 + \beta_1 x_1 + \beta_2 x_2 + \beta_{11} x_1^2 + \beta_{22} x_2^2 + \beta_{12} x_1 x_2$. Polynomial model (real variables): similar to above (change coded variables 'x' by real variable 'X'). Values x were −1, 0, and +1 (for both x_1 and x_2). Values X_1 were 1.25%, 1.875%, and 2.5%; values X_2 were 0.5%, 1.5%, and 2.5%. Y_1 = moisture content; Y_2 = tensile stress at break; Y_3 = tensile strain at break; Y_4 = apparent Young's Modulus.

* $p < 0.05$: effects have p-values less than 0.05, indicating that they are significantly different from zero at the 95% confidence level.

Table 3
Maximum and minimum values of the response functions in coded and real levels of independent variables.

Independent variables	MO (%) Y_1	σ_{max} (MPa) Y_2	$\Delta L/L_0$ Y_3	E (MPa) Y_4
Maximum (coded level of variables)				
x_1	−1.00	1.00	1.00	−0.63
x_2	−1.00	−0.09	−1.00	−0.32
Maximum value	95.71	0.60	1.18	0.53
Minimum (coded level of variables)				
x_1	1.00	−1.00	−1.00	−1.00
x_2	1.00	1.00	−1.00	1.00
Minimum value	91.36	0.21	0.29	0.18
Maximum (real level of variables)				
X_1	1.25	2.50	2.50	1.48
X_2	0.5	1.41	0.50	1.18
Maximum value	95.71	0.60	1.18	0.53
Minimum (real level of variables)				
X_1	2.50	1.25	1.25	1.25
X_2	2.50	2.50	0.50	2.50
Minimum value	91.36	0.21	0.29	0.18

stress increased with [$CaCl_2$] or [Alg]. Finally, the model estimating tensile stress was statistically significantly (Table 2) ($p < 0.05$; $R^2 = 0.86$) and using the notation of Eq. (1), the best fit of the coded model was the following (Eq. 4):

$$Y_2 = 0.4693 + 0.1257 \cdot x_1 - 0.0237 \cdot x_2 - 0.0046 \cdot x_1^2 - 0.1130 \cdot x_2^2 + 0.0039 \cdot x_1 x_2 \quad (4)$$

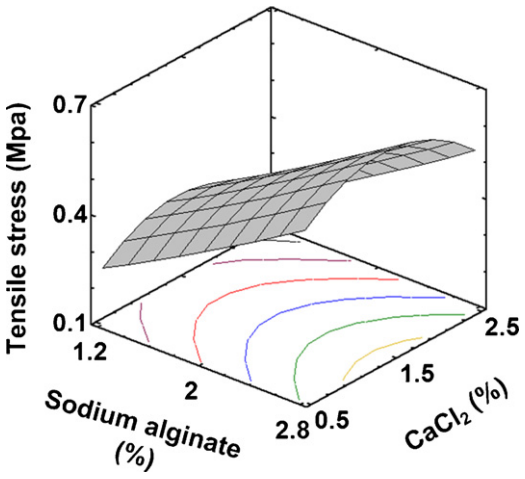

Fig. 5. Response surface for maximum tensile stress (σ_{max}) as a function of the concentration of sodium alginate and calcium chloride.

Regression coefficients and analysis of variance for tensile stress (Y_2) are shown in Table 2 and maximum and minimum values of the model are shown in Table 3. The maximum tensile stress varied between 0.2 and 0.6 MPa.

In practice, the stoichiometric amounts required to saturate the G-blocks of sodium alginate solutions is surpassed several times to reach the highest gel strength (Ca^{2+} = 127 mM or 1.41%), so the number of times of stoichiometric Ca^{2+} required at low concentrations of [Alg] is greater than for high concentrations. Therefore, for a solution of [Alg] = 1.0%, it required about 27 times the concentration of Ca^{2+} stoichiometric requirement, and for a solution of [Alg] = 3.0% required about 9 times.

Numerous studies concluded that the gel strength increases with increasing calcium concentration, since these studies used increasing concentrations of Ca^{2+} source to limit values relatively low (compared to those used in this study), for example up to 30 mM (Stokke et al., 2000), 35 mM (Zhang et al., 2005), 40 mM (Davidovich-Pinhas & Bianco-Peled, 2010). In this work, much higher concentrations (e.g., 225 mM Ca^{2+}) were used that allowed us to observe behavior of the response variables in a wider range [$CaCl_2$].

3.3.3. Tensile strain at break ($\Delta L/L_0$)

Tensile strain at break ($\Delta L/L_0$) was calculated by dividing the elongated distance of the fiber bundle at break by the initial length of the specimen (L_0 = 50 mm). A large tensile strain corresponds to a deformable material. Fig. 6 shows contour plots of RS for tensile

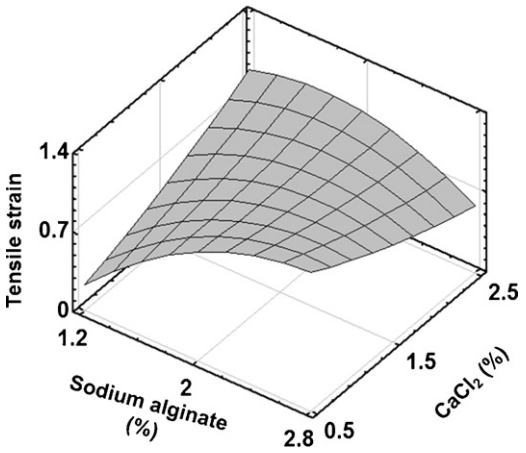

Fig. 6. Response surface for tensile strain ($\Delta L/L_0$) as a function of the concentration of sodium alginate and calcium chloride.

strain ($\Delta L/L_0$) as a function of [Alg] and [$CaCl_2$]. A statistically significant model ($p < 0.05$; $R^2 = 0.78$) was estimated and using the notation of Eq. (1) the best fit coded model was the following (Eq. 5):

$$Y_3 = 0.8870 + 0.1896 \cdot x_1 + 0.0622 \cdot x_2 - 0.1436 \cdot x_1^2 + 0.0517 \cdot x_2^2 - 0.2543 \cdot x_1 x_2 \quad (5)$$

Regression coefficients and analysis of variance for tensile strain at break are shown in Table 2 and values obtained from the model are exhibited in Table 3. The R^2 was <0.80, this could be attributed to the simplification of the model (Eq. (1) and Table 2), but also to experimental conditions (Draget et al., 2006). Fig. 6 shows values of tensile strain for calcium alginate fibers close to 100%, being the maximum value of tensile strain calculated (Table 3) of 1.18 for [Alg] = 2.5% and [$CaCl_2$] = 0.5%. Low tensile stress values showed high values of tensile strain and this may due to the low G residues content of the sample of alginate (16%). Other authors reported that the tensile strain was insensitive to [$CaCl_2$] or [Alg] (Zhang et al., 2005). Moreover, the tensile strain values obtained were higher than those reported in another study (Roopa & Bhattacharya, 2008) for cylindrical samples (40 mm in diameter and 10 mm in height), whose values were between 17.6% and 38.8% ([Alg] = 0.75 and 2.25%, respectively).

3.3.4. Apparent Young's modulus

The apparent Young's modulus of elasticity is defined as the initial slope of the stress–strain curve (before the break point). The apparent Young's modulus (E) was calculated using the slope of the curve between tensile stress and tensile strain (σ vs $\Delta L/L_0$) in the linear viscoelastic range (~15% secant modulus) (Fig. 7a).

Fig. 7b shows contour plots of RS for apparent Young's modulus (E). A statistically significant model ($p < 0.05$; $R^2 = 0.89$) was estimated and using the notation of Eq. (1) the best fit coded model is the following (Eq. 6):

$$Y_4 = 0.5164 - 0.0223 \cdot x_1 - 0.0720 \cdot x_2 - 0.0352 \cdot x_1^2 - 0.1814 \cdot x_2^2 + 0.0686 \cdot x_1 x_2 \quad (6)$$

Regression coefficients and analysis of variance for apparent Young's modulus (coded and real values) are shown in Table 2 and maximum and minimum values of the model are presented in Table 3. This bell-shaped behavior of E (Fig. 7b) as a function of concentration has also been observed in mixed gellan gels when

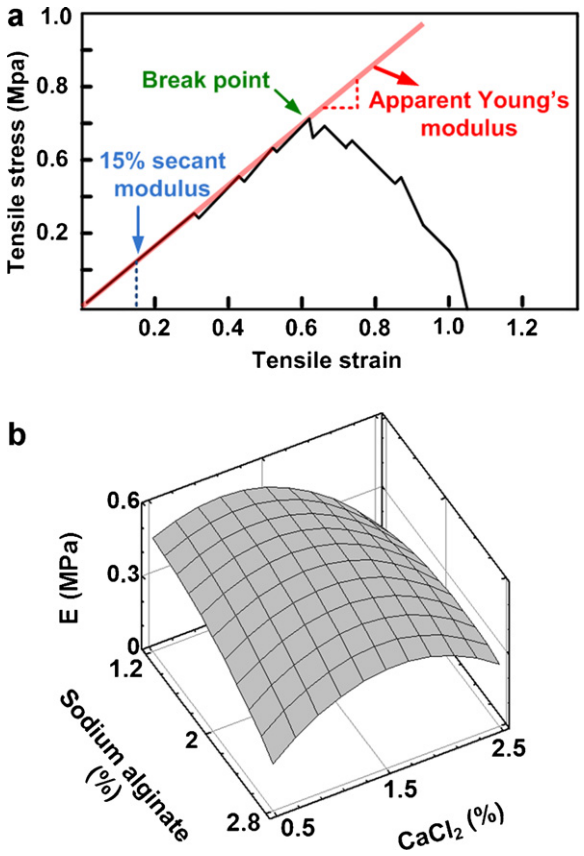

Fig. 7. (a) Apparent Young's modulus (slope of the stress–strain curve before the break point) at 15% secant modulus. (b) Response surface for apparent Young's modulus (E) as a function of the concentration of sodium alginate and calcium chloride.

[$CaCl_2$] increased (Mao et al., 2000). Highest values of apparent Young's modulus reported here are around 0.5 MPa, within the order of magnitude found for gels about 1 MPa (Yada, 2004) but higher than data reported for calcium alginate gels in other studies (Davidovich-Pinhas & Bianco-Peled, 2010; Suklim et al., 2004); however, samples of sodium alginate used has a higher content of G, 30% to 75% (Davidovich-Pinhas & Bianco-Peled, 2010). For foods scientists, the tensile stress at break often correlates better with the mouthfeel of a gel than does the elastic modulus (Draget et al., 2006). Figs. 5, 6 and 7b suggest that food fibers with different mechanical properties may be designed by properly selecting the levels of [$CaCl_2$] and [Alg]. Alginate occurs in the plant as of different metals, primarily sodium and calcium and its biological functions are salts principally of a structural nature (provide flexibility and strength) and as ion exchange species (Craigie, Morris, Rees, & Thom, 1984). The G-blocks have a high affinity for Ca^{2+}, and it is these ions which are mainly responsible for gel strength (Percibal, 1979; Sikorski et al., 2007). In general, the stiffness of the plant reflects the content of G-blocks, as result of their ability to form strong gels by crosslinking with calcium.

According to the results obtained, as the calcium alginate gel reaches its maximum strength, the amount of Ca^{+2} used for inter- and intra-chain associations is higher compared to that stoichiometrically required to saturate the G-blocks. It is possible that Ca^{+2} is not only required to saturate the carboxylates groups, but may also get involved to a lesser extent in Ca^{+2} associations with other components of the alginate. Some studies indicate that Ca^{2+} is also involved in the gelation of the M-blocks; however, the mechanical strength of calcium alginate gels is mainly due to junctions formed by the G-blocks with a strong auto-cooperative binding of Ca^{2+} between the chains in the gel state. The M-blocks and MG-blocks

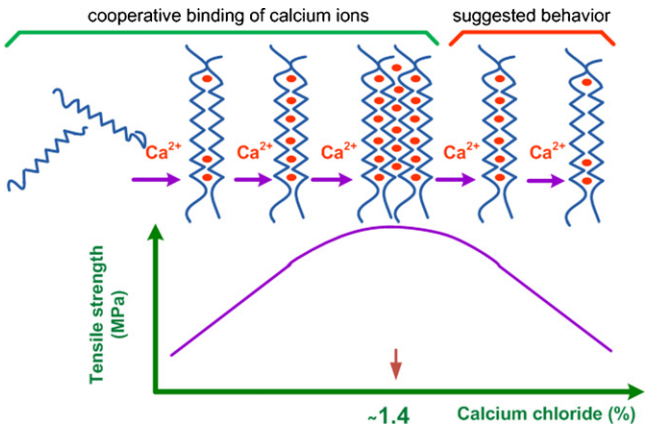

Fig. 8. Scheme suggesting a mechanism that explains the strengthening and weakening of calcium alginate fibers as a function of concentration of calcium chloride.

have much lower selectivity for Ca^{2+} and no autocooperative binding mechanism. Smidsrod (1974) concludes that the modulus of rigidity of gels formed by different cations is directly dependent on their ability to bind to the polyuronides by a cooperative inter-chain binding mechanism.

The results shown in Figs. 5, 6 and 7b indicate that may choose the gel strength tailor-made as a function of the [Alg] and [$CaCl_2$].

3.4. Toward a molecular understanding

In order to explain our experimental results, the effect of [$CaCl_2$] on MP of calcium alginate fibers a sketch was presented in Fig. 8. At low [$CaCl_2$], the Ca^{2+} ions contribute to the formation of junction zones that are assumed to consist of dimeric units or "egg-box dimers" (Vreeker et al., 2008). As a result, the gel is formed and MP are directly related to the number of "egg-box" sites formed and the increase in network crosslink density results in a higher fracture stress (Zhang et al., 2005). In the alginate, gel strength is directly related to the total content of G units and the average length of the G-blocks in the gelling polymer. A saturation point is reached when a maximum number of "egg-box" sites is attained leaving long polymeric chains between them (e.g., coinciding with a maximum tensile stress when [$CaCl_2$] ≈ 1.4%). Davidovich-Pinhas and Bianco-Peled (2010) reported an increase in the number of monomeric units within junction zones of alginate gels at high calcium concentration and suggested an increase lateral chain association which reduced the number of junction zones, thus, leading to a decrease in the modulus. The presence of a maximum value in tensile stress may indicate that an optimum number and size of binding sites in calcium alginate gels is attained. However, the literature is unclear as to whether the increase in modulus is caused by a higher strength of the junction zones or by a large number of them (Draget, 2000, Chap. 22).

Results of this study suggest that the "egg-box" model used to describe ionotropic gelation of alginate only partly explain the relation with microstructural and mechanical properties of the gelled material. According to the egg-box association scheme between G units (Grant et al., 1973), calcium ions induce chain-chain associations forming stable junction zones of dimers and later lateral interactions between dimers (left-hand side in Fig. 8). The decrease in gel strength observed after reaching the maximum force at a [$CaCl_2$] ≈ 1.4% or 127 mM, is a suggestion proposed based on the egg-box model (right-hand side in Fig. 8). The experimental evidence leading to this hypothesis is based on: (1) After the maximum in tensile strength due to interchain association is achieved the system will reverse to the formation of dimers with no association between dimers. As [$CaCl_2$] further increases, Ca^{2+} will only partially fill the G-blocks. Changes in cation concentration can alter the number of alginate strands held together in the "egg-box" model, thus altering the strength of the gel network (Simpson et al., 2004). It was found that the diffusion of calcium ions through the gel network was dependent on the initial concentration of calcium, the ionic strength of the alginate solution, and the size of pores in the gel which is formed (Potter, Balcom, Carpenter, & Hall, 1994). At higher [$CaCl_2$] the ionic strength of the sodium alginate solution may play a definite role in the gelling mechanism. It has been suggested that electrostatic interactions are the main driving force for the observed strengthening effects (Draget et al., 2006). (2) Due to the probable presence of intermolecular hydrophobic interactions that are involved in gelation of G-blocks (Tako & Kohda, 1997), leading to a reduction in connectivity between dimers in neighboring chains. As the size of these assemblies increases, their number decrease, with consequent reduction in connectivity and collapse (tight interchain chelation) (Morris, Rees, Thom, & Boyd, 1978). (3) The reasons for this behavior are not understood, but it appears that G-blocks lose affinity for Ca^{+2}. In this regard, the data register of X-ray diffraction for calcium alginate fibers indicate that the junction zone involves random pairs of polymer chains to form dimers through Ca^{2+} coordination according to the egg-box model and for reasons not fully understood, coordination of the Ca^{2+} cations reduces the ability for lateral packing of the dimers (Sikorski et al., 2007).

4. Conclusions

Calcium alginate fibers of continuous and uniform diameter were successfully produced using a microfluidic device and the mechanical properties were studied in controlled manner. For the sample of alginate used, It was shown that the tensile stress of fibers increased with the Ca^{2+} concentration up to a certain point (calcium chloride concentration around 1.4%) and beyond this value the tensile stress decreased. The presence of a maximum in tensile stress may indicate that a determined number and size of binding sites along the polymeric chains of fibers of calcium alginate is attained, and their mechanical properties are directly related to the number of "egg-box" sites formed.

This value (1.4% or 127 mM Ca^{2+}) is several times the stoichiometric requirement to saturate the polymer carboxylates groups. In order to explain the behaviour of the tensile strength beyond the maximum the "egg-box" model was completed. This suggest that the "egg-box" model used to describe ionotropic gelation of alginate only partly explain the relation with microstructural and mechanical properties of the gelled material. And allows the design and manufacturing of gels of calcium alginate with different mechanical properties by properly selecting the levels of concentration of calcium chloride and sodium alginate.

Acknowledgments

We gratefully acknowledge funding sources CONICYT (Comisión Nacional de Investigación Científica y Tecnológica) and FONDECYT project 1095199. We also appreciate the effort of Dr. Sobukola O. P. of the University of Agriculture Abeokuta, Nigeria, in the valuable discussions.

References

Belitz, H.-D., Grosch, W., & Schieberle, P. (Eds.). (2004). *Food Chemistry*. Berlin: Springer.

Bergo, P., & Sobral, P. J. A. (2007). Effects of plasticizer on physical properties of pigskin gelatin films. *Food Hydrocolloids*, *21*(8), 1285–1289.

Bhattarai, N., Li, Z., Edmondson, D., & Zhang, M. (2006). Alginate-based nanofibrous scaffolds: Structural, mechanical and biological properties. *Advanced Materials*, *18*, 1463–1467.

Braccini, I., & Pérez, S. (2001). Molecular basis of Ca^{2+}-induced gelation in alginates and pectins: The egg-box model revisited. *Biomacromolecules*, *2*(4), 1089–1096.
Craigie, J. S., Morris, E. R., Rees, D. A., & Thom, D. (1984). Alginate block structure in phaeophyceae from Nova Scotia: Variation with species, environment and tissue-type. *Carbohydrate Polymers*, *4*(4), 237–252.
Davidovich-Pinhas, M., & Bianco-Peled, H. (2010). A quantitative analysis of alginate swelling. *Carbohydrate Polymers*, *79*(4), 1020–1027.
Draget, K. (2000). Alginates. In G. O. Phillips, & P. A. Williams (Eds.), *Handbook of Hydrocolloids*. Woodhead Publishing Limited: Cambridge England.
Draget, K., Moe, S., Skjak-Braek, G., & Smidsrod, O. (2006). Alginates. In A. M. Stephen, G. O. Phillips, & P. A. Williams (Eds.), *Food Polysaccharides and Their Applications*. CRC Press-Taylor and FrancisGroup.
Espino-Díaz, M., Ornelas-Paz, J. D. J., Martínez-Téllez, M. A., Santillán, C., Barbosa-Cánovas, G. V., Zamudio-Flores, P. B., & Olivas, G. I. (2010). Development and characterization of edible films based on mucilage of opuntia ficus-indica(L.). *Journal of food science*, *75*(6), E347–E352.
Fabra, M. J., Talens, P., & Chiralt, A. (2010). Influence of calcium on tensile, optical and water vapour permeability properties of sodium caseinate edible films. *Journal of Food Engineering*, *96*, 356–364.
Fan, L., Du, Y., Huan, R., Wang, Q., Wang, X., & Zhang, L. (2005). Preparation and characterization of alginate/gelatin blend fibers. *Journal of Applied Polymer Science*, *96*, 1625–1629.
Grant, G. T., Morris, E. R., Rees, D. A., & Smith, P. J. C. (1973). Biological interactions between polysaccharides and divalent cations: The egg-box model. *FEBS Letters*, *32*, 195–198.
Lazaridou, A., Biliaderis, C. D., & Kontogiorgios, V. (2003). Molecular weight effects on solution rheology of pollulan and mechanical properties of its films. *Carbohydrate Polymers*, *52*, 151–166.
Mao, R., Tang, J., & Swanson, B. G. (2000). Texture properties of high and low acyl mixed gellan gels. *Carbohydrate Polymers*, *41*(4), 331–338.
Mikolajczyk, T., & Wolowska-Czapnik, D. (2005). Multifunctional alginates fibres with anti-bacterial properties. *Fibres & Textiles in Eastern Europe Industrial Engineering Chemistry Research*, *13*(3(51)), 35–40.
Moon, S., Ryu, B.-Y., Choi, J., Jo, B., & Farris, R. J. (2009). The morphology ad mechanical properties of sodium alginate based electrospun poly(ethylene oxide) nanofibers. *Polymer Engineering and Science*, *49*, 52–59.
Morris, E. R., Rees, D. A., Thom, D., & Boyd, J. (1978). Chiroptical and stoichiometric evidence of a specific, primary dimerisation process in alginate gelation. *Carbohydrate Research*, *66*(1), 145–154.
Percibal, E. (1979). The polysaccharides of green, red and brown seaweeds: Their basic structure, biosynthesis and function. *British Phycological Journal*, *14*(2), 113–117.
Potter, K., Balcom, B. J., Carpenter, T. A., & Hall, L. D. (1994). The gelation of sodium alginate with calcium ions studied by magnetic resonance imaging (MRI). *Carbohydrate Research*, *257*(1), 117–126.
Ribeiro, A. C. F., Barros, M. C. F., Teles, A. S. N., Valente, A. J. M., Lobo, V. M. M., Sobral, A. J. F. N., & Esteso, M. A. (2008). Diffusion coefficients and electrical conductivities for calcium chloride aqueous solutions at 298.15 K and 310.15 K. *Electrochimica Acta*, *54*(2), 192–196.
Roopa, B. S., & Bhattacharya, S. (2008). Alginate gels: I. Characterization of textural attributes. *Journal of Food Engineering*, *85*(1), 123–131.
Shin, S.-J., Park, J.-Y., Lee, J.-Y., Park, H., Park, Y.-D., Lee, K.-B., Whang, C.-M., & Lee, S.-H. (2007). On the fly continuous generation of alginate fibers using a microfluidic device. *Langmuir*, *23*, 9104–9108.
Sikorski, P., Mo, F., Skjak-Braek, G., & Stokke, B. T. (2007). Evidence for egg-box-compatible interactions in calciumâˆ'alginate gels from fiber X-ray diffraction. *Biomacromolecules*, *8*(7), 2098–2103.
Sime, W. J. (1990). *Food gels*. London/New York: Elsevier Applied Science.
Simpson, N. E., Stabler, C. L., Simpson, C. P., Sambanis, A., & Constantinidis, I. (2004). The role of the $CaCl_2$-guluronic acid interaction on alginate encapsulated BTC3 cells. *Biomaterials*, *25*(13), 2603–2610.
Skurtys, O., & Aguilera, J. M. (2008a). Applications of microfluidic devices in food engineering. *Food Biophysics*, *3*, 1–15.
Skurtys, O., & Aguilera, J. M. (2008b). Structuring bubbles and foams in gelatine solutions within a circular microchannel device. *Journal of Colloid and Interface Science*, *318*, 380–388.
Skurtys, O., & Aguilera, J. M. (2009). Formation of O/W macroemulsions with a circular microfluidic device using saponin and potato starch. *Food Hydrocolloids*, *23*(7), 1810–1817.
Skurtys, O., Bouchon, P., & Aguilera, J. M. (2008). Formation of bubbles and foams in gelatine solutions within a vertical glass tube. *Food Hydrocolloids*, *22*, 706–714.
Smidsrod, O. (1974). Molecular basis for some physical properties of alginates in the gel stat. *Faraday Discussion Chemical Society*, *57*, 263–274.
Stokke, B. T., Draget, K. I., Smidsrod, O., Yuguchi, Y., Urakawa, H., & Kajiwara, K. (2000). Small-angle X-ray scattering and rheological characterization of alginate gels. 1. Ca–Alginate gels. *Macromolecules*, *33*, 1853–1863.
Suklim, K., Flick, G. J., Marcy, J. E., Eigel, W. N., Haugh, C. G., & Granata, L. A. (2004). Effect of cold-set binders: Alginates and microbial transglutaminase on the physical properties of restructured scallops. *Journal of Texture Studies*, *35*, 634–642.
Tako, M., & Kohda, Y. (1997). Calcium induced association characteristics of alginate. *Journal of Applied Glycoscience*, *44*(2), 153–159.
Tonnesen, H. H., & Karlsen, J. (2002). Alginate in drug delivery systems. *Drug development and industrial Pharmacy*, *28*(6), 621–630.
van der Goot, A., Peifhambardoust, S., Akkermans, C., & van Oosten-Manski, J. (2008). Creating novel structures in food materials: The role of well-defined shear flow. *Food Biophysics*, *3*, 120–125.
Vreeker, R., Li, L., Fang, Y., Appelqvist, I., & Mendes, E. (2008). Drying and rehydratation of calcium alginate gels. *Food Biophysics*, *3*, 361–369.
Walstra, P. (2003). Soft solids. In *Physical Chemistry of Foods*. Marcel Dekker: New York Basel., p. 683.
Wang, C., Liu, H., Gao, Q., Liu, X., & Tong, Z. (2008). Alginate–calcium carbonate porous microparticle hybrid hydrogels with versatile drug loading capabilities and variable mechanical strengths. *Carbohydrate Polymers*, *71*(3), 476–480.
Yada, R. Y. (2004). *Proteins in Food Processing*. Cambridge: CRC Woodhead Publishing Limited.
Zhang, J., Daubert, C. R., & Foegeding, E. A. (2005). Fracture analysis of alginate gels. *Journal of food science*, *70*(7), E425–E431.

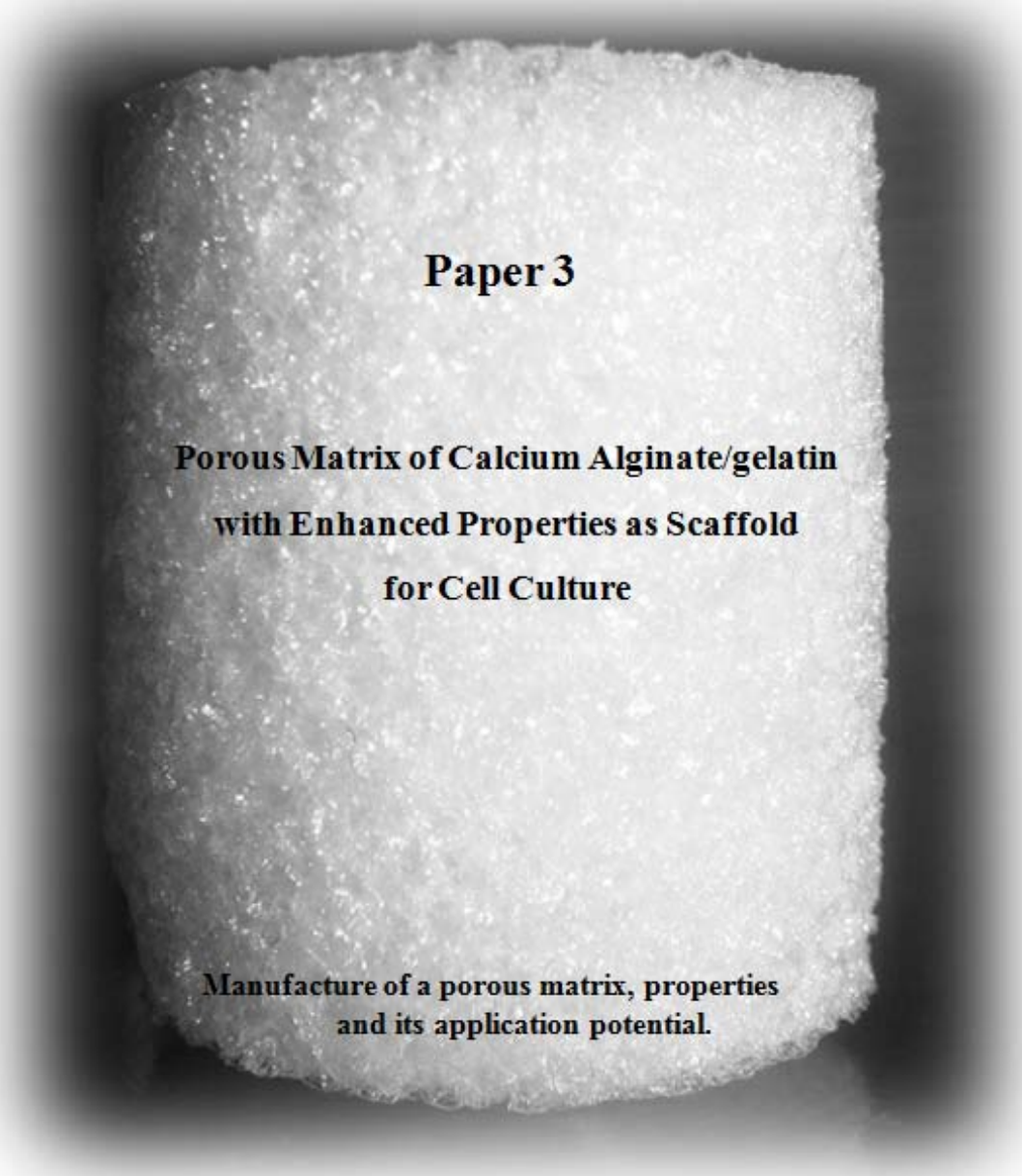

Paper 3

Porous Matrix of Calcium Alginate/gelatin with Enhanced Properties as Scaffold for Cell Culture

Manufacture of a porous matrix, properties and its application potential.

JOURNAL OF THE MECHANICAL BEHAVIOR OF BIOMEDICAL MATERIALS 46 (2015) 331–342

Available online at www.sciencedirect.com

ScienceDirect

www.elsevier.com/locate/jmbbm

Research Paper

Porous matrix of calcium alginate/gelatin with enhanced properties as scaffold for cell culture

Teresa R. Cuadros[a,*], *Alejandro A. Erices*[b], *José M. Aguilera*[a]

[a]*Department of Chemical and Bioprocess Engineering, School of Engineering, Pontificia Universidad Católica de Chile, PO Box 306, Santiago 22, Chile*

[b]*Department of Cell and Molecular Biology, Faculty of Biological Sciences, Pontificia Universidad Católica de Chile, PO Box 114-D, Santiago, Chile*

ARTICLE INFO

Article history:
Received 19 June 2014
Received in revised form
20 August 2014
Accepted 27 August 2014
Available online 3 February 2015

Keywords:
Alginate
Gelatin
Aerated porogen
Scaffold
High porosity
Cell culture

ABSTRACT

Hydrophilic polysaccharides can be used to prepare porous matrices with a range of possible applications. One such application involves acting as scaffolds for cell culture. A new homogeneous and highly porous biopolymeric porous matrix (BPM) of calcium alginate/gelatin was produced by following a simple process. The key to this process was the selection of the porogen (aerated gelatin). The preparation technique comprises the following steps: incorporating the porogen into the solution of alginate (3%), molding, cross-linking the alginate in 1.41% $CaCl_2$ (maximum gel strength; Cuadros et al., 2012. Carbohydr. Polym. 89, 1198–1206), molding, leaching and lyophilization. Cylinders of BPM were shown to have a relative density of 0.0274 ± 0.002, porosity of $97.26 \pm 0.18\%$, an average internal pore size of 204 ± 58 μm and enhanced mechanical properties, while imbibing more than 11 times their dry weight in water. In vitro cell culture testing within BPM using mesenchymal stem cells was demonstrated by MTT assays and expression of alkaline phosphatase. The BPM provided a suitable microenvironment for seeding, adhesion, proliferation and osteogenic differentiation of cells. The preparation technique and resulting porous matrix represent potential tools for future study and further applications.

1. Introduction

Porous matrices from biomaterials take the form of solid foams, sponges, clusters of air cells, cellular solids or scaffolds. Several biopolymers are used to generate porous matrices which included collagen (Chimenti et al., 2011), gelatin (Chimenti et al., 2011; Liu and Ma, 2009; Sisson et al., 2010; Van Vlierberghe et al., 2007), silk (Jin et al., 2004), alginate (Alnaief et al., 2011; De Moura et al., 2005; Eiselt et al., 2000; Kaklamani et al., 2014; Ming-Hua et al., 2004), and chitosan (Geng et al., 2005; Ming-Hua et al., 2004).

Polysaccharides are widely used for their solubility in water, stability to pH variations and lack of toxicity (Barbosa et al., 2005). Alginate is a natural linear polysaccharide copolymer composed of two uronic acids units: β-(1,4) linked D-mannuronic acid (M) and α-(1–4) linked L-guluronic acid (G).

*Corresponding author. Tel.: +562 23544927, 562 23544264; fax :+562 23545803.
E-mail address: tcuadroc@uc.cl (T.R. Cuadros).

http://dx.doi.org/10.1016/j.jmbbm.2014.08.026
1751-6161/

It contains varying quantities and sequences of three types of blocks (M–M, G–G, and M–G) and has the ability to form strong thermoresistant gels. These are produced by cross-linking with calcium ions within the G-block units to form local molecular arrangements known as "egg box" (Alnaief et al., 2011; Drury and Mooney, 2003; Grant et al., 1973; Sikorski et al., 2007; Simpson et al., 2004). This is performed under mild conditions at low temperatures and in the absence of organic solvents.

Alginate is widely used because of its non-toxicity, biodegradability and high biocompatibility (Kaklamani et al., 2014). Alginate gel is widely used in medical applications (Mikos et al., 2006; Ribeiro et al., 2004; Wang et al., 2008), such as tissue engineering (TE) (Petrenko et al., 2011). Gelatin is a protein derived from denatured collagen and is the major constituent of skin, bones and connective tissues. As a thermally reversible gelling agent, it can be used for encapsulation in food, cosmetics and pharmacology. It is also particularly useful in tissue engineering given its biodegradability, biocompatibility and non-immunogenicity (Wang et al., 2012; Yao et al., 2012). Calcium chloride is one source of divalent cations that has been widely used in biomedicine (Fan et al., 2005; Szymanski and Feinberg, 2014) for a long time, without any reports of calcium ions causing damage and/or affecting cell survival (Cao et al., 2012; Simpson et al., 2004). Calcium is preferred for applications in bone tissue as it is the principal ion in the extracellular matrix (ECM) (Morais et al., 2013). Furthermore, the calcium ion is both intra- and extracellular and has tremendous versatility as it is responsible for controlling several cellular processes such as: fertilization, proliferation, development, learning and memory, contraction and secretion (Berridge et al., 2000).

In general, high-G alginates produce strong but brittle gels, while high-M alginates produce weaker, more elastic and freeze/thaw stable gels (Sriamornsak et al., 2007). It has been shown that the strength of the alginate gel network is an important factor that influences the growth characteristics of encapsulated cells. While changes in gel strength affect the growth characteristics of the cells, high-M alginates are not sensitive to such changes (Simpson et al., 2004). The effect of the concentrations of $CaCl_2$ on the mechanical properties of calcium alginate fibres was studied; in it the maximum tensile stress was determined and was produced with a 1.41% (w/v) or 127 mM concentration of calcium chloride (Cuadros et al., 2012). A similar concentration of $CaCl_2$ (100 mM) has been used for two decades as a standard protocol for encapsulation and no toxic effects have been reported (Simpson et al., 2004).

To mimic the biological functions of native extracellular matrices, highly biocompatible scaffolds that promote cell adhesion and growth are essential (Leong et al., 2003). Besides biocompatibility, scaffolds must also demonstrate high porosity and interconnectivity of pores in order to promote cell seeding and growth. This is because the regeneration of tissues requires different microenvironments with suitable pore sizes. For TE cell in-growth and improvement of the transportation of nutrients requires porosities higher than 90% (Freyman et al., 2001; Leong et al., 2003). In terms of pore size, a range between 200 and 400 μm has been suggested for in vitro bone tissue regeneration (Leong et al., 2003), while another study recommends sizes between 300 and 500 μm (Hutmacher, 2000). The matrix must also have sufficient mechanical integrity during in vitro cell culture to maintain the spaces required for cell in-growth and tissue development (Drury et al., 2004). Mesenchymal stem cells (MSCs) are primitive multipotent cells that are able to differentiate various cell types. They can easily be isolated and propagated in vitro and are therefore suitable for bone TE as they exhibit two important properties: self-renewal and multi-lineage differentiation (Eslaminejad et al., 2006; Heng et al., 2004).

Several manufacturing techniques have been developed to confer porosity and homogeneity to porous matrices in order to improve the uptake, distribution and transport of different fluids and their components. There are many top-down techniques, including porogen-leaching (Studenovská et al., 2008; Weng and Wang, 2001; Zhang et al., 2006), gas foaming (Eiselt et al., 2000), thermally induced phase separation (TIPS) (liquid–liquid demixing and solid–liquid demixing, freeze-fixation, freeze-gelation) (Cheng-Hsuan et al., 2007; Holzwarth and Ma, 2011; Liu and Ma, 2009; Van Vlierberghe et al., 2007; Zmora et al., 2002), and lyophilization (direct method). Lyophilization is normally included at the end of any procedure for manufacturing porous matrices, as it is a way of directly removing the water from the frozen system. However, these top-down techniques have limitations, such as lack of mechanical strength, problems with residual solvent, lack of control over microstructure, presence of toxic residual porogens, nonporous external surface, close pore architecture, limited interconnected pores, small pores sizes or highly irregular pores, besides being tedious and time-consuming to fabricate (Leong et al., 2003; Martynov et al., 2010; Yao et al., 2012). For example, in freezing methods such as fixation by freezing and freeze-gelation, the architecture of the air cells showed elongated pores, the size of which differed from the top to the bottom of the matrix (Cheng-Hsuan et al., 2007; Ming-Hua et al., 2004). Producing biocompatible scaffolds for TE requires structures that have suitable macro-properties such as spatial form, mechanical strength, density and porosity, and micro properties such as pore size, pore size distribution and interconnectivity (Leong et al., 2003).

This study expects to overcome most of the limitations of the literature. The authors propose the development of a top-down production method resulting in a structure that is suitable for TE. The suitability of the structure is defined by both the macro properties as spatial form, strength, density and porosity homogeneous scaffolds; and micro properties such as pore size and interconnectivity. Therefore, the objective of this study is to develop a top-down technique for preparing a biopolymeric porous matrix (BPM) made primarily of alginate. A further objective was to determine the physical, mechanical and microstructural properties of the BPM. In vitro tests were also conducted to demonstrate the adhesion, growth and cell differentiation within the porous matrix.

2. Materials and methods

2.1. *Materials*

Sodium alginate (Alg) powder (Gelymar, Natural Extracts S.A., Chile) from *Macrocystis pyrifera* with an average composition

of 16% G [α-L-guluronic acid], 38% M [β-D-mannuronic acid] and 46% of MG alternating units (low viscosity, 50–200 cP for 1% solution at 20 °C). Gelatin Leiner, extra fine grade of 240 Bloom powder (Code 901553) was kindly supplied by Floramatic Ltd., Chile. A solution of calcium chloride ($CaCl_2$) with a concentration of 1.41% w/v was prepared based on anhydrous salt $CaCl_2 \cdot 2H_2O$ (CA-0520, Heyn, Santiago, Chile). Glass tubes (2.0 cm internal diameter and 15 cm height) open at both ends were used to prepare cylindrical specimens.

2.2. *Preparation of porous matrices*

A biopolymeric porous matrix (BPM) and control matrix (CM) of calcium alginate/gelatin were produced by following the scheme presented in Fig. 1and using three solutions (I, II, III) containing two biopolymers (alginate and gelatin) prepared with distilled water. Solution I consisted of 3% Alg (w/w) and was stored at 15 °C. In solution II, gelatin 10% (w/w) was dissolved in cold water and heated to 70 °C to complete dissolution. In solution III, gelatin 10% (w/w) was dissolved in cold water and heated to 70 °C to complete dissolution, and upon cooling (between 28 and 30 °C) it was subjected to mechanical agitation with a blender (10,000 RPM for 1 min) and converted into a flowable foam (room temperature, 20 °C).

Biopolymeric porous matrix (BPM) of a mixture alginate/gelatin was prepared as follows. Solution I and the foamed gelatin solution (solution III) were mixed in a 70:30 weight ratio, filled into glass tubes and stored overnight at 4 °C, to induce further gelling of gelatin. After a brief bath (~2 s) of the tubes in water at 60 °C, the contents of the tubes were immersed for 3 h in a 1.41% (w/v) $CaCl_2$ solution (maximum strength of alginate gel (Cuadros et al., 2012)), re-introduced in the glass tubes and stored overnight at 4 °C. Gelled pieces were cut into cylinders (22 mm height) and leached thrice with distilled water (with stirring) at 65 °C (30 min each) to remove as much gelatin (the porogen) as possible. The samples of the leached CaAlg porous gel were lyophilized in a VirTis Lyophilizer (Genesis 25 ES Freeze Dryer, SP Industries, Gardiner NY) after rapid cooling to −40 °C and exposure to vacuum at −10 °C over three days (to complete drying).

Control matrix (CM) was prepared by mixing the solutions I (15 °C) and II (30 °C) to yield a final solution containing 3% alginate and 1% gelatin (minimum concentration required to

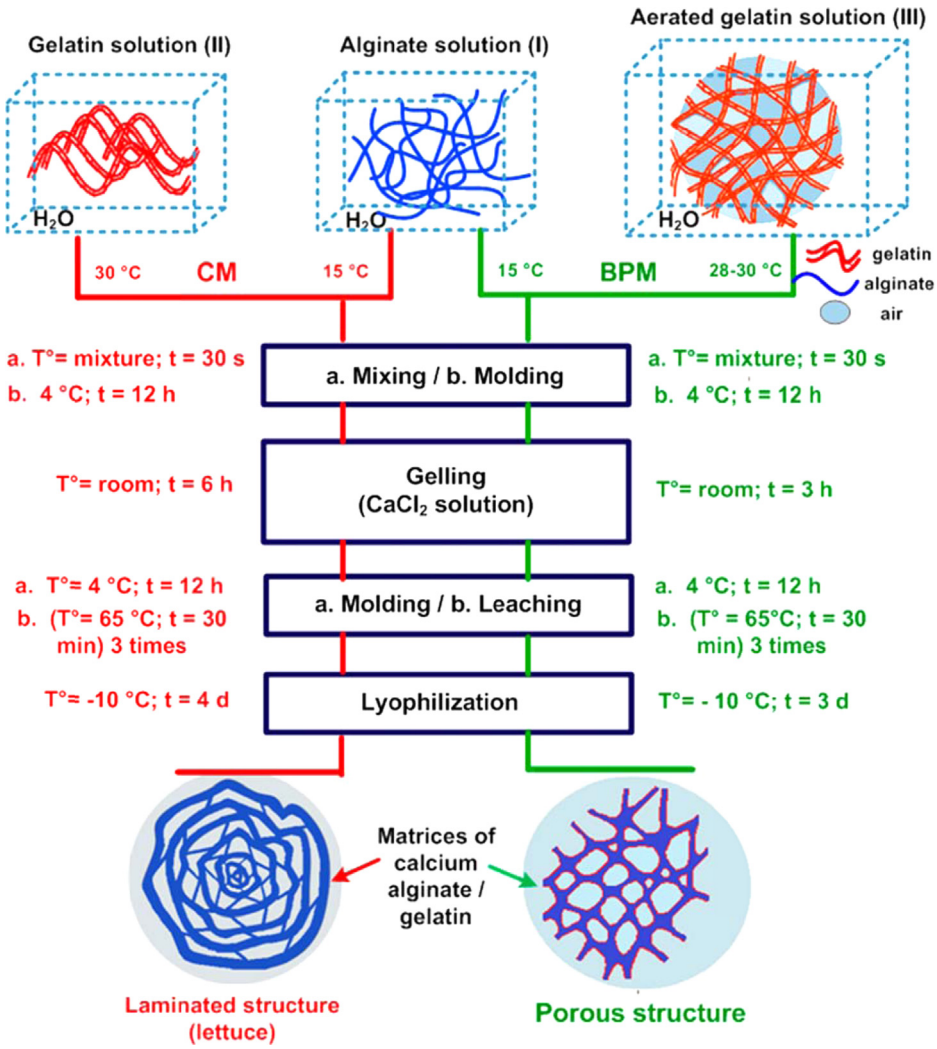

Fig. 1 – Scheme of preparation procedure for control matrix (CM) and biopolymeric porous matrix (BPM). Stages with temperature (*T*) and time (*t*) (not to the same scale).

mold the alginate), filled into glass tubes and stored overnight at 4 °C, to induce further gelling of gelatin. After a brief bath (~2 s) of the tubes in water at 60 °C, the contents of the tubes were immersed for 6 h in a 1.41% (w/v) $CaCl_2$ solution, re-introduced in the glass tubes and stored overnight at 4 °C. Gelled pieces were cut into cylinders (22 mm height) and leached thrice with distilled water (with stirring) at 65 °C (30 min each) to remove as much gelatin as possible. Then samples were lyophilized after rapid cooling to −40 °C and exposed to vacuum at −10 °C over four days (to complete drying). Then, both freeze-dried matrices (BPM and CM) were stored in desiccators over phosphorous pentoxide at zero relative humidity before further analysis.

Three terms that are used throughout this paper are wet samples, lyophilized samples and rehydrated samples. The wet samples refer to the gelled samples in the manufacturing process, prior to lyophilization. The lyophilized samples are the samples that are obtained at the end of the manufacturing process, while rehydrated samples are the lyophilized samples that have been subjected to hydration.

2.3. Morphological analyses

The porous structure of BPM was observed with a light microscope (Olympus SZX7, Optical Co. Ltd., Tokyo, Japan) and images were taken with a digital camera (CoolSnap-Pro Color, Photometrics Roper Division, Inc., Tucson, AZ). The surface morphology of BPM and the CM were also examined using a scanning electron microscopy (SEM JEOL-JSM 5300, Jeol Ltd., Tokyo, Japan) operated at an acceleration voltage of 20 kV. Freeze-dried specimens were fixed to a metal stub with double-sided tape and covered with gold using a sputter coater. The average pore diameter (pore size) of the BPM structure was estimated after image processing and measured using Image Pro-Plus 4.5 imaging software (Media Cybernetics, Inc., Silver Spring, MD). The BPM subjected to tests of in vitro cell culture was viewed with an Olympus CK2 inverted optical microscope. Cell viability was assessed by an MTT assay (Molecular Probes, Eugene, OR, USA) and cellular activity by evaluating the alkaline phosphatase activity (Sigma-Aldrich Inc, St. Louis, MO, USA).

2.4. Volume

Variations in volume were calculated for the two specimens (CM and BPM) as V/V_O, where V_O is the volume of the solutions before gelation (6.9 cm^3), and V, the measured volume of the wet, lyophilized, rehydrated and compressed cylindrical gels. Volumes were calculated by two methods: (1) as a cylinder after measuring the diameter and height of the samples, and (2) by volumetric displacement using poppy seeds (0.5–1 mm average size) and purified and calcined sand (0.1–0.3 mm, Heyn, Santiago, Chile).

2.5. Porosity

Porosity (ϕ) was determined using the density method based on the air space within the matrix, known as apparent porosity (ϕ_{app}). This is defined as the ratio of the volume of air space or voids to the total volume. Apparent porosity is calculated based on the solid density (ρ_S), and apparent density (ρ_{app}) by using Eq. (1) and expressed as (%)

$$\phi_{app} = 1 - \left(\frac{\rho_{app}}{\rho_S}\right)100 \quad (1)$$

where ρ_{app}/ρ_S is defined as the relative density. Solid density (ρ_S) is the density of the solid material, excluding any internal pores (filled with air). One way to calculate this is by dividing the sample weight by the volume after destroying all air spaces. This destruction was not possible in the BPM because the material is strong and flexible. As the solid fraction of BPM is an alginate/gelatin mixture, the solid density (ρ_S) has been estimated by taking the value for materials such as cellulose and most foods polymers (e.g., starch, protein, gelatin), this value is in the order of 1.5 g/cm^3 (Gibson and Ashby, 1997; Liu and Ma, 2009; Nussinovitch et al., 2004; Peleg, 1997). ρ_{app} was calculated as the ratio of the mass (m) to the sample volume (V).

2.6. Rehydration of dried samples or water uptake

Freeze-dried samples were immersed in excess water (i.e., in a ratio 1:500, w/w) at 20 °C for 30 h until they reached constant weight. The water uptake capacity (WU) of samples was calculated by Eq. (2):

$$\mathrm{WU} = \frac{(W - Wo)}{Wo} \quad (2)$$

where Wo is the weight of dried gel and W is the weight of gel at equilibrium.

2.7. Mechanical properties

Mechanical properties [maximum elastic stress, and apparent Young's modulus] of wet, freeze-dried and rehydrated samples were obtained at room temperature (20 °C) using a Universal Texture Analyser TA.XT2i (Stable Micro Systems, Godalming, Surrey, UK) calibrated using a 5 kg load cell. Cylindrical samples were subjected to uniaxial compression stress with a descending lubricated acrylic plate (70 mm diameter) up to 80% deformation at a constant rate of 0.5 mm/s. During testing the sectional area of compressed samples, even under fairly large deformation, remained almost unchanged. A compressive strength was defined as the maximum stress observed at the end of linear elastic region of the stress–strain curve (e.g., between 5 and 12% strain) and an apparent Young's modulus (E) was calculated as the slope of the line stress vs strain by Eqs. (3) and (4):

$$\sigma = \frac{F}{A_O} \quad (3)$$

$$\varepsilon = \frac{\Delta H}{H_O} \quad (4)$$

where stress$=\sigma$ and strain$=\mathcal{E}$, F=force; ΔH=absolute deformation, $H_O - H(t)$; A_O and H_O are the initial cross-sectional area and height of the sample, respectively. The compression force versus distance data were determined in quintuplicate and reported as an average value.

2.8. Cell culture

These tests were intended to demonstrate the growth of human adipose-derived MSCs in the porous 3D structures. BPM scaffolds, made into sheets of 3 mm thickness in Petri dishes, were autoclaved, cut into pieces and placed in 24-wells of culture dishes. MSCs were suspended (10^6 cells/mL) in a Dulbecco's modified Eagles's medium (DMEM; Gibco, Paisley, UK) supplemented with 10% fetal bovine serum (FBS, HyClone, Logan) and antibiotics, seeded (100 μL of cell suspension) on BPM and maintained at 37 °C in a humidified atmosphere containing 5% CO_2. After 24 h, to allow cell adhesion, wells were replenished with a culture medium. To analyze cell adhesion and viability, MTT assay ([3-(4,5-dimethylthiazol-2-yl)-2,5-diphenyltetrazolium bromide], Molecular Probes, Eugene, OR) was developed after 7 days. MTT is taken up by cells and reduced in the mitochondria to an insoluble blue product observed under the microscope. To analyze MSCs osteogenic differentiation cells were induced with an osteogenic medium (0.1 mM dexamethasone, 10 mM β-glycerol phosphate and 50 mM ascorbate-2-phosphate) during two weeks, and alkaline phosphatase activity was assessed by a cytochemical analysis or colorimetric assay as an osteogenic marker (Erices et al., 2000, 2002).

2.9. Statistical analysis of data

One-way analysis of variance (ANOVA) assuming a confidence level of 95% ($p<0.05$) was performed using Statgraphics Centurion XV software 2006 (Manugistics Inc., Statistical Graphics Corporation, Rockville, USA). Data were expressed as mean ± standard deviation.

3. Results

Recapitulating, the method of preparation of BPM involved the following steps: (1) incorporation of porogen (aerated gelatin, solution II) to alginate 3% (solution I); (2) molding and cooling (4 °C, gelation of gelatin); (3) gelation of alginate at room temperature in 1.41% $CaCl_2$ (maximum gel strength) and molding at 4 °C (to define the form); (4) leaching with hot water to remove the gelatin, and (5) lyophilization, (Fig. 1).

3.1. Manufacturing process. Physical and microstructural appearance

To develop the production process for this scaffold, it was necessary to review and replicate various top-down methods and evaluate their resulting matrices. Among these methods, techniques for generating pores in the matrix, such as porogen–leaching, were tested, resulting in heterogeneous matrices. Subsequently, interest developed in gas entrapment by injection and the use of surfactants, among others. From this, the idea of using foam forming proteins emerged. Some proteins were tested, but better results in terms of behavior and properties were obtained using gelatin. The final step was to determine the optimum levels of concentration and proportion by trial and error.

The alginate solutions showed stability for a long period at room temperature in a pH range of 5–10 (Draget et al., 2006; Fennema, 1985). The resulting scaffold (BPM) demonstrates a near-neutral pH (7.2) in an aqueous solution and stability for long periods (dehydrated samples were stored over two years at ambient conditions). The volume of solution II (10% gelatin) increased by ~100% (99.99 ± 1.72%) due to the incorporation of air, resulting in a foamy white fluid (solution III). The presence of air favored the subsequent gelation of the alginate, as the gelling time of the aerated structure was half the time of the non-aerated sample.

The alginate gelation time was determined experimentally by dissecting the sample and seeing whether it was completely solid. Gelation or crosslinking of the alginate starts from the outside of the sample and moves to the center. In other words, diffusion of Ca^{2+} ions goes from outside to inside and finishes when there is no fluid present. Gelation of the BPM took half the time (3 h) because the spaces provided by the air bubbles had been replaced by the calcium chloride solution. Therefore, Ca^{2+} ions entered the pores (homogeneously distributed) and alginate gelation took less time than that for the non-aerated CM samples. In the case of the CM, gelation of the alginate lasted for 6 h and the lyophilization for four days because the sample was not aerated. Notwithstanding, the times for gelation and lyophilization of the cylindrical samples BPM and CM were sufficient.

Fig. 2 shows images obtained by optical microscopy of a sequence of intermediates in the preparation of the BPM. Because of the low resolution of the light microscopy the image of solution I did not reveal any outstanding features (Fig. 2A). However, in the case of the aerated solution III used as a porogen (Fig. 2B), fibrils of gelatin appear to form a grid that traps the air bubbles. The inset shows a magnified section of Fig. 2B. Fig. 2C shows the mixture of solutions I and III and reveals a uniform distribution of the mixed solution around the air bubbles. In Fig. 2D (wet sample of BPM), the gelled and molded alginate gel reveals air cells or pores with a diameter of 50–200 μm. The air bubbles (dark in color) can also be seen to be entangled. Therefore, when the sample was lyophilized, the empty spaces remained connected and had an increased diameter of 204 ± 58 μm. The pores are interconnected because the porogen (gelatin fibrils or grid, (Fig. 2B)) used was removed, leaving free spaces (partially) after leaching.

Fig. 3 shows the macroscopic morphology of the wet (top) and lyophilized CM (left hand side column) and BPM samples. The outer surfaces of the samples in Fig. 3A and B do not have any pores, while in the cross section the structure looks like a "lettuce" (Fig. 3C). This structure features solid walls which encase irregular and elongated pores that increase in size as they move away from the center (probably an effect of freezing) (Petrenko et al., 2011). From the images of the BPMs, the effect of the porogen on the wet samples is evident (Fig. 3D and G). In the lyophilized samples (Fig. 3E, F, H and I) the space occupied by each of the air bubbles increased due to dehydration, without considerably affecting the volume. The volume of the wet sample BPM was not affected by lyophilization (decreased slightly).

SEM images in Fig. 4correspond to the external surfaces (top) and cross sections (down) of both lyophilized samples. Fig. 4A confirms that the outer surface of CM did not have pores and

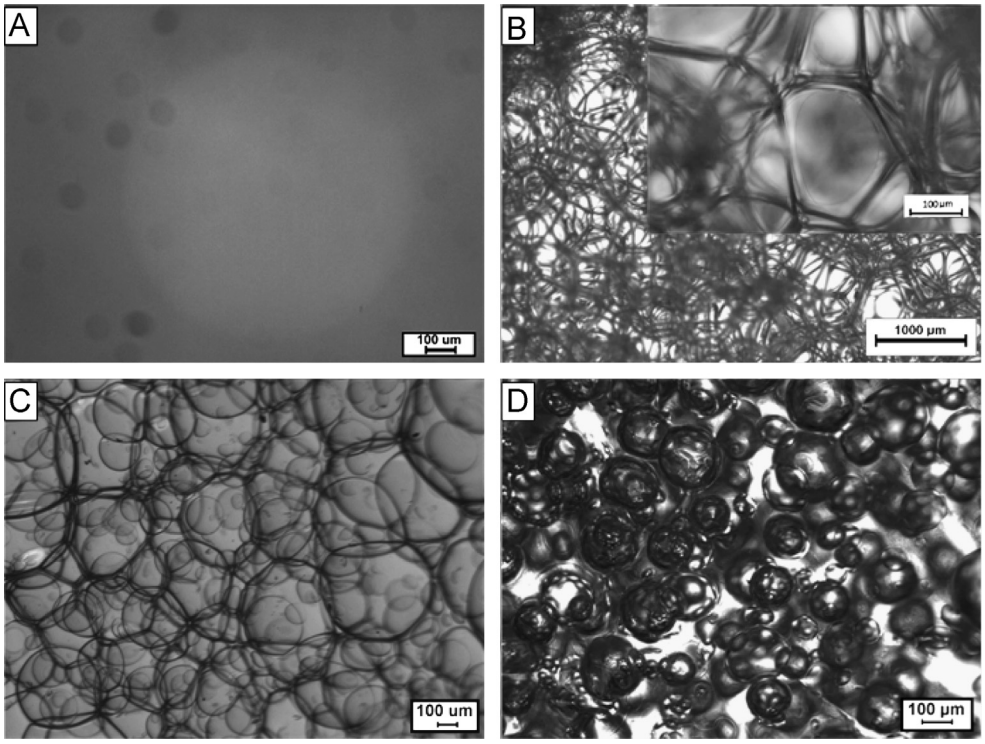

Fig. 2 – Optical microscopy of the manufacturing sequence of the BPM sample. (A) Solution I, sodium alginate 3%, (B) solution II, aerated 10% gelatin, (C) mixture of solutions I and II, (D) wet porous gel of calcium alginate (BPM). The inset shows a magnified section of (B).

was covered by a skin, while the outer surface of the BPM (Fig. 4B) exhibited pores open to the exterior. In cross section, the laminated structure of CM was confirmed, while BPM displayed a uniformly distributed and interconnected porous network with average pore sizes of 250±135 μm and 204±58 μm for external and internal pores, respectively (Table 1).

3.2. *Physical properties*

The average porosity and relative density of lyophilized BPM were 97.26±0.18% and 0.027±0.002, respectively (Table 1). The volume of BPM decreased with respect to V_O for the wet, lyophilized and rehydrated states (88%, 84% and 81%, respectively). For CM, these values corresponded to 95%, 76% and 95%, respectively (Fig. 5). Interestingly, the lyophilized BPM showed only a slight decrease in volume when it was rehydrated (from 84% to 81% relative to V_O), while lyophilized CM increased from 76% to 95% (Fig. 5). Water uptake by hydrated BPM and CM were more than 11 and 7 times their dry weight, respectively (Table 1), although for BPM the change in volume was minimal (decrease). In contrast to lyophilized CM samples that were destroyed when subjected to compression up to 80% (Fig. 5—inset A), the BPM did not (Fig. 5—inset B) and after removing the applied stress, it partially recovered its initial volume (resilience).

3.3. *Mechanical properties*

The stress of a material depends on the speed at which the load is applied. If the load is applied quickly, the stress is greater; if it is applied slowly, the stress is lower. At higher speeds, alignment of the chains decreases as the chains do not have sufficient time to align. Furthermore, at low deformation rates, the chains are aligned in the direction of the applied force. It is common for ligaments, tendons, skin, bones, etc. to be subject to fast and slow rates, with behavior varying, depending on the type of tissue. The mechanical tests for BPM were performed at an average deformation rate of 0.5 mm/s among others (0.016 mm/s (Caliari et al., 2011), 0.1 mm/s (Kaklamani et al., 2014), 0.16 mm/s (Cheng-Hsuan et al., 2007), 0.333 mm/s (Jin et al., 2004), 1 mm/s (Chimenti et al., 2011), with some other speeds not mentioned (Chang et al., 2009)).

The values of maximum elastic stress for the wet samples were similar to those obtained for the rehydrated samples. This was also the case for the apparent Young's modulus, for both the CM and BPM samples (Table 1). The wet CM and BPM samples showed a creep zone (elastic–plastic) in the stress–strain curves (Fig. 6A top) when the deformation exceeded 50%. However, this creep zone was not observed in the rehydrated CM and BPM samples (Fig. 6A bottom). Lyophilized samples of BPM during compression showed a sigmoid stress–strain curve (Fig. 6B) that is, an initial linear elastic portion followed by a central region of almost constant stress during cell wall collapse, and ending in a third section at high strains indicative of the densification of the collapsed material (Fig. 6B inset). BPM lyophilized did not fracture during deformation (although small cracks were observed) and underwent densification almost without altering its cross section (Fig. 6B). In contrast, the lyophilized CM sample was

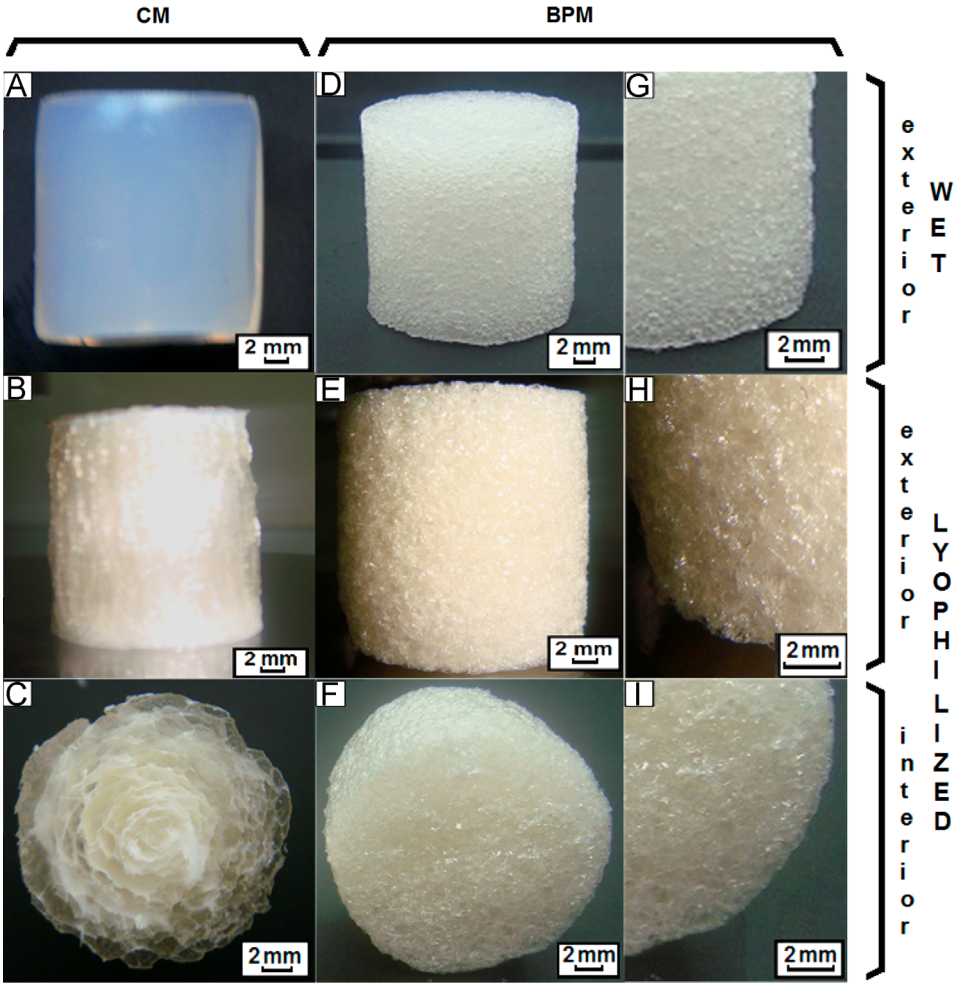

Fig. 3 – Macroscopic appearance, calcium alginate gel wet and lyophilized. First column, control matrix (CM); second and third columns, porous matrix (BPM). ((A), (D) and (G)) Wet gels; ((B), (E) and (H)) lyophilized whole pieces of the gels; ((C), (F) and (I)) cross-sectional view from a piece of the lyophilized gels.

fractured at a strain around 10% and the rupture continued until the text was completed (80% compression) (Fig. 5A). The lyophilized BPM and CM samples had a Young's modulus above 4 and 3.4 MPa, and a maximum elastic stress of around 0.4 and 0.2 MPa, respectively (Table 1). Consequently, the lyophilized BPM sample had better mechanical properties than the lyophilized CM sample, as well as higher values of porosity and water absorption. Furthermore, the change in volume when the wet sample was lyophilized was lower for the BPM than for the CM. The change in volume when the lyophilized sample was rehydrated is also lower for the BPM than the CM (Table 1).

3.4. *Cell culture*

In samples of CM, cell seeding was not possible. The structure of the CM sample was fragile and was destroyed in handling. Hence, the cell culture was performed only with samples of BPM. MTT assay was tested in the first stage, it was used to verify cell survival and proliferation so MTT reduced to purple formazan in living cells (Fig. 7B). The subsequent steps of solubilization and measurement, at a certain wavelength, were not made.

The gelatin that remains attached to the structural skeleton promotes cell adhesion (attachment points) of MSCs within the BPM and the subsequent cellular functions (Petrenko et al., 2011). So, BPM (Fig. 7A) was tested to demonstrate the adhesion, growth and cell differentiation, and the presence of living cells after cultivation. The homogeneity and interconnection of the pores were verified by the homogeneous distribution of stained cells (Fig. 7B). MSCs were easily loaded and attached within the BPM and the cell–scaffold interaction was compatible with cellular functions like viability, proliferation and differentiation. MSCs were maintained longer than a month growing in the BPM, and also were effectively induced to the osteogenic lineage in response to regular stimulus (Fig. 7D).

The incorporation of living cells in alginate crosslinked with calcium has previously been suggested (Cao et al., 2012). Calcium is an intracellular ion and is responsible for controlling several cellular processes. The concentration of intracellular free Ca^{2+} ranges from 100 nM in the cytoplasm, nucleus and mitochondria to 100 μm in the endoplasmic reticulum

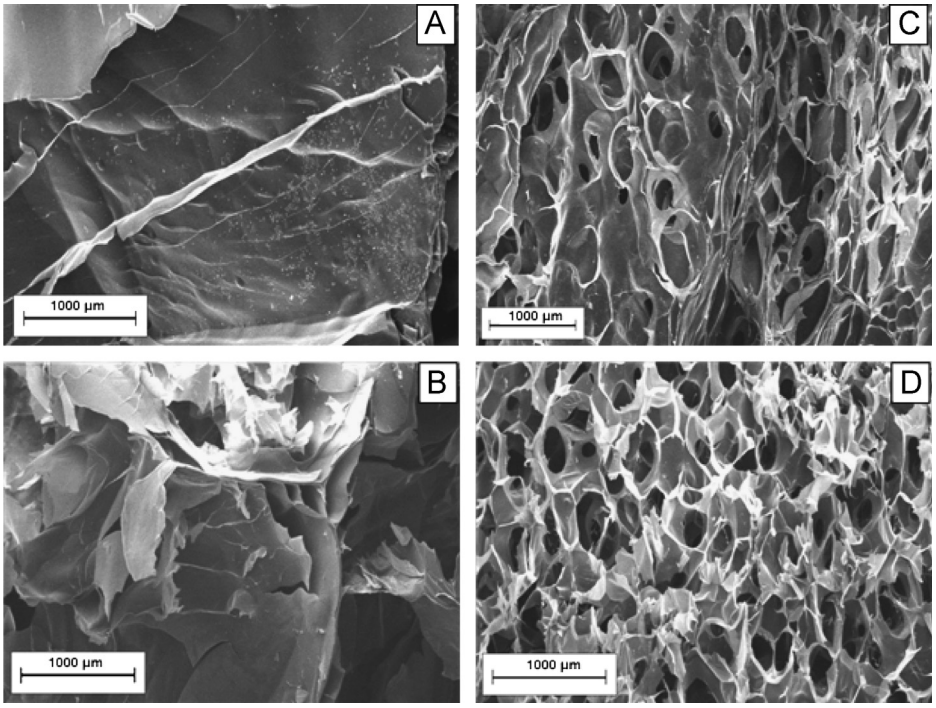

Fig. 4 – SEM images of lyophilized samples. Left: control matrix (CM); right, porous matrices (BPM). ((A) and (C)) Exterior surface; ((B) and (D)) cross section.

Table 1 – Summary of properties of calcium alginate/gelatin matrices.

Property[a]	Control matrix (CM)	Biopolymer porous matrix (BPM)
External appearance	Solid skin	Porous
Internal appearance	Gaps between concentric layers	Porous
Relative density, ρ_{app}/ρ_S	0.048±0.005	0.027±0.002
Density (g/cm^3)	0.064±0.007	0.044±0.002
Pore size[b], diameter (μm)		
Exterior	Not present	250±135
Interior	Blanks, no pores	204±58
Volume, V/V_o		
Wet	0.95±0.038	0.88±0.031
Lyophilized	0.76±0.050	0.84±0.035
Compressed	(destroyed)	0.42±0.007
Rehydrated	0.95±0.007	0.81±0.015
Porosity (%)	95.2±0.54	97.26±0.18
Rehydration, (W−Wo)/Wo	7.32±0.26	11.31±0.49
Maximum elastic stress (kPa)		
Wet gel	17.9±2.4	8.8±1.2
Lyophilized	192.8±13.5	397.3±38.8
Rehydrated	19.1±3.8	9.2±1.3
Young's modulus, E (kPa)		
Wet gel	171.0±16	97.2±19
Lyophilized	3472.4±162	4054.4±194
Rehydrated	190.9±11	72.3±9

[a] Shaded rows correspond to lyophilized samples.
[b] Average sizes of open spaces in images SEM were calculated by image analyzer tools.

(Berridge et al., 2000). It has been shown that direct exposure to high concentrations of calcium leads to mitochondrial toxicity, apoptosis and cell death (Orrenius et al., 2003). Given this, one might assume that the use of $CaCl_2$ at a concentration of 127 mM is relatively high and could lead to cell death. However, this was not the case in the present study. Cell growth occurred in the BPM, which could be because the calcium ions form part of the matrix (through cross-linking of the alginate), with no free or excess calcium ions. The situation will be different when living cells are incorporated into the alginate before cross-linking occurs. In this case, contact with $CaCl_2$ at 127 mM would be detrimental to the

cells. However, lower levels of survival and proliferation of cells has even been demonstrated in concentration of up to 500 mM of $CaCl_2$.

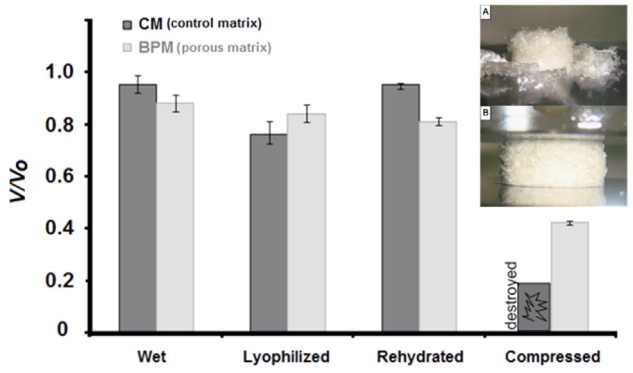

Fig. 5 – Variation in volume (*V*) with respect to the initial volume (V_o, before gelation) during different stages of the manufacturing process of the CM and BPM samples. Inset A shows destruction of the structure of CM after compression; inset B shows that BPM keeps the sample integrity and cross-section.

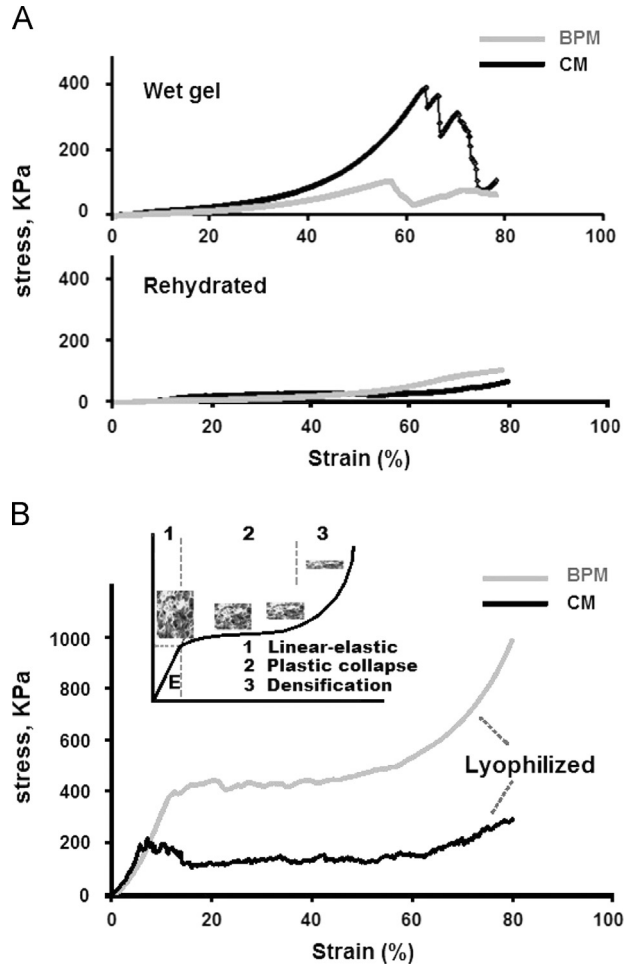

Fig. 6 – Stress–strain curves for CM and BPM. (A) Wet and rehydrated gels. (B) Lyophilized gels. Inset: typical behavior of a dry polymer foam.

4. Discussion

The most important step in the production technique proposed in this study is the selection and incorporation of a porogen (aerated gelatin, solution III) into the alginate solution (solution I). At this stage of the process, the following can be observed: (1) zero or almost zero movement of air bubbles, and immediately thereafter (in seconds), (2) the complete immobilization of the bubbles by gelling the gelatin. This was achieved by using the appropriate concentration of gelatin (10%) and proportion of the mixture (30%), both of which were determined experimentally. The theoretical basis for the zero (or almost zero) movement of the air bubbles is based on the balance of two opposing forces, as described by Stokes law (Eq. (5)) and Archimedes principle (Eq. (6)). Stokes law refers to the friction force (*Fr*) experienced by spherical objects (air bubbles) moving at low velocities (laminar) within a viscous fluid. Archimedes principle states that a body immersed in a fluid at rest, receives a push (*E*) from the bottom up equal to the weight of the fluid it displaces. The bubble experiences a frictional force (*Fr*) that opposes forward speed or ascent (v), dynamic viscosity of the fluid (η) and bubble radius (r).

$$Fr = 6 \times \pi \times r \times \eta \times v \tag{5}$$

$$E = -m \times g = -\rho \times g \times V \tag{6}$$

where ρ=fluid density (alginate); g=acceleration of gravity; V=volume of air bubbles or "volume of fluid displaced", and m=mass of air bubbles.

The BPM preparation technique does not include a step for cross-linking with gelatin. However, a fraction of gelatin remained on the matrix after leaching. This retention probably occurred due to strong interaction and miscibility between the gelatin and alginate molecules through the intermolecular hydrogen bonds, as shown by the alginate/gelatin blend fibres (Fan et al., 2005; Yao et al., 2012). The percentage of residual gelatin was calculated gravimetrically (between leached and non-leached samples) for the lyophilized samples. The CM and BPM samples had around ~15.6% and ~47.5% of residual gelatin, respectively. The lyophilized CM sample had significant amounts of residual gelatin; this is because the wet samples are solid gels without external or internal pores, making it difficult the gelatin release from the compact structure in the leaching step.

The high porosity and pore size, particularly on the outer surface (Table 1), make the BPM an appropriate material for impregnating with biological fluids. The biopolymeric interaction (alginate/gelatin) in the BPM affects the product's structure–property relationships. The alginate/gelatin fibres showed greater water retention compared to pure alginate fibres (Fan et al., 2005). Furthermore, the ability of the BPM to maintain its volume when subjected to lyophilization and rehydration is desirable for many specific applications (Drury and Mooney, 2003). The slight shrinkage observed in the wet and lyophilized BPM samples could be explained by the fact that the cohesive forces of the structural skeleton are slightly greater than those of expansion. Swelling did not occur when the lyophilized sample was in the presence of an excess of water. In contrast, the lyophilized CM sample expanded to a

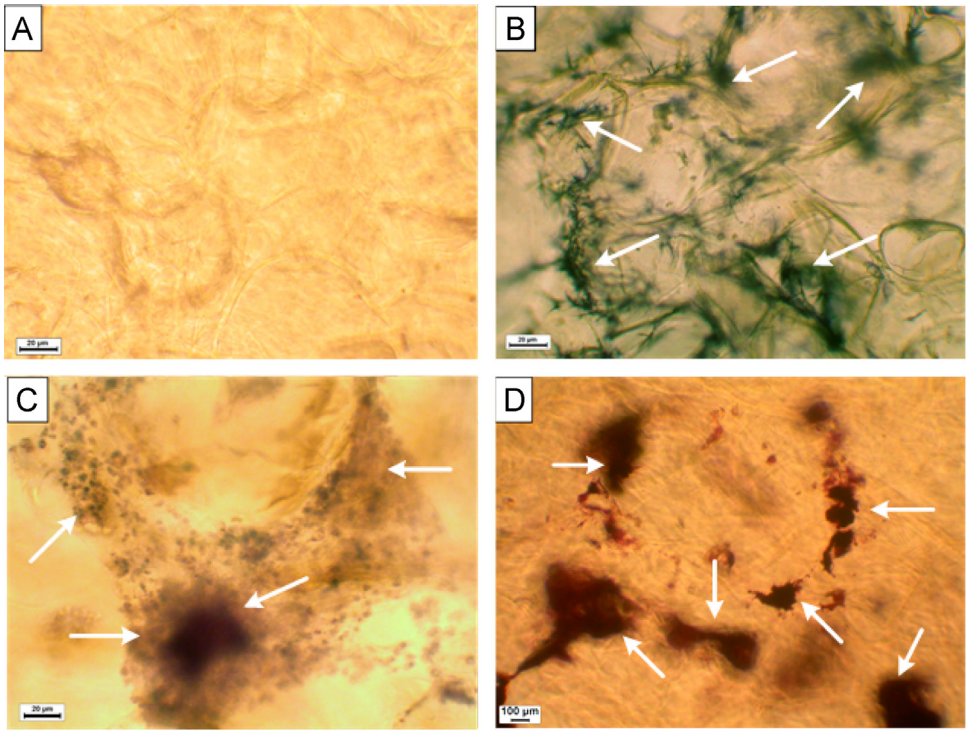

Fig. 7 – Light microscopy of BPM tested as a 3D culture systems (in vitro). (A) Control (BPM without cells). (B) MSCs grown during two weeks (see arrows) under proliferation conditions inside the BPM and stained with MTT. (C) After osteogenic induction during two weeks MSCs (shown by arrows) were still alive inside the BPM. (D) Osteogenic differentiation of MSCs visualized by alkaline phosphatase activity (see arrows).

similar volume to that of the wet sample. It could be due to different molecular arrangements; in the BPM samples air bubbles are an obstacle and the chains are arranged differently; regarding the CM samples the chains are arranged like sheets of irregular pore sizes.

The Young modulus of rehydrated samples was lower than those of lyophilized samples since water acts as a plasticizer in hydrophilic biopolymeric structures. Values of density, maximum elastic stress and apparent Young's modulus of BPM (Table 1) are comparable to those of commercially available polymeric foams (Gibson and Ashby, 1997; Peleg, 1997). Still, it may be possible to increase or decrease the value of these properties by varying the concentration (Bron et al., 2011) and source of the alginate (e.g., at higher contents of guluronic acid, the gel will be stronger but less elastic (Lee et al., 2012; Petrenko et al., 2011; Sriamornsak et al., 2007; Trens et al., 2007)). Young's moduli of calcium alginate scaffolds produced by freeze-drying at different cooling rates were 1136±264 kPa and 385±213 kPa, but exhibited lack of structural homogeneity, broad pore size distributions and poor interconnectivity of pores (Zmora et al., 2002). Regarding the porous structure itself, the optimum pore size depends on the application; an average pore size of 106±39.6 μm was sufficient for free penetration of mesenchymal stromal cells (Petrenko et al., 2011) and a pore size of 200 μm allowed rapid penetration of the cells in bone tissue engineering (Eslaminejad et al., 2007). It has been observed that larger pores of 300–500 μm improved diffusion rates to and from the center of a scaffold (Hutmacher, 2000).

An important requirement is that the matrix possesses adequate mechanical properties to maintain the required spaces for cells in-growth, propagation and tissue regeneration (Drury and Mooney, 2003; Hollister, 2005; Leong et al., 2003). The stiffness of the soft tissues ranges from 0.1 to 100 kPa (e.g., 0.1 kPa for brain, 40 kPa for osteoid) (Huang et al., 2012). Young's moduli similar to the physiological stiffness of the human myocardium have been estimated by different authors between 200 and 500 kPa (Chimenti et al., 2011). Scaffolds with high elastic modulus for skeletal tissue repair (bone and cartilage) are needed to handle the stresses induced by the in vivo culture (e.g., cell proliferation) and withstand the physiological loads imposed on the scaffolds (Leong et al., 2003) without showing symptoms of fatigue or failure (Hutmacher, 2000). Some macroporous matrices of chemically crosslinked gelatin manufactured by combining the TIPS and porogen-leaching techniques showed Young's modulus of 0.8 MPa (Liu and Ma, 2009). The lyophilized BPM sample showed enhanced physical and mechanical properties: porosity of 97.26%; an average internal pore size of 204±58 μm; an apparent Young's modulus of 4.06 MPa; and a maximum elastic stress of 0.4 MPa. As a comparison, sponges of β-tricalcium phosphate–alginate–gelatin revealed values for the same properties of 89.79%, 325.3 μm, 1.82 MPa and 0.196 MPa, respectively (Eslaminejad et al., 2007).

Results suggest that the BPM produced using this alternative method is biocompatible for three-dimensional cell culture and suitable as a platform for engineering organs and tissues (Tonsomboon and Oyen, 2013). The presence of

gelatin in the BPM is the key to cell adhesion. It has already been shown that the presence of gelatin in the pore walls of alginate-based matrices facilitated the adhesion, growth and differentiation of human bone marrow mesenchymal stromal cells (Petrenko et al., 2011). It has also been shown that alginate/gelatin microspheres showed higher cell proliferation compared to those pure alginate (Yao et al., 2012). Alginates exhibit a low cell adhesion, because they are not biologically active (Morais et al., 2013). Porous microspheres of alginate/gelatin mixtures achieved 95% cell viability (Yao et al., 2012). Likewise, the BPM could be degraded more easily (due to the attached gelatin) due to enzymes and metabolites excreted by the MSCs.

This method of manufacturing BPM may circumvent problems of other porous matrices based on gelatin and/or alginate, e.g., inconsistent morphologies and pore sizes (Zmora et al., 2002), use of toxic organic solvents (Liu and Ma, 2009), and presence of porogen residues (and/or agglomeration) (Leong et al., 2003). The incorporation of an innocuous porogen (aerated gelatin) is the key step of this manufacturing process, resulting in a porous structure which lacks cytotoxicity, far otherwise promotes cell growth. The results showed that the cell culture in contact with the BPM showed uniformity and high activity that can be attributed to the following characteristics: suitable microenvironment, pore size and interconnection, and mechanical strength.

5. Conclusions

We have presented a method of top-down production for a new biopolymeric porous matrix (BPM) of calcium alginate/gelatin. The procedure is simple because it does not require complicated steps to be performed. The procedure includes adding a porogen (aerated gelatin), molding, cooling, gelation by diffusion (in 1.41% $CaCl_2$, maximum gel strength), leaching, and lyophilization. The BPM cylinders had excellent physical, mechanical, and microstructural properties (Table 1). The resulting structure was highly porous and homogeneous, with relative density of 0.027 ± 0.002, porosity $97.26 \pm 0.18\%$, average pore size of $204 \pm 58\ \mu m$, an apparent Young's modulus of 4.05 MPa, and a maximum elastic stress of 0.4 MPa. Particularly noteworthy is the absorption of water by the lyophilized BPM sample, which exceeded 11 times its dry weight with only a slight reduction in volume.

The key for cell culture in the BPM was the presence of gelatin (trapped in the structure) that promotes cell adhesion and the subsequent functions. The BPM was tested and provided an excellent environment for cell adhesion, proliferation and differentiation osteogenesis. Given the properties of the BPM, these matrices could be studied in greater depth as a support for tissue engineering among other potential applications.

Acknowledgments

We gratefully acknowledge funding by CONICYT (Comisión Nacional de Investigación Científica y Tecnológica de Chile) to T.R. Cuadros.

REFERENCES

Alnaief, M., Alzaitoun, M.A., García-González, C.A., Smirnova, I., 2011. Preparation of biodegradable nanoporous microspherical aerogel based on alginate. Carbohydr. Polym. 84, 1011–1018.

Barbosa, M.A., Granja, P.L., Barrias, C.C., Amaral, I.F., 2005. Polysaccharides as scaffolds for bone regeneration. ITBM-RBM 26, 212–217.

Berridge, M.J., Lipp, P., Bootman, M.D., 2000. The versatility and universality of calcium signalling. Nat. Rev. Mol. Cell Biol. 1, 11–21.

Bron, J.L., Vonk, L.A., Smit, T.H., Koenderink, G.H., 2011. Engineering alginate for intervertebral disc repair. J. Mech. Behav. Biomed. Mater. 4, 1196–1205.

Caliari, S.R., Ramirez, M.A., Harley, B.A.C., 2011. The development of collagen-GAG scaffold–membrane composites for tendon tissue engineering. Biomaterials 32, 8990–8998.

Cao, N., Chen, X.B., Schreyer, D.J., 2012. Influence of calcium ions on cell survival and proliferation in the context of an alginate hydrogel. ISRN Chem. Eng. 2012, 9.

Cuadros, T.R., Skurtys, O., Aguilera, J.M., 2012. Mechanical properties of calcium alginate fibers produced with a microfluidic device. Carbohydr. Polym. 89, 1198–1206.

Chang, C., Duan, B., Zhang, L., 2009. Fabrication and characterization of novel macroporous cellulose–alginate hydrogels. Polymer 50, 5467–5473.

Cheng-Hsuan, H., Sung-Pei, T., Ming-Hwa, H., Da-Ming, W., Chung-En, L., Cheng-Hsuan, H., Hsien-Chung, T., Hsyue-Jen, H., 2007. Analysis of freeze-gelation and cross-linking processes for preparing porous chitosan scaffolds. Carbohydr. Polym. 67, 124–132.

Chimenti, I., Rizzitelli, G., Gaetani, R., Angelini, F., Ionta, V., Forte, E., Frati, G., Schussler, O., Barbetta, A., Messina, E., Dentini, M., Giacomello, A., 2011. Human cardiosphere-seeded gelatin and collagen scaffolds as cardiogenic engineered bioconstructs. Biomaterials 32, 9271–9281.

De Moura, M.R., Guilherme, M.R., Campese, G.M., Radovanovic, E., Rubira, A.F., Muniz, E.C., 2005. Porous alginate-Ca^{2+} hydrogels interpenetrated with PNIPAAm networks: interrelationship between compressive stress and pore morphology. Eur. Polym. J. 41, 2845–2852.

Draget, K., Moe, S., Skjak-Braek, G., Smidrod, O., 2006. Alginates. In: Stephen, A.M., Phillips, G.O., Williams, P.A. (Eds.), Food Polysaccharides and Their Applications. CRC Press, Boca Raton, FL, pp. 289–334.

Drury, J.L., Dennis, R.G., Mooney, D.J., 2004. The tensile properties of alginate hydrogels. Biomaterials 25, 3187–3199.

Drury, J.L., Mooney, D.J., 2003. Hydrogels for tissue engineering: scaffold design variables and applications. Biomaterials 24, 4337–4351.

Eiselt, P., Yeh, J., Latvala, R.K., Shea, L.D., Mooney, D.J., 2000. Porous carriers for biomedical applications based on alginate hydrogels. Biomaterials 21, 1921–1927.

Erices, A., Conget, P., Minguell, J., 2000. Mesenchymal progenitor cells in human umbilical cord blood. Br. J. Haematol. 109, 235–242.

Erices, A., Conget, P., Rojas, C., Minguell, J., 2002. Gp130 activation by soluble interleukin-6 receptor/interleukin-6 enhanced osteoblastic differentiation of human bone marrow-derived mesenchymal stem cells. Exp. Cell Res. 280, 24–32.

Eslaminejad, M., Mirzadeh, H., Mahamadi, Y., Nickmahzar, A., 2007. Bone differentiation of marrow-derived mesenchymal stem cells using B-tricalcium phosphate–alginate–gelatin hybrid scaffolds. J. Tissue Eng. Regen. Med. 1, 417–424.

Eslaminejad, M.B., Nikmahzar, A., Taghiyar, L., Nadri, S., Massumi, M., 2006. Murine mesenchymal stem cells isolated

by low density primary culture system. Dev. Growth Differ. 48, 361–370.
Fan, L., Du, Y., Huan, R., Wang, Q., Wang, X., Zhang, L., 2005. Preparation and characterization of alginate/gelatin blend fibers. J. Appl. Polym. Sci. 96, 1625–1629.
Food Chemistry. In: Fennema, O.R. (Ed.), Marcell Dekker, New York, NY.
Freyman, T.M., Yannas, I.V., Gibson, L.J., 2001. Cellular materials as porous scaffolds for tissue engineering. Prog. Mater. Sci. 46, 273–282.
Geng, X., Kwon, O.-H., Jang, J., 2005. Electrospinning of chitosan dissolved in concentrated acetic acid solution. Biomaterials 26, 5427–5432.
Gibson, L., Ashby, M., 1997. Cellular Solids: Structure and Properties. Cambridge University Press.
Grant, G.T., Morris, E.R., Rees, D.A., Smith, P.J.C., 1973. Biological interactions between polysaccharides and divalent cations: the egg-box model. FEBS Lett. 32 (1), 195–198.
Heng, B.C., Cao, T., Stanton, L.W., Robson, P., Olsen, B., 2004. Strategies for directing the differentiation of stem cells into the osteogenic lineage in vitro. J. Bone Miner. Res. 19, 1379–1394.
Holzwarth, J.M., Ma, P.X., 2011. Biomimetic nanofibrous scaffolds for bone tissue engineering. Biomaterials 32, 9622–9629.
Hollister, S.J., 2005. Porous scaffold design for tissue engineering. Nat. Mater. 4, 518–524.
Huang, G., Wang, L., Wang, S., Han, Y., Wu, J., Zhang, Q., Xu, F., Lu, T.J., 2012. Engineering three-dimensional cell mechanical microenvironment with hydrogels. Biofabrication 4, 042001.
Hutmacher, D.W., 2000. Scaffolds in tissue engineering bone and cartilage. Biomaterials 21, 2529–2543.
Jin, H.-J., Chen, J., Karageorgiou, V., Altman, G.H., Kaplan, D.L., 2004. Human bone marrow stromal cell responses on electrospun silk fibroin mats. Biomaterials 25, 1039–1047.
Kaklamani, G., Cheneler, D., Grover, L.M., Adams, M.J., Bowen, J., 2014. Mechanical properties of alginate hydrogels manufactured using external gelation. J. Mech. Behav. Biomed. Mater. 36, 135–142.
Lee, H.-Y., Jin, G.-Z., Shin, U.S., Kim, J.-H., Kim, H.-W., 2012. Novel porous scaffolds of poly(lactic acid) produced by phase-separation using room temperature ionic liquid and the assessments of biocompatibility. J. Mater. Sci.: Mater. Med. 23, 1271–1279.
Leong, K.F., Cheah, C.M., Chua, C.K., 2003. Solid freeform fabrication of three-dimensional scaffolds for engineering replacement tissues and organs. Biomaterials 24, 2363–2378.
Liu, X., Ma, P.X., 2009. Phase separation, pore structure, and properties of nanofibrous gelatin scaffolds. Biomaterials 30, 4094–4103.
Martynov, S., Wang, X., Stride, E.P., Edirisinghe, M.J., 2010. Preparation of a micro-porous alginate gel using a microfluidic bubbling device. Int. J. Food Eng. 6 (3), 1–12.
Mikos, A.G., Herring, S.W., Ochareon, P., Elisseeff, J., Lu, H.H., Kandel, R., Schoen, F.J., Toner, M., Mooney, D., Atala, A., Van Dyke, M.E., David, K., Vunjak-Novakovic, G., 2006. Engineering complex tissues. Tissue Eng. 12, 3307–3339.
Ming-Hua, H., Pei-Yun, K., Hsyue, H., Tzu-Yang, H., Lein-Tuan, H., Juin-Yih, L., Da-Ming, W., 2004. Preparation of porous scaffolds by using freeze-extraction and freeze-gelation methods. Biomaterials 25, 129–138.
Morais, D.S., Rodrigues, M.A., Silva, T.I., Lopes, M.A., Santos, M., Santos, J.D., Botelho, C.M., 2013. Development and characterization of novel alginate-based hydrogels as vehicles for bone substitutes. Carbohydr. Polym. 95, 134–142.
Nussinovitch, A., Jaffe, N., Gillilov, M., 2004. Fractal pore-size distribution on freeze-dried agar-texturized fruit surfaces. Food Hydrocoll. 18, 825–835.
Orrenius, S., Zhivotovsky, B., Nicotera, P., 2003. Regulation of cell death: the calcium-apoptosis link. Nat. Rev. Mol. Cell Biol. 4, 552–565.
Peleg, M., 1997. Review: mechanical properties of dry cellular solid foods. Food Sci. Technol. Int. 3, 227–240.
Petrenko, Y.A., Ivanov, R.V., Petrenko, A.Y., Lozinsky, V.I., 2011. Coupling of gelatin to inner surfaces of pore walls in spongy alginate-based scaffolds facilitates the adhesion, growth and differentiation of human bone marrow mesenchymal stromal cells. J. Mater. Sci.: Mater. Med. 22, 1529–1540.
Ribeiro, C.C., Barrias, C.C., Barbosa, M.A., 2004. Calcium phosphate–alginate microspheres as enzyme delivery matrices. Biomaterials 25, 4363–4373.
Sikorski, P., Mo, F., Skjak-Braek, G., Stokke, B.T., 2007. Evidence for egg–box-compatible interactions in calcium alginate gels from fiber X-ray diffraction. Biomacromolecules 8, 2098–2103.
Simpson, N.E., Stabler, C.L., Simpson, C.P., Sambanis, A., Constantinidis, I., 2004. The role of the $CaCl_2$-guluronic acid interaction on alginate encapsulated BTC3 cells. Biomaterials 25, 2603–2610.
Sisson, K., Zhang, C., Farach-Carson, M.C., Chase, D.B., Rabolt, J.F., 2010. Fiber diameters control osteoblastic cell migration and differentiation in electrospun gelatin. J. Biomed. Mater. Res. Part A 94, 1312–1320.
Sriamornsak, P., Thirawong, N., Korkerd, K., 2007. Swelling, erosion and release behavior of alginate-based matrix tablets. Eur. J. Pharm. Biopharm. 66, 435–450.
Studenovská, H., Slouf, M., Rypácek, F., 2008. Poly(HEMA) hydrogels with controlled pore architecture for tissue regeneration applications. J. Mater. Sci.: Mater. Med. 19, 615–621.
Szymanski, J.M., Feinberg, A.W., 2014. Fabrication of freestanding alginate microfibers and microstructures for tissue engineering applications. Biofabrication 6, 024104.
Tonsomboon, K., Oyen, M.L., 2013. Composite electrospun gelatin fiber-alginate gel scaffolds for mechanically robust tissue engineered cornea. J. Mech. Behav. Biomed. Mater. 21, 185–194.
Trens, P., Valentin, R., Quignard, F., 2007. Cation enhanced hydrophilic character of textured alginate gel beads. Colloids Surf., A: Physicochem. Eng. Aspects 296, 230–237.
Van Vlierberghe, S., Cnudde, V., Dubruel, P., Masschele, B., Cosijns, A., De Paepe, I., Jacobs, P.J., Van Hoorebeke, L., Remon, J.P., Schacht, E., 2007. Porous gelatin hydrogels: 1. Cryogenic formation and structure analysis. Biomacromolecules 8, 331–337.
Wang, A., Cui, Y., Li, J., Van Hest, J.C.M., 2012. Fabrication of gelatin microgels by a "cast" strategy for controlled drug release. Adv. Funct. Mater. 22, 2673–2681.
Wang, C., Liu, H., Gao, Q., Liu, X., Tong, Z., 2008. Alginate–calcium carbonate porous microparticle hybrid hydrogels with versatile drug loading capabilities and variable mechanical strengths. Carbohydr. Polym. 71, 476–480.
Weng, J., Wang, M., 2001. Producing chitin scaffolds with controlled pore size and interconnectivity for tissue engineering. J. Mater. Sci. Lett. 20, 1401–1403.
Yao, R., Zhang, R., Luan, J., Lin, F., 2012. Alginate and alginate/gelatin microspheres for human adipose-derived stem cell encapsulation and differentiation. Biofabrication 4, 025007.
Zhang, J., Zhang, H., Wu, L., Ding, J., 2006. Fabrication of three dimensional polymeric scaffolds with spherical pores. J. Mater. Sci. 41, 1725–1731.
Zmora, S., Glicklis, R., Cohen, S., 2002. Tailoring the pore architecture in 3-D alginate scaffolds by controlling the freezing regime during fabrication. Biomaterials 23, 4087–4094.

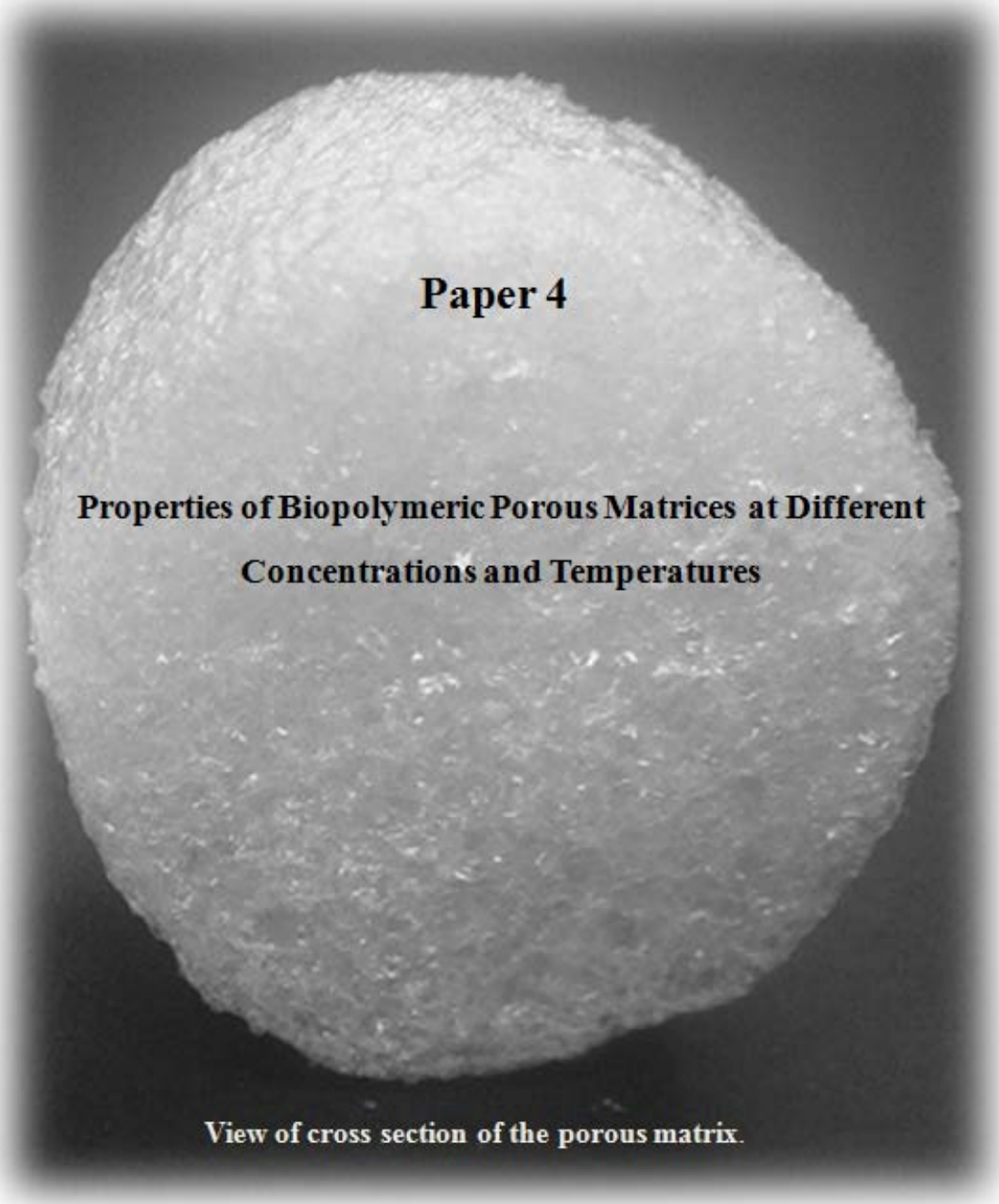

Paper 4

Properties of Biopolymeric Porous Matrices at Different Concentrations and Temperatures

View of cross section of the porous matrix.

PROPERTIES OF BIOPOLYMERIC POROUS MATRICES AT DIFFERENT CONCENTRATIONS AND TEMPERATURES

1. Introduction

The behaviour of physically cross-linked gels of polysaccharides such as alginate have not yet been fully studied because they form gels with unique properties (Davidovich-Pinhas and Bianco-Peled, 2010). Properties such as water absorption and volume change are important for bio-adhesion (Bron et al., 2011), mechanical strength (Drury et al., 2004), drug release ability (Ferreira Almeida and Almeida, 2004; Grassi et al., 2001; Ostberg and Graffner, 1994), permeability (Hambleton et al., 2009), and degradation rate (Morais et al., 2013). Alginate gels are widely used because of their physiological compatibility (Davidovich-Pinhas and Bianco-Peled, 2010) and are common additives in drugs and food formulation (Dong et al., 2006; Mehling et al., 2009; Wang et al., 2008), cosmetics (Tonnesen and Karlsen, 2002), and in other fields such as biomedical (Mikos et al., 2006; Nokhodchi and Tailor, 2004; Qin, 2008; Ribeiro et al., 2004; Shapiro and Cohen, 1997).

Alginates have no nutritional value, but are accepted and recognized as being safe in food (Draget et al., 2006). Alginate is a natural polysaccharide which is soluble in water and consists of alternating segments of 1→4 linked α -L-guluronic acid (G) and β-D-mannuronic acid (M). The size, number and sequence of these segments depend on the physical and chemical properties of the alginate (Draget et al., 1994). Alginates exhibit affinity to multivalent cations such as Ca^{2+} and are able to bind those ions selectively, and cooperatively form the ionically cross-linked alginate gel (Draget et al., 2006; Hennink and van Nostrum, 2012; Zhang et al., 2013). Alginate has the ability to form strong thermo-resistant gels by creating a cross-linking area or local molecular arrangement known as the “egg box” (Aguilera and Stanley, 1999; Bajpai and Sharma, 2004; Draget et al., 2006; Grant et al., 1973). The cross-linking can occur at room temperature and physiological pH (Hennink and van Nostrum, 2012). Therefore, alginate gels are often used as a matrix for the encapsulation of living cells and for the

release of proteins and drugs. Both sodium alginate and calcium salt are nontoxic and biocompatible and alginate gels are stable within a temperature range of 0-100 °C (Tonnesen and Karlsen, 2002). Gelatin is a protein derived from denatured collagen, which is a major component of skin, bones and connective tissue. Gelatin forms gels when the temperature changes and is a thermally reversible gelling agent for encapsulation (Yao et al., 2012).

The objective of this study is to describe the physical, mechanical and microstructural properties of biopolymeric porous matrices (BPMs) calcium alginate/gelatine at different concentrations and temperatures. The BPMs were prepared using a method developed in a previous study (Cuadros et al., 2014).

2. Materials and Methods

2.1. Materials

Sodium alginate (Alg) powder (Gelymar, Natural Extracts S.A., Chile) from *Macrocystis pyrifera* with average composition of 16% G [α-L-guluronic acid], 38% M [β-D-mannuronic acid] and 46% of MG alternating units, (low viscosity, 50-200 cP for 1% solution at 20°C). Gelatin Leiner, extra fine grade of 240 Bloom powder (Code 901553 was kindly supplied by Floramatic Ltda., Chile). A solution of calcium chloride ($CaCl_2$) with a concentration of 1.41% w/v was prepared based on anhydrous salt ($CaCl_2.2H_2O$ p.a., CA- 0520, Heyn, Santiago, Chile). Glass tubes (2.0 cm internal diameter and 15 cm height) open at both ends were used.

2.2. Preparation of porous matrices

The method for preparing biopolymeric porous matrices (BPMs) was developed in our laboratory in a previous study (Cuadros et al., 2014). BPMs were prepared at 1.5%, 2.25% and 3% Alg (w/w) (solution I) and was stored at 15 °C.

Control matrices (C) were prepared by mixing the solutions I (15 °C) and solution II (30 °C) to yield a final solution containing alginate (1.5%, 2.25% or 3.0%) and 1% gelatin (minimum concentration required to mold the alginate), filled into glass tubes and stored overnight at 4 °C, to induce further gelling of gelatin. After a brief bath (~2 s) of the tubes in water at 60 °C, the contents of the tubes were immersed for 6 h in a 1.41% (w/v)

$CaCl_2$ solution, reintroduced in the glass tubes and stored overnight at 4 °C. Gelled pieces were cut into cylinders (22 mm height) and leached thrice with distilled water (with stirring) at 65 °C (30 min each) to remove as much gelatin as possible. Then samples were lyophilized after rapid cooling to -40 °C and exposed to vacuum at -10 °C over four days (to complete drying). Then, both freeze-dried matrices (BPM and CM) were stored in desiccators over phosphorous pentoxide at zero relative humidity before further analysis.

Solution of 10% gelatin (w/w) was prepared with water at 70 °C until the powder was fully dissolved, and upon cooling (around 28 °C) it was subjected to mechanical agitation with a blender (10,000 rpm for 1 min) and converted into a flowable foam (solution III). Then, the solution I and solution III were mixed in a 70:30 weight ratio, filled into glass tubes and stored overnight at 4 °C, to induce further gelling of gelatin. After a brief bath (~2 s) of the tubes in water at 60 °C the contents of the tubes were immersed for 3 h in a 1.41% (w/v) $CaCl_2$ solution (Cuadros et al., 2012), re-introduced in the glass tubes and stored overnight at 4 °C. Gelled pieces were cut into cylinders (22 mm height) and leached thrice with distilled water at 65 °C (30 min each) to remove as much gelatin (the porogen) as possible. The leached samples were lyophilized in a VirTis Lyophilizer (Genesis 25ES Freeze Dryer, SP Industries, Gardiner NY) after rapid cooling to -40 °C and exposure to vacuum to -10 °C over three days (to complete drying).

Figure 1 presents an overview of the procedure and the types of obtained samples: porous matrices such as, samples “A” (leached) and samples “B” (non-leached); and non-porous as “C” or control samples. The numbers 1, 2 and 3 correspond to the concentrations 1.5%, 2.25% and 3.0% of alginate (solution I), respectively. For example, in A2, the letter A indicates that the matrix is subjected to leaching and the number 2 indicates that the alginate concentration or solution I is 2.25%.

Three terms are used, the wet samples are the gelled samples used in the manufacturing process, prior to lyophilization. The lyophilized samples, are the samples that are obtained at the end of the manufacturing process, and rehydrated samples are the lyophilized samples that have been subjected to hydration.

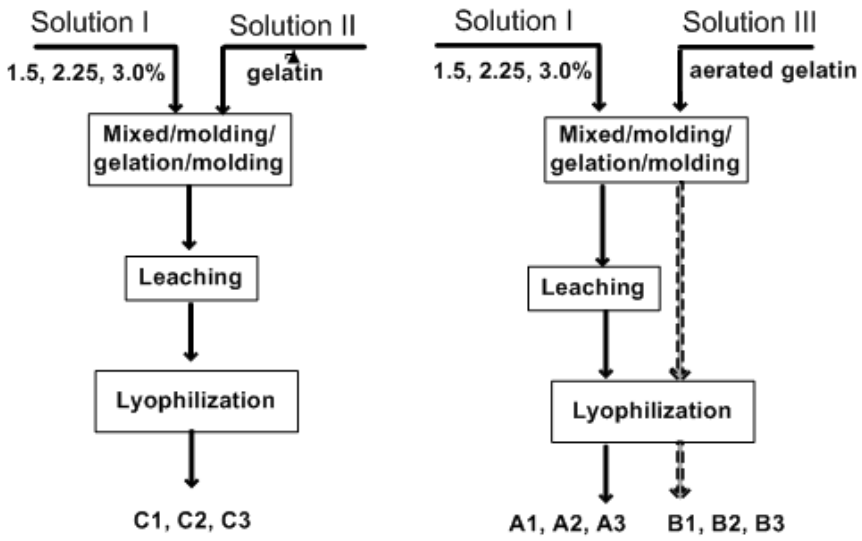

Figure 1. Overview of preparation. A and B porous matrices, C control.

2.3. Morphological analyses

The porous structures of BPMs were observed with a light microscope (Olympus SZX7, Optical Co. Ltd., Tokyo, Japan) and images were taken with a digital camera (CoolSnap-Pro Color, Photometrics Roper Division, Inc., Tucson, AZ). The surface morphology of samples were examined and the pore diameters measured using scanning electron microscopy SEM JEOL-JSM 5300 (Jeol Ltd., Tokyo, Japan) operated at an acceleration voltage of 20 kV. Freeze dried specimens were fixed to a metal stub with double-sided tape and covered with gold using a sputter coating. Pore sizes of the BPMs structures were estimated after image processing (Zúñiga and Aguilera, 2009) and measured using Image Pro-Plus 4.5 imaging software (Media Cybernetics, Inc., Silver Spring, MD).

2.4. Volume

Variations in volume were calculated as V/V_O, where *Vo* is the volume of the mixture solutions before gelation (6.9 cm^3), and *V*, the measured volume of wet, lyophilized and rehydrated cylindrical gels. Volumes were calculated by two methods: 1) as a cylinder

after measuring the diameter and height of the samples, and 2) by volumetric displacement using poppy seeds (0.5-1 mm average size) and purified and calcined sand (0.1-0.3 mm, Heyn, Santiago, Chile).

2.5. Porosity

Porosity (ϕ), was determined using the density method based on the air space within the matrix, known as apparent porosity (ϕ_{app}). This is defined as the ratio of the volume of air space or voids to the total volume. Apparent porosity is calculated based on the solid density (ρ_S), and apparent density (ρ_{app}) by using equation (1) and expressed as (%):

$$\phi_{app} = 1 - (\frac{\rho_{app}}{\rho_S})100 \quad (1)$$

(ρ_{app} / ρ_S) is defined as the relative density. Solid density (ρ_S), is the density of the solid material, excluding any internal pores (filled with air). One way to calculate this is by dividing the sample weight by the volume after destroying all of the air spaces. This destruction was not possible in the BPM because the material is strong and flexible. As the solid fraction of BPM is an alginate/gelatin mixture, the solid density (ρ_S) has been estimated by taking the value for materials such as cellulose and most foods polymers (e.g., starch, protein, gelatin), this value is in the order of 1.5 g/cm^3 (Gibson and Ashby, 1997; Liu and Ma, 2009; Nussinovitch et al., 2004; Peleg, 1997). ρ_{app} was calculated as the ratio of the mass (m) to the sample volume (V).

2.6. Water uptake at different temperatures

Freeze-dried samples were immersed in excess water (i.e., in a ratio 1:500, w/w) at pH 7.0 and at 20, 25, 30, 35, 40, 45, 50 °C under constant stirring until they reached constant weight. The water uptake (WU) of samples was calculated by equation (2):

$$WU = (W(t) - Wo)/Wo \quad (2)$$

where *Wo* are the weight of lyophilized gel (initial) and *W(t)* are the weight of gel at time *t*.

2.7. Mechanical properties

Apparent Young's modulus of wet, freeze-dried and rehydrated samples were obtained at room temperature (20 °C). Also, the apparent Young's modulus of samples rehydrated at different temperatures (20, 25, 30, 35, 40, 45 and 50 °C) were measured using a Universal Texture Analyser TA.XT2i (Stable Micro Systems, Godalming, Surrey, UK) calibrated using a 5 Kg load cell.

Cylindrical samples were subjected to uniaxial compression stress with a descending lubricated acrylic plate (70 mm diameter) up to 80% deformation at a constant rate of 0.5 mm/s. A compressive strength was defined as the maximum stress observed at the end of linear elastic region of the stress-strain curve (e.g., between 5-12% strain) and an apparent Young´s modulus (E) was calculated as slope of the line stress vs strain by equations (3) and (4):

$$\sigma = \frac{F}{A_O} \tag{3}$$

$$\varepsilon = \frac{\Delta H}{H_O} \tag{4}$$

Where, Stress = (σ) and strain = ($\mathcal{E}$), F = force ; ΔH = absolute deformation, $H_O - H(t)$; A_O and H_O are the initial cross-sectional area and height of the sample, respectively. The compression force versus distance were determined in quintuplicate and reported as an average value (Zúñiga and Aguilera, 2009).

2.8. Statistical analysis of data

One-way analysis of variance (ANOVA) assuming confidence level of 95% ($p<0.05$) was performed using Statgraphics Centurion XV software 2006 (Manugistics Inc., Statistical Graphics Corporation, Rockville, USA). Data were expressed as mean ± standard deviation.

3. Results

3.1 Microstructural appearance, volume, porosity and apparent Young's modulus

For the purposes of this study, a control sample (C, or non-porous) and two porous samples (A and B) were obtained. Differences in weight between the lyophilized B samples (non-leached) and A samples (leached) allowed us to calculate the amount of residual and removed gelatin. Table 1 presents a summary of these findings. Figure 2 contains SEM images of two samples, one control (C2, Figures 2a and 2b) and one porous (A2, Figures 2c and 2d), both with 2.25% alginate.

Table 1. Gelatine content (%) in the lyophilized samples. Control (C), and Porous Matrices (A and B).

Control			Porous matrices					
C1	C2	C3	B1	B2	B3	A1	A2	A3
35.21	23.73	15.56	66.66	65.57	58.80	59.26	57.58	47.50

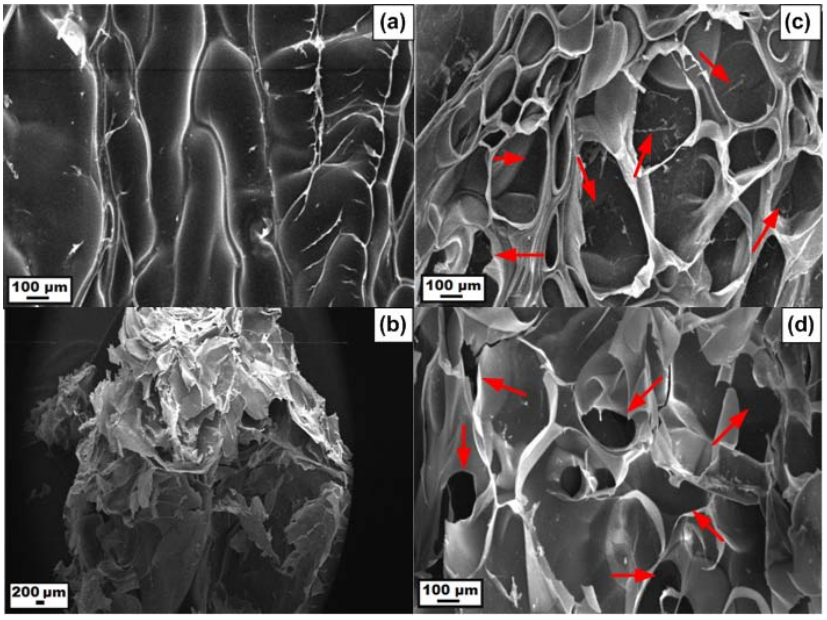

Figure 2. SEM images of lyophilized samples of alginate matrices at 2.25%. C2 on the left and A2 on the right. (a) and (c) internal pores, (b) and (d) external pores. Arrows show pore interconnectivity or communication.

The average diameter of the pores decreases as the concentration of alginate increases for both the B and A samples (Table 2). By contrast, the C samples do not have pores and exhibit non-porous surfaces (Figure 2b) as solid sheets. Image 2d (A samples, see arrows) show that pores are interconnected, the external pores are larger than the internal pores (Table 2), the B samples showed larger pores on the outside. The external pores are gateways to the incorporation of nutrients and active components in the matrix.

Table 2. Average pore size of the lyophilized porous matrices for A and B.

Pore diameter, mm	Alginate concentration					
	Samples B			Samples A		
	B1, 1.5%	B2, 2.25%	B3, 3.0%	A1, 1.5%	A2, 2.25%	A3, 3.0%
Internal pore	354.73 ±83^{bc}	281.87 ±69^{abc}	249.53 ±58^{ab}	380.77 ±88^{c}	352.28 ±71^{bc}	204.3 ±58^{a}
External pore	397.37 ±13^{d}	322.89 ±89^{d}	279.72 ±78^{d}	313.39 ±15^{d}	292.95 ±14^{d}	257.02 ±14^{d}

The results are average of ten determinations of three different batches, and values behind ± indicate standard deviation. This means that the same superscripts are not significantly different within the groups ($p > 0.05$).

Equilibrium time of rehydration of the samples was 30 h. This was previously determined as shown for dehydrated samples A3, B3 and C3 (Figure 3a) at 3% alginate, which were immersed in water until they reached equilibrium (constant weight). It was noted that the weight of the rehydrated samples was lower than the weight of the wet samples. The weight gain in water (rehydrated samples) relative to the weight of the wet samples (weight after gelling alginate, during manufacture) at room temperature (20 °C), expressed as percentage was: C1 (44.67%), C2 (28.85%), C3 (45.39%), B1 (71.79%), B2 (70.31%), B3 (56.41%), A1 (83.60%), A2 (83.53%), A3 (71.36%).

The weight loss of wet samples (through dehydration) is greater than the weight gain of the lyophilized samples through rehydration. This indicates that, the ability of the matrices to capture water (wet gels) is partially recovered when the lyophilized gels are subjected to rehydration.

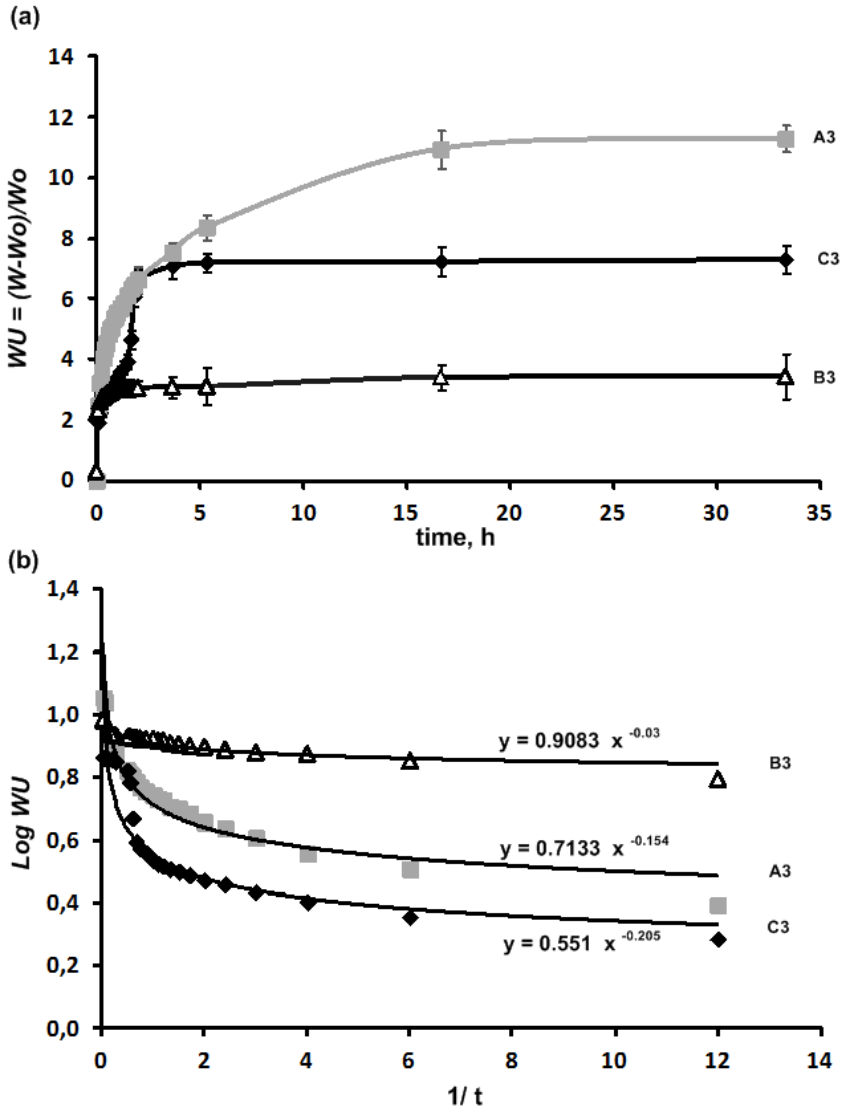

Figure 3. (a) Water uptake kinetics at 20°C for porous samples (A and B) and control (C) at 3% alginate. (b) Fit parameters to the power law model that describes the kinetics of water uptake for the same samples. The bars indicate standard deviation.

Figure 4 shows the changes in volume of the gel in three sequential states: wet, lyophilized and rehydrated, the data showed significant differences between these samples. The C samples showed higher variations in volume at different concentrations than the porous A and B samples. Interestingly, the wet B samples increased in volume when they were lyophilized, while A samples decreased. No significant differences were

observed in terms of variations in volume for the porous samples with respect to the concentration of alginate ($p > 0.05$).

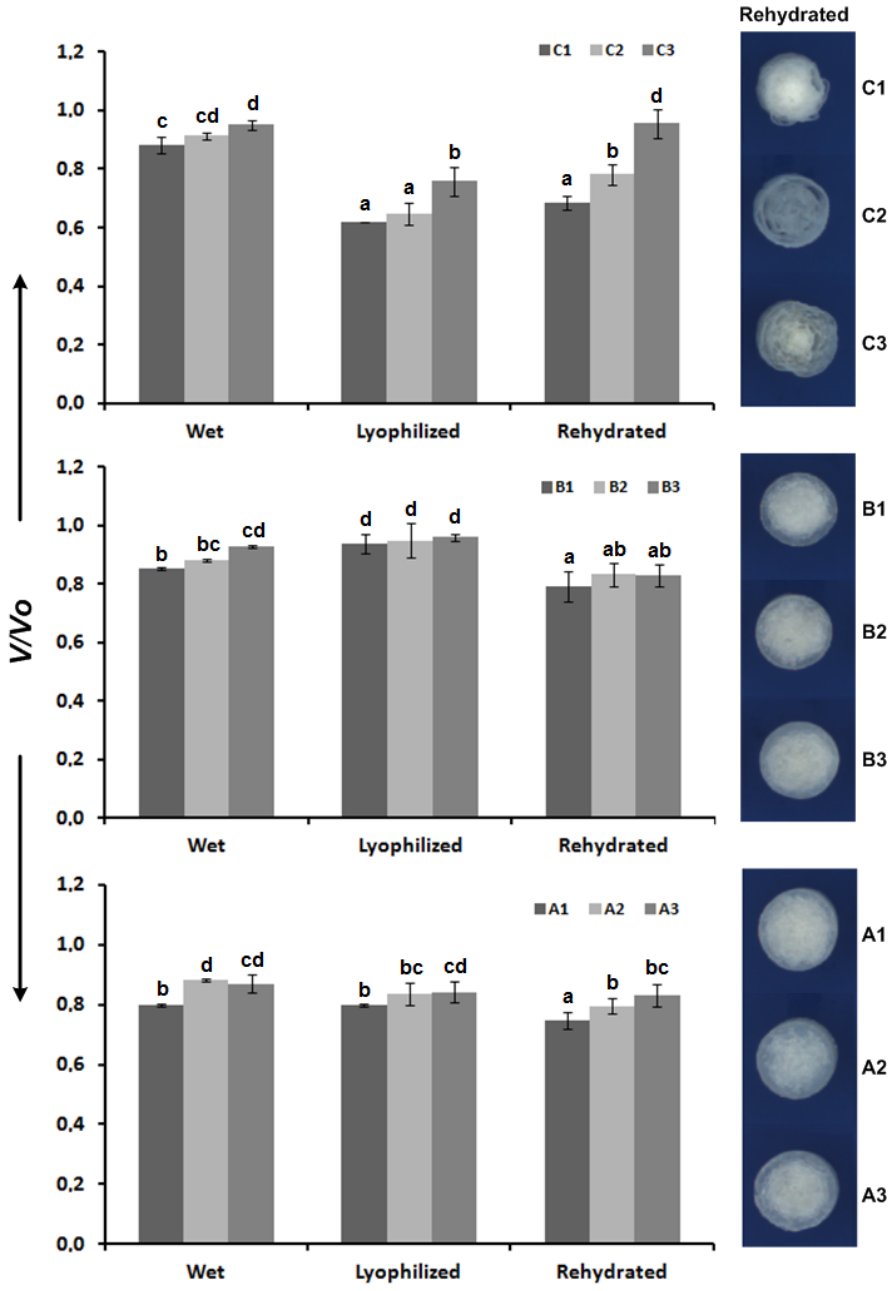

Figure 4. Variation in volume of C (control) and porous matrices B and A during different states: wet, lyophilized and rehydrated. Images of the cross sections of the rehydrated samples are presented to the right of each graph. The dependence on the concentration of alginate for each state is not statistically significant ($p>0.05$). The bars indicate standard deviation.

Figure 5 shows the average porosity of the lyophilized samples at different concentrations of alginate (1.5%, 2.25% and 3.0%). The B samples are less porous than the A samples and a decrease in porosity was observed for both samples when the concentration of alginate increased. With respect to the porous samples, the A1 sample showed the hightest porosity (97.79 ± 0.04 %) and the B3 sample the lowest (96.62 ± 0.11 %).

The results for the three sample types (A, B and C) in the three states of preparation (wet, lyophilized, rehydrated) suggest that there is a direct relationship between the concentration of alginate and apparent Young's modulus (Figure 6). The Young's modulus values fell about one order of magnitude when lyophilized samples (Figure 6b) were rehydrated (Figure 6a).

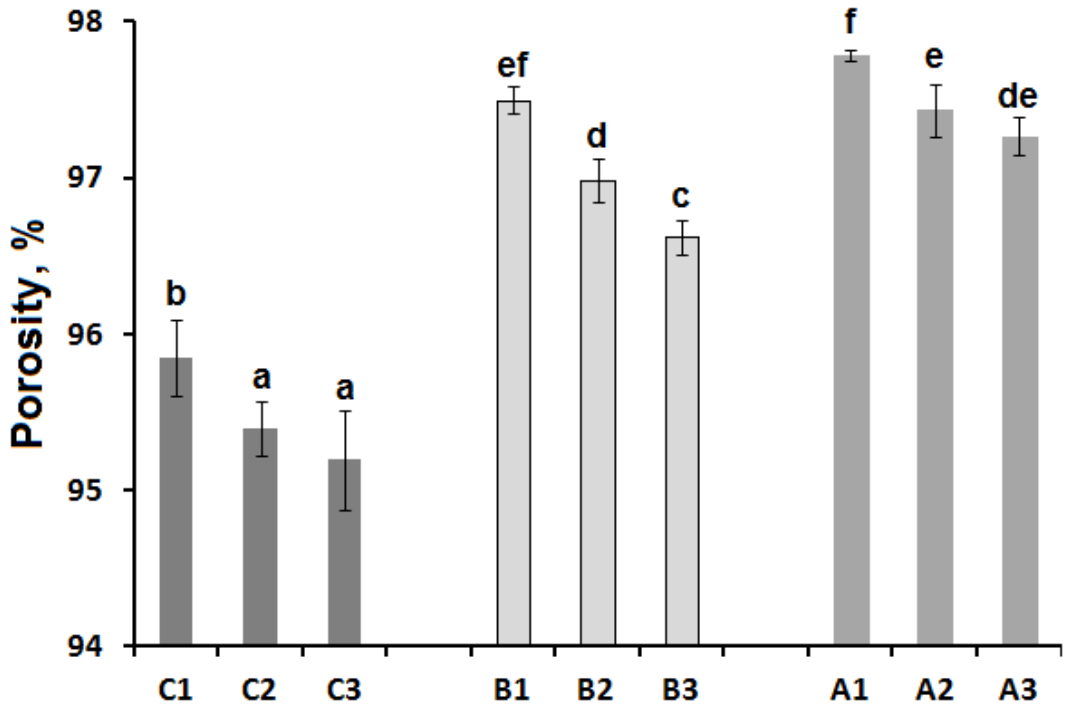

Figure 5. Porosity values of lyophilized samples, control C and porous matrices B and A, to differents concentrations of alginate: 1, 2 and 3 are 1.5%, 2.25% and 3.0%, respectively ($p<0.05$). The bars indicate standard deviation.

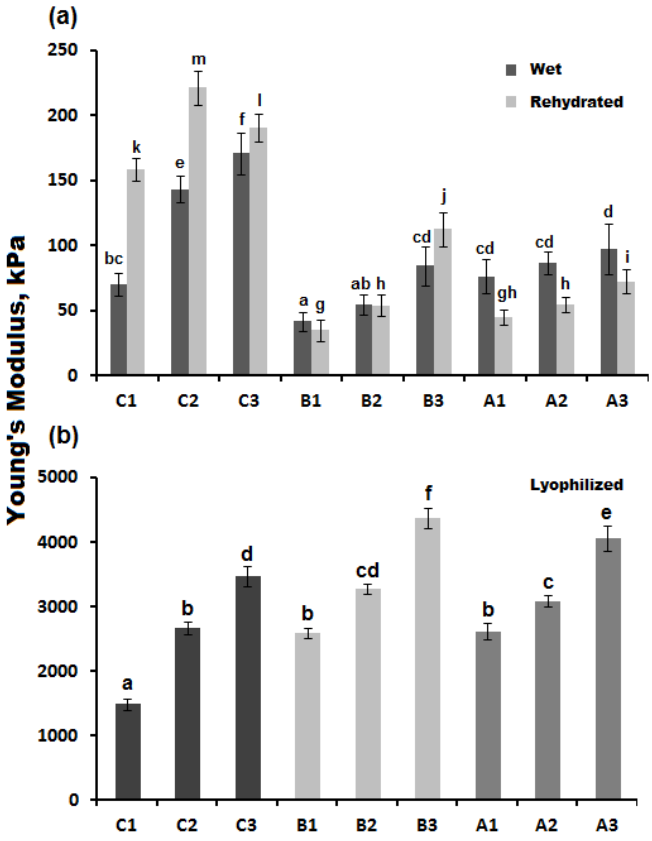

Figure 6. Value of Young's modulus for C samples (control) and porous matrices A and B at 20 °C. (a) wet samples and rehydrated. (b) lyophilized samples (scale of the largest vertical axis) ($p<0.05$). The bars indicate standard deviation.

Note that although the control samples (C) do not have an organized structure, the samples rehydrated and wet have apparent Young's modulus higher values than those of the A and B samples under similar conditions.

3.2. Volume, water absorption and mechanical properties at different temperatures of hydration

Volume changes, water uptake and apparent Young's modulus at 20 °C to 50°C were determined and the results are presented in this section. Figure 7 (top) shows that the volumes of the rehydrated samples decreased linearly (slightly) as temperature increased.

The A samples showed higher water uptake values, followed by B and C, respectively, Figure 7 (centre). This behaviour suggests that water uptake increases as the pore size increases and decreases as the concentration of alginate increases. Water uptake at 1.5% and 2.25% alginate (samples 1 and 2) presented similar values, while water absorption decreases as the temperature increases at 3.0% alginate. For BPMs, the sample A1 had the highest water uptake (over 16 times its dried weight) and B3 the lowest (over 8 times its dried weight), with internal pore sizes of 381 ± 88 μm and 249 ± 58 μm, respectively (Table 2).

Water uptake is directly related to the apparent Young's modulus and inversely related to the alginate concentration. It should be noted that the values of the Young's modulus for the C samples are higher than for those of the B and A samples despite the lack of an organized structure (Figure 7, lower images). The structures of the BPMs were more stable as hydration temperature increased compared to the C samples. The BPMs showed linear behavior at 1.5% alginate while at higher concentrations (2.25% and 3.0%) it peaked at around 25 °C. This same behavior was observed in the water uptake, albeit with a lower peak.

4. Discussion

Calcium alginate beads have been successfully used (in aqueous medium) to encapsulate various sensitive components at room temperature, including drug components (Grassi et al., 2001), proteins (Kierstan and Bucke, 2000), living cells (Stabler et al., 2001), enzymes (Blandino et al., 1999), and spermatozoa (Torre et al., 2000), among others. If the BPMs are intended for use in pharmacology, i.e. to maintain a component of interest such as a drug, it is necessary to know the physical and mechanical characteristics of these structures as well as their ability to absorb water. These features influence the way in which the drugs or other components are released. There is a delay in the delivery of drugs at higher concentrations of alginate (Tonnesen and Karlsen, 2002). Physical and mechanical properties of the lyophilized BPMs exhibit the typical behaviour of polymeric foams (Cuadros et al., 2014; Gibson and Ashby, 1997) and have high water

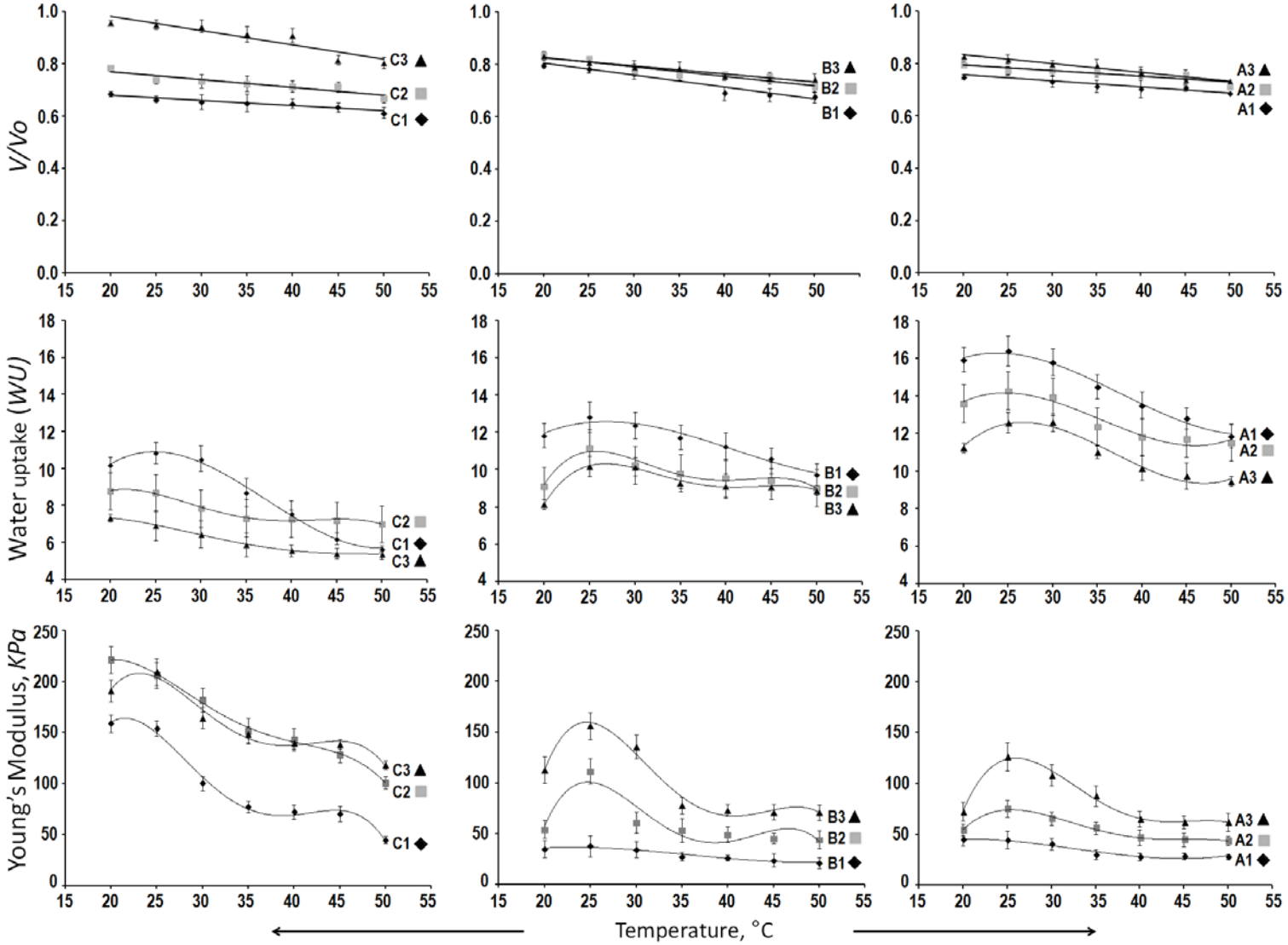

Figure 7. Behavior of control samples C, porous matrices B and A at different temperatures of rehydration. The bars indicate standard deviation.

uptake capacity at temperatures between 20 and 50 °C. Water uptake was several times the dried weight of the materials in water (up to 16 times), while the volume decreased slightly. Also, as the concentration of alginate increases, the volume and water uptake decrease slightly, while the apparent Young's modulus increases.

Larger pores mean larger spaces, which could contain a high number of water molecules bonded together and in contact with the pore walls in the matrix (de Moura et al., 2005; Pasparakis and Bouropoulos, 2006). It is possible to adjust water uptake data empirically using a power-law model [$\log W = k\,(t)^{-n}$] with a single exponent. Thus, at 3.0% alginate concentration, the three types of samples show a similar rehydration mechanism (Figure 3a) whose empirical values of *k* and *n* were established (Figure 3b). Similar results were reported for other calcium alginate preparations, in gels of the rude component or mixed with others (Chang et al., 2009; Davidovich-Pinhas and Bianco-Peled, 2010; Morais et al., 2013; Pasparakis and Bouropoulos, 2006; Sriamornsak et al., 2007). Rehydration of dried non-porous calcium alginate beads (4% alginate) reached an increase of up to 35 times the dried weight, demonstrating high water uptake ability (Pasparakis and Bouropoulos, 2006). The unique characteristic of BPMs is that despite gaining weight with rehydration (up to 16 times the dried weight), the volume remained almost unchanged (between wet and lyophilized samples) (Figure 4).

In the hydration process, the osmotic pressure was probably similar to the strength of cross-linking bonds responsible for the structure's stability and rigidity. When the pores are filled with water, the system reaches equilibrium with the aqueous medium and none of the usual swelling occurred in contrast to that which was observed with the macroporous cellulose-alginate hydrogels. In effect, the volume increased in sample C but the opposite behaviour was observed for BPMs, with the volume decreasing slightly (Figure 3).

At equilibrium, the pressure is set to zero due to the balance between two opposing forces, both external and internal (structure) (Davidovich-Pinhas and Bianco-Peled, 2010). Rehydration volumes remain almost constant (slight shrinkage), which means that the pore walls remain rigid despite the presence of water molecules inside of the matrix. The water acts as a plasticizer in biopolymers that reduces the interaction

between adjacent chains and produces increasing mobility and flexibility. This explains the decrease in the values of the apparent Young's modulus as water uptake increases (Aguilera and Stanley, 1999). However, the theory of rubbery elasticity is not completely valid for alginate gels. The literature indicates that this is controversial (Davidovich-Pinhas and Bianco-Peled, 2010) and that there is some uncertainty about its validity because the cross-linking structure found in alginates is so unique (Mitchell, 1980). It has also been found that the compression of long alternating sequences of MG/MG junctions is responsible for gel shrinkage (syneresis) in alginate gels given their dependence on the length of the MG blocks (Donati et al., 2005). The water uptake capacity is affected when the cross-linked network of calcium alginate is contained within another gel such as a gel composed of interpenetrated networks of calcium alginate and PNIPAAm [Poly (N-isopropyl acrylamide)] (de Moura et al., 2005) and macroporous cryogels of poly(glycidol-co-ethyl glycidyl carbamate) (Petrov et al., 2011).

Although the A samples were leached (in three stages), their structure still contains a high percentage of gelatine. This gelatin content suggests the possible formation of a protein-polysaccharide complexes through ionic interaction. A higher content of gelatine (B samples) improved the behaviour of some of composite gel properties (higher volumes and mechanical properties) and may have caused it to degrade. The presence of gelatine in the BPMs does not affect the safety of the samples.

BPMs at different temperatures have higher Young's modulus as the concentration of alginate increases and the pore size of the matrix decreases (de Moura et al., 2005). Similar to the water absorption, the BPMs could absorb, store, and protect compounds of interest such as drugs, with low and high solubility. Furthermore, the properties of the structure could be modified by varying the concentration and type of alginate (G content) (Tonnesen and Karlsen, 2002).

In summary, larger pore size increases water absorption and decreases the apparent Young's modulus. Thus, these properties may vary and can be controlled by varying the concentration of alginate (Figure 7).

5. Conclusions

Biopolymeric porous matrices (BPMs) of calcium alginate/gelatin were used to generate different samples, A and B, leached and non-leached, respectively. Each type of porous matrix was prepared at different concentrations (1.5%, 2.25% and 3.0%) and its physical mechanical and rehydration properties were evaluated. The BPMs had good physical and mechanical properties in the different sequential states of preparation (wet, lyophilized, and rehydrated) at room temperature. The BPMs had pore sizes which ranged from between 204 ± 58 to 380 ± 88 μm with high porosities from 96.62 ± 0.11% (B3) to 97.79 ± 0.04% (A1). The concentration of alginate had no effect on the volume of the samples within each group (i.e., wet, rehydrated, lyophilized). The volumes of the lyophilized A samples decreased slightly, but the B samples had a greater volume than the corresponding wet samples. The apparent Young's modulus reached values of up to 100 kPa for rehydrated gels and over 4000 kPa for lyophilized samples.

The BPMs have high water uptake capacity in the temperature range from 20 °C to 50 °C and reached several times their dried weight in water (up to 16 times), while the volume decreased slightly. Water uptake increased with a decrease in the concentration of alginate. In summary, larger pore size increases the water absorption and decreases the apparent Young's modulus.

The results described here may provide scientists who work on gels with new evidence for the design and manufacture of pre-defined microstructures. BPMs have excellent physical and mechanical properties that could be used for the design of tailored matrices in delivering bioactive compounds with applications in pharmacology, food, biology, and the environmental sciences.

References

Aguilera, J. M. and Stanley, D. W. (Eds.). (1999). *Microstructural Principles of Food Processing and Engineering*. Gaithersburg, MD, Aspen.

Bajpai, S. K. and Sharma, S. (2004). Investigation of swelling/degradation behaviour of alginate beads crosslinked with Ca^{2+} and Ba^{2+} ions. *Reactive and Functional Polymers, 59*, 129-140.

Blandino, A., Macías, M. and Cantero, D. (1999). Formation of calcium alginate gel capsules: Influence of sodium alginate and $CaCl_2$ concentration on gelation kinetics. *Journal of Bioscience and Bioengineering, 88*, 686-689.

Bron, J. L., Vonk, L. A., Smit, T. H. and Koenderink, G. H. (2011). Engineering alginate for intervertebral disc repair. *Journal of the Mechanical Behavior of Biomedical Materials, 4*, 1196-1205.

Cuadros, T. R., Skurtys, O. and Aguilera, J. M. (2012). Mechanical properties of calcium alginate fibers produced with a microfluidic device. *Carbohydrate Polymers, 89*, 1198-1206.

Cuadros, T.R., Erices, A. and Aguilera, J.M. (2014). Porous matrix of calcium alginate/gelatin with enhanced properties as scaffold for cell culture. *Journal of the Mechanical Behavior of Biomedical Materials*, 46, 331-342.

Chang, C., Duan, B. and Zhang, L. (2009). Fabrication and characterization of novel macroporous cellulose–alginate hydrogels. *Polymer, 50*, 5467-5473.

Davidovich-Pinhas, M. and Bianco-Peled, H. (2010). A quantitative analysis of alginate swelling. *Carbohydrate Polymers, 79*, 1020-1027.

de Moura, M. R., Guilherme, M. R., Campese, G. M., Radovanovic, E., Rubira, A. F. and Muniz, E. C. (2005). Porous alginate-Ca2+ hydrogels interpenetrated with PNIPAAm networks: interrelationship between compressive stress and pore morphology. *European Polymer Journal, 41*, 2845-2852.

Donati, I., Holtan, S., Mørch, Y. A., Borgogna, M. and Dentini, M. (2005). New hypothesis on the role of alternating sequences in calcium alginate g els. *Biomacromolecules, 6*, 1031-1040.

Dong, Z., Wang, Q. and Du, Y. (2006). Alginate/gelatin blend films and their properties for drug controlled release. *Journal of Membrane Science, 280*, 37-44.

Draget, K., Moe, S., Skjak-Braek, G. and Smidrod, O. (2006). Alginates. In A. M. Stephen, G. O. PhillipsandP. A. Williams (Eds.). *Food Polysaccharides and Their Applications* (pp. 289-334). Boca Raton, FL, CRC Press.

Draget, K., Skjak Bræk, G. and Smidsrød, O. (1994). Alginic acid gels: the effect of alginate chemical composition and molecular weight. *Carbohydrate Polymers, 25*, 31-38.

Drury, J. L., Dennis, R. G. and Mooney, D. J. (2004). The tensile properties of alginate hydrogels. *Biomaterials, 25*, 3187-3199.

Ferreira Almeida, P. and Almeida, A. J. (2004). Cross-linked alginate-gelatine beads: a new matrix for controlled release of pindolol. *Journal of Controlled Release, 97,* 431-439.

Gibson, L. and Ashby, M. (1997). *Cellular solids: structure and properties* Cambridge University Press.

Grant, G. T., Morris, E. R., Rees, D. A. and Smith, P. J. C. (1973). Biological interactions between polysaccharides and divalent cations: the egg-box model. *Febs Letters, 32,* 195-198.

Grassi, M., Colombo, I. and Lapasin, R. (2001). Experimental determination of the theophylline diffusion coefficient in swollen sodium-alginate membranes. *Journal of Controlled Release, 76,* 93-105.

Hambleton, A., Debeaufort, F., Bonnotte, A. and Voilley, A. (2009). Influence of alginate emulsion-based films structure on its barrier properties and on the protection of microencapsulated aroma compound. *Food Hydrocolloids, 23,* 2116-2124.

Hennink, W. E. and van Nostrum, C. F. (2012). Novel crosslinking methods to design hydrogels. *Advanced Drug Delivery Reviews, 64, Supplement,* 223-236.

Kierstan, M. and Bucke, C. (2000). The immobilization of microbial cells, subcellular organelles, and enzymes in calcium alginate gels. *Biotechnology and Bioengineering, 67,* 726-736.

Liu, X. and Ma, P. X. (2009). Phase separation, pore structure, and properties of nanofibrous gelatin scaffolds. *Biomaterials, 30,* 4094-4103.

Mehling, T., Smirnova, I., Guenther, U. and Neubert, R. H. H. (2009). Polysaccharide-based aerogels as drug carriers. *Journal of Non-Crystalline Solids, 355,* 2472-2479.

Mikos, A. G., Herring, S. W., Ochareon, P., Elisseeff, J., Lu, H. H., Kandel, R., Schoen, F. J., Toner, M., Mooney, D., Atala, A., Van Dyke, M. E., David, K. and Vunjak-Novakovic, G. (2006). Engineering complex tissues. *Tissue Engineering, 12,* 3307-3339.

Mitchell, J. R. (1980). The rheology of gels. *Journal of Texture Studies, 11,* 315-337.

Morais, D. S., Rodrigues, M. A., Silva, T. I., Lopes, M. A., Santos, M., Santos, J. D. and Botelho, C. M. (2013). Development and characterization of novel alginate-based hydrogels as vehicles for bone substitutes. *Carbohydrate Polymers, 95,* 134-142.

Nokhodchi, A. and Tailor, A. (2004). In situ cross-linking of sodium alginate with calcium and aluminum ions to sustain the release of theophylline from polymeric matrices. *Il Farmaco, 59*, 999-1004.

Nussinovitch, A., Jaffe, N. and Gillilov, M. (2004). Fractal pore-size distribution on freeze-dried agar-texturized fruit surfaces. *Food Hydrocolloids, 18*, 825-835.

Ostberg, T. and Graffner, C. (1994). Calcium alginate matrices for oral multiple unit administration: III. Influence of calcium concentration, amount of drug added and alginate characteristics on drug release. *International Journal of Pharmaceutics, 111*, 271-282.

Pasparakis, G. and Bouropoulos, N. (2006). Swelling studies and in vitro release of verapamil from calcium alginate and calcium alginate–chitosan beads. *International Journal of Pharmaceutics, 323*, 34-42.

Peleg, M. (1997). Review: mechanical properties of dry cellular solid foods. *Food Science and Technology International, 3*, 227-240.

Petrov, P., Utrata-Wesołek, A., Trzebicka, B., Tsvetanov, C. B., Dworak, A., Anioł, J. and Sieroń, A. (2011). Biocompatible cryogels of thermosensitive polyglycidol derivatives with ultra-rapid swelling properties. *European Polymer Journal, 47*, 981-988.

Qin, Y. (2008). Alginate fibres: an overview of the production processes and applictions in wound management. *Polymer International, 57*, 171-180.

Ribeiro, C. C., Barrias, C. C. and Barbosa, M. A. (2004). Calcium phosphate-alginate microspheres as enzyme delivery matrices. *Biomaterials, 25*, 4363-4373.

Shapiro, L. and Cohen, S. (1997). Novel alginate sponges for cell culture and transplantation. *Biomaterials, 18*, 583-590.

Sriamornsak, P., Thirawong, N. and Korkerd, K. (2007). Swelling, erosion and release behavior of alginate-based matrix tablets. *European Journal of Pharmaceutics and Biopharmaceutics, 66*, 435-450.

Stabler, C., Wilks, K., Sambanis, A. and Constantinidis, I. (2001). The effects of alginate composition on encapsulated βTC3 cells. *Biomaterials, 22*, 1301-1310.

Tonnesen, H. H. and Karlsen, J. (2002). Alginate in drug delivery systems. *Drug development and industrial pharmacy, 28*, 621-630.

Torre, M. L., Maggi, L., Vigo, D., Galli, A., Bornaghi, V., Maffeo, G. and Conte, U. (2000). Controlled release of swine semen encapsulated in calcium alginate beads. *Biomaterials, 21*, 1493-1498.

Wang, C., Liu, H., Gao, Q., Liu, X. and Tong, Z. (2008). Alginate-calcium carbonate porous microparticle hybrid hydrogels with versatile drug loading capabilities and variable mechanical strengths. *Carbohydrate Polymers, 71*, 476-480.

Yao, R., Zhang, R., Luan, J. and Lin, F. (2012). Alginate and alginate/gelatin microspheres for human adipose-derived stem cell encapsulation and differentiation. *Biofabrication, 4*, 025007.

Zhang, H., Zhang, F. and Wu, J. (2013). Physically crosslinked hydrogels from polysaccharides prepared by freeze–thaw technique. *Reactive and Functional Polymers, 73*, 923-928.

Zúñiga, R. N. and Aguilera, J. M. (2009). Structure-fracture relationships in gas-filled gelatin gels. *Food Hydrocolloids, 23*, 1351-1357.